

**The role of sympathetic neurons in modulating  
resident muscularis macrophage functions during  
postoperative ileus and mucosal antimicrobial  
responses in homeostasis**

**Sympathetic neurons in intestinal homeostasis and disease**

Doctoral thesis

to obtain a doctorate (PhD)

from the Faculty of Medicine

of the University of Bonn

**Shilpashree Mallesh**

From Bangalore, India

2022

**The role of sympathetic neurons in modulating  
resident muscularis macrophage functions during  
postoperative ileus and mucosal antimicrobial  
responses in homeostasis**

**Sympathetic neurons in intestinal homeostasis and disease**

Doctoral thesis

to obtain a doctorate (PhD)

from the Faculty of Medicine

of the University of Bonn

**Shilpashree Mallesh**

From Bangalore, India

2022

Written with authorization of  
the Faculty of Medicine of the University of Bonn

First reviewer: Prof. Dr. Sven Wehner

Second reviewer: Prof. Dr. Daniel Robert Engel

Day of oral examination: 18. November 2021

For the institute of Klinik für Allgemein-, Viszeral-, Thorax- und Gefäßchirurgie

Director: Prof. Dr. Jörg C. Kalff

## Table of content

<b>List of abbreviations .....</b>	<b>7</b>
<b>1. Introduction .....</b>	<b>11</b>
1.1 Structure of the murine small intestine .....	11
1.2 Intestinal mucosal epithelium.....	12
1.3 Structure of the mammalian nervous system.....	14
1.3.1 The Enteric Nervous System .....	16
1.3.2 The Parasympathetic Nervous System.....	16
1.3.3 The Sympathetic Nervous System.....	17
1.4 Neuro-immune interactions.....	18
1.5 Intestinal tissue-resident macrophages .....	19
1.6 The postoperative ileus.....	21
1.6.1 Pathophysiology of POI.....	21
1.6.1.1 Neurogenic phase- the early or effector phase of POI.....	22
1.6.1.2 Inflammatory phase- the late and clinically relevant phase of POI .....	23
1.6.2 Activation of resident macrophages in the early phase of POI.....	24
1.6.3 Generalized impairment of GI motility .....	25
1.7 Objectives.....	26
<b>2. Material and Methods .....</b>	<b>27</b>
2.1 Material.....	27
2.1.1 Devices .....	27
2.1.2 Consumable materials .....	28
2.1.3 Reagents.....	29
2.1.4 Buffers and solutions.....	30
2.1.5 Kits.....	31
2.1.6 Antibodies .....	32
2.1.7 Primers for qPCR.....	32
2.1.8 Primers (Quantitect).....	34

2.1.9 Primers (Taqman).....	34
2.1.10 Mouse lines.....	34
2.1.11 Software applications.....	34
2.2 Methods.....	36
2.2.1 Animals.....	36
2.2.2 The surgical denervation procedure (sSTX).....	36
2.2.3 The chemical denervation procedure (cSTX).....	37
2.2.4 Cholecystokinin (CCK) test.....	37
2.2.5 The mouse model of non-infectious postoperative ileus.....	37
2.2.6 Isolation of primary leukocytes from the muscularis externa.....	38
2.2.7 Gastrointestinal transit time measurement.....	38
2.2.8 Whole mounts preparation and Immunofluorescence staining.....	39
2.2.9 Hanker yates staining.....	39
2.2.10 Flow cytometry-based cell sorting.....	40
2.2.11 RNA isolation from sorted cells.....	40
2.2.12 RNA isolation of the complete tissue.....	40
2.2.13 <i>Ex vivo</i> stimulation assay.....	41
2.2.14 Reverse transcription and quantitative real-time polymerase chain reaction (PCR).....	41
2.2.15 RNA sequencing.....	42
2.2.16 Western blot.....	42
2.2.17 Fluorescence microscopy.....	43
2.2.18 Statistical analysis.....	43
<b>3. Results.....</b>	<b>44</b>
3.1 Sympathetic denervation modulates resident muscularis macrophage inflammatory response upon intestinal manipulation and reduces postoperative symptoms in mice.....	44
3.1.1 Selection of the sympathetic denervation approach.....	44
3.1.1.1 The genetic approach (gSTX).....	44
3.1.1.2 The surgical approach (sSTX).....	45
3.1.1.3 The chemical approach (cSTX).....	46

3.1.2 Selection of the STX approach targeting only sympathetic but not parasympathetic neurons.....	49
3.1.3 Selection of the treatment time point.....	51
3.1.4 Changes in the muscularis externa upon cSTX .....	53
3.1.5 Distinct changes in CX3CR1 <sup>+</sup> muscularis macrophages upon cSTX .....	55
3.1.6 <i>Ex vivo</i> stimulation of CX3CR1 <sup>+</sup> muscularis macrophages with LPS/M-CSF .....	56
3.1.7 Effects of cSTX in the early phase of non-infectious acute POI.....	58
3.1.8 CX3CR1 <sup>+</sup> muscularis macrophage anti-inflammatory genes are reduced upon cSTX in the early phase of POI.....	59
3.1.9 Sympathetic neuronal loss results in reduced symptoms of postoperative ileus. ....	60
3.2 Effects of sympathetic denervation on mucosal antibacterial defense.....	64
3.2.1 Changes in the mucosa after cSTX .....	64
3.2.2 Increased epithelial tight junction genes after cSTX .....	65
3.2.3 cSTX increased antimicrobial defense genes .....	67
<b>4. Discussion.....</b>	<b>69</b>
4.1 Effects of cSTX on the muscularis externa and resident CX3CR1 <sup>+</sup> Macrophages in health and disease .....	69
4.1.1 cSTX targets sympathetic neurons without affecting vagal innervation .....	70
4.1.2 cSTX shapes the muscularis externa profile to a pro-inflammatory status and reduces resident CX3CR1 <sup>+</sup> macrophage anti-inflammatory cytokines under baseline conditions.....	72
4.1.3 cSTX alters macrophage anti-inflammatory profile also in the early phase of POI.....	75
4.1.4 Sympathetic neurons play a pro-inflammatory role in the late and clinically relevant phase of POI .....	77
4.2 Effects of cSTX on the mucosal antimicrobial defense genes and insights into their role in immune driven disorders.....	78
4.2.1 cSTX affects epithelium barrier integrity and antimicrobial defense responses .....	79

4.3 Concluding remarks.....	81
<b>5. Abstract .....</b>	<b>83</b>
<b>6. List of Figures .....</b>	<b>85</b>
<b>7. List of tables .....</b>	<b>87</b>
<b>8. References.....</b>	<b>88</b>
<b>9. Acknowledgments .....</b>	<b>108</b>

**List of abbreviations**

6-OHDA	6-hydroxydopamine
$\alpha$ 7nAChR	$\alpha$ 7 nicotinic receptor-expressing
Adra1a	Alpha- 1A adrenergic receptor
Adra1b	Alpha- 1b adrenergic receptor
Adra1d	Alpha- 1d adrenergic receptor
Adra2a	Alpha- 2A adrenergic receptor
Adra2b	Alpha- 2B adrenergic receptor
Adrb1	Beta-1 adrenergic receptor
Adrb2	Beta-2 adrenergic receptor
Adrb3	Beta-3 adrenergic receptor
ANOVA	Analysis of Variance
ANS	Autonomous nervous system
Arg1	Arginase 1
BAC	Benzalkonium chloride
BCA	Bicinchoninic acid assay
BMP2	Bone morphogenetic protein 2
BSA	Bovine serum albumin
CCK	Cholecystokinin
CD163	Cluster of Differentiation 163
cDNA	Complementary deoxyribonucleic acid
ChAT	Choline acetyltransferase
CNS	Central nervous system

CRF	Corticotrophin-releasing factor
CSF-1R	Colony Stimulating Factor 1 Receptor
cSTX	Chemical sympathectomy
CX3CR1	C-X3-C Motif Chemokine Receptor 1
DC	Dendritic cells
Defa1	Defensin Alpha 1
DMEM	Dulbecco's Modified Eagle Medium
DNA	Deoxyribonucleic acid
ENS	Enteric nervous system
FACS	Fluorescence-activated cell sorting
FCS	Fetal calf serum
FITC-dextran	Fluorescein Isothiocyanate-Dextran
g	Grams
GAP	Goblet-associated antigen passages
GC	Geometric center
GFP	Green fluorescent protein
GIT	Gastrointestinal tract
GO	Gene ontology
gSTX	Genetic sympathectomy
h	Hour
HRP	Horse-radish peroxidase
IEC	Intestinal epithelial cells
IL-10	Interleukin- 10

IL-1b	Interleukin- 1 beta
IL-6	Interleukin 6
IM	Intestinal manipulation
iNOS	Inducible nitric oxide synthase
i.p	Intraperitoneal
KCl	Potassium chloride
KRB	Krebs–Ringer buffer
LPS	Lipopolysaccharide
Lyz1	Lysozyme C-1 precursor
μ	Micro
mACHR-4	Muscarinic acetylcholine receptor
M-CSF	Macrophage colony-stimulating factor
MHC	Major histocompatibility complex
MPO	Myeloperoxidase
NaCl	Sodium chloride
NE	Norepinephrine
nNOS	Nitric oxide synthase
NPY	Neuropeptide Y
PBS	Phosphate-Buffered Saline
PCA	Principal component analysis
PCR	Polymerase chain reaction
pH	Potential of hydrogen
PNS	Peripheral nervous system

POI	Postoperative ileus
PVDF	Polyvinylidene fluoride
Reg3g	Regenerating islet-derived protein 3
Retnla1	Resistin-like alpha precursor
RNA	Ribonucleic acid
RPM	Revolutions per minute
RT-PCR	Real-time Polymerase Chain Reaction
SEM	Standard error of mean
SMA	Superior mesenteric artery
SNS	Sympathetic nervous system
sSTX	Surgical sympathectomy
STX	Sympathectomy
TH	Tyrosine hydroxylase
TNF- $\alpha$	Tumour Necrosis Factor alpha
VIP	Vasoactive intestinal polypeptide
YM1	Chitinase-like protein 3 (Chil3)

## 1. Introduction

### 1.1 Structure of the murine small intestine

The small and large intestine, form a significant part of the gastrointestinal tract (GI tract). As a key component of the digestive system, the small intestine allows the breakdown of food and absorption of nutrients via blood vessels, nerves, and muscles (Collins et al., 2021). It consists of three parts: duodenum- the first and shortest segment, jejunum- the mid-segment, and ileum- the third and last segment of the small bowel. The small bowel

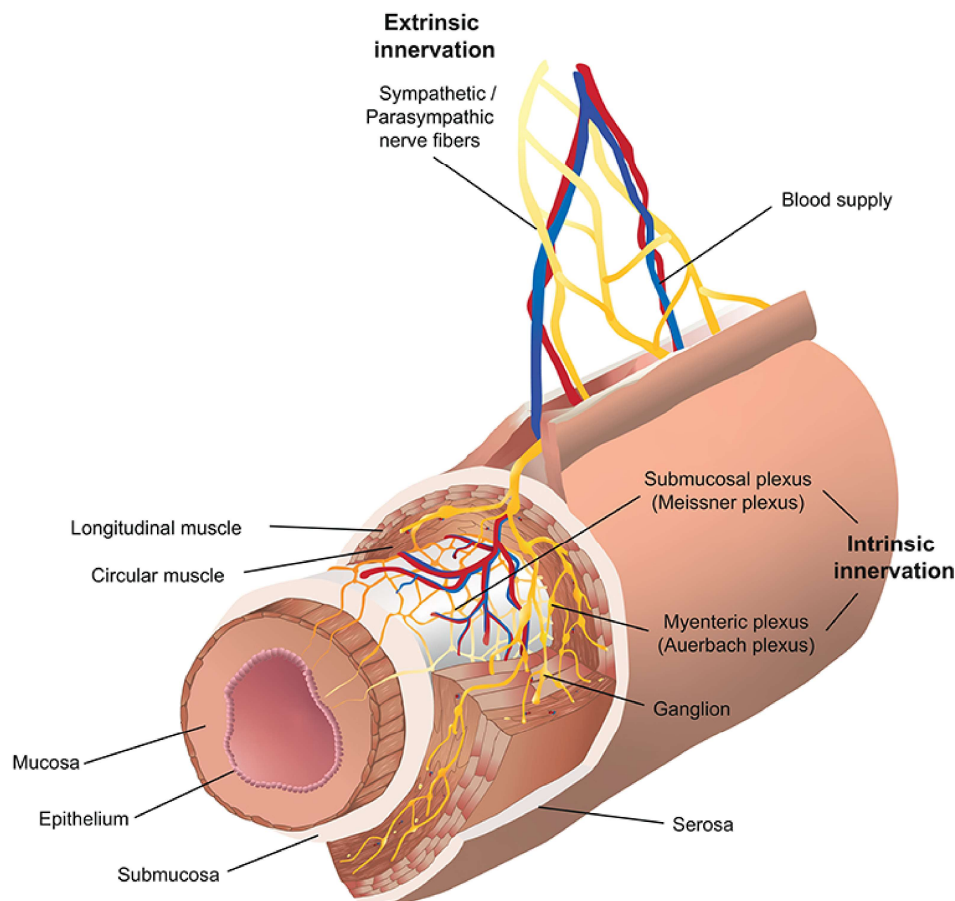


**Figure 1: Schematic view of the intestinal wall showing the organization of different layers.**

The myenteric plexus is located between circular and longitudinal muscle layers. The mucosa is the innermost layer whereas the submucosal plexus lies below the circular muscle layer. Coordinated contractions of circular and smooth muscle layers are responsible for the rhythmic peristaltic movement of the intestine. The image is adapted from Jakob et al. 2020. Copyright (2020) Jakob, Murugan and Klose. This figure is licensed under a Creative Commons Attribution 4.0 International License <https://creativecommons.org/licenses/by/4.0/>.

is made up of four complex functional layers: mucosa, submucosa, muscularis externa and serosa (**Figure 1A**) (Jakob et al., 2020).

The mucosa is the innermost layer of the intestine that lines the gut lumen (Randall et al., 2011). The mucosal layer includes epithelium that is supported by the lamina propria. The epithelium of the small intestine is organized in a series of finger-like projections called villi, and each villus is surrounded by invaginations called crypts (Bowcutt et al., 2014). The mucosa is supported by the submucosal layer that contains nerves, blood vessels, and lymphatics. The submucosa is further surrounded by a two-layer musculature called muscularis externa that is comprised of an outer layer of the longitudinal and inner layer of circular smooth muscle cells. The coordinated contraction and relaxation of the smooth muscle cells drive the peristaltic movement of the gut (Muller et al., 2014) and the enteric nervous system plays a major role in regulating the frequency of these peristaltic movements (Furness, 2012).

## 1.2 Intestinal mucosal epithelium

The intestinal mucosa is densely innervated by extrinsic and intrinsic neurons, and the interaction between these neurons and epithelium has been well documented (Sharkey et al., 2018). Gut epithelium plays a pivotal role in maintaining homeostasis by absorbing nutrients and providing a protective barrier against luminal agents. This barrier consists of tight junctions, desmosomes, and adherens junctions. The tight junction is a multi-protein complex that allows transepithelial transport of uncharged solutes and bacterial polysaccharides but prevents paracellular translocation of bacteria into the host environment (van Itallie et al., 2008; Watson et al., 2005). The epithelial cells are connected by tight junctions mainly occludins claudins, ZO-1, and ZO-2 (Zihni et al., 2016; Lee et al., 2018) (**Figure 2A**). Altered tight junction barrier permeability due to disruption of the epithelium can trigger mucosal inflammatory bowel diseases (IBD) such as Crohn's disease and ulcerative colitis. The epithelium is made of a single layer of specialized cell types that are constantly revived by stem cells in the crypts of Lieberkühn (Mittal und Coopersmith, 2014). In 1974, Cheng and Leblond first described four major intestinal epithelial cells: paneth cells, goblet cells, enterocytes, and enteroendocrine cells (**Figure 2B**) (Cheng und Leblond, 1974). The absorptive enterocytes are found on the villus, while

goblet cells and enteroendocrine cells are present on both villi and crypts. Tuft cells on the villi-crypt axis sense for luminal bacteria and paneth cells in the crypt secrete bactericidal products. Microfold cells (or M-cells) in the epithelium provide a gateway for luminal antigens (Clevers, 2013).

The epithelium prevents the translocation of bacteria and is shielded by a mucin layer, antibacterial lectins, and defensins (Zheng et al., 2020). Mucins are secreted by intestinal goblet cells and act as a barrier against microbes invading the epithelium. Intestinal epithelial cells produce antimicrobial proteins that help the host defense system fight against microbial challenges. Enterocytes secrete Regenerating islet-derived protein 3-gamma (REG3 $\gamma$ ) throughout the small intestine while paneth cells produce defensins and lysozymes in small intestinal crypts (Gallo und Hooper, 2012; Bevins und Salzman, 2011). REG3 $\gamma$  selectively targets and disrupts the surface membrane of gram-positive bacteria (Bevins und Salzman, 2011). Defensins are bactericidal against gram-positive and gram-negative bacteria. They disrupt the membrane integrity and inhibit bacterial cell wall biosynthesis (Zasloff, 2002; Sass et al., 2010; Schneider et al., 2010). In addition, these defensins possess a chemotactic activity and can recruit leukocytes (Bevins und Salzman,

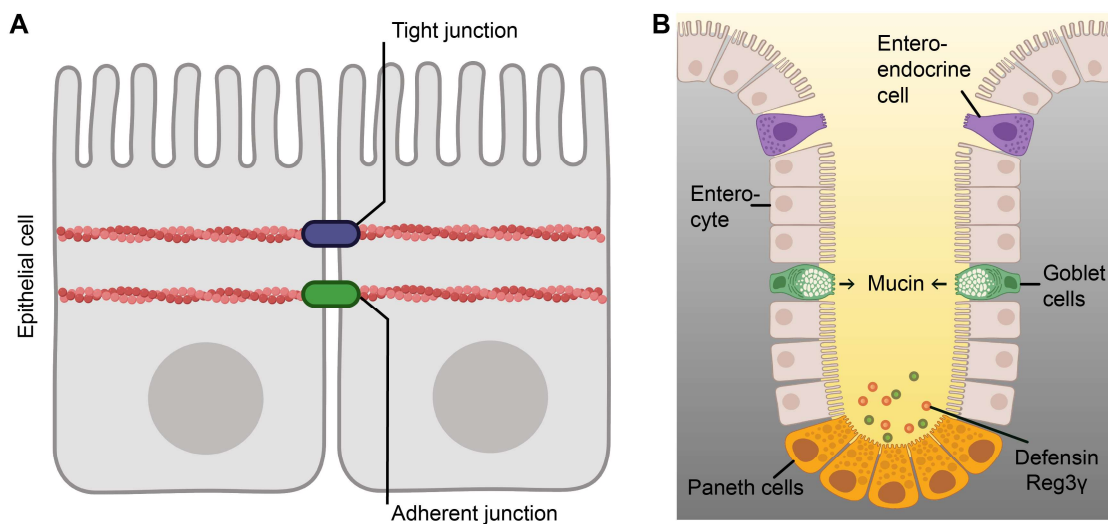


**Figure 2: Epithelial cells of the intestine**

(A) Epithelial cells are connected by transmembrane tight junctions that act as a barrier modulating solute movement across the epithelium and prevent paracellular luminal translocation. (B) Paneth cells in the crypt of the small intestine secrete defensins and lysozymes. Enterocytes secrete REG3 $\gamma$ . Goblet cells secrete mucin that forms a thick protective layer surfacing the epithelium. This mucin layer concentrates antimicrobial proteins such as REG3 $\gamma$  and defensins near the surface of the epithelium.

2011). Dysregulated functions of these antimicrobial proteins are associated with IBD (Wehkamp et al., 2005).

### 1.3 Structure of the mammalian nervous system

The central nervous system (CNS) and the peripheral nervous system (PNS) are the two fundamental parts of the mammalian nervous system. Nerve structures in the brain and spinal cord are part of the CNS, while all other nerves in the body are part of the PNS (Catala und Kubis, 2013). Both CNS and PNS have somatic and autonomous parts that regulate various bodily processes. PNS has both afferent sensory and efferent motor fibers that innervate various organs including the spleen and intestine (Rao und Gershon, 2016; Hu et al., 2020). The sensory spinal nerves of the dorsal root ganglia and motor spinal nerves of the anterior horn represent the somatic PNS system and work under voluntary control. In contrast, the involuntary physiologic processes such as digestion, heart rate, respiration, and blood pressure are regulated by the PNS via the autonomous nervous system (ANS) (Jänig, 1989; Catala und Kubis, 2013). The ANS can be further subdivided into the enteric nervous system (**Figure 3A**) (ENS), the sympathetic nervous system (**Figure 3B**), and the parasympathetic nervous system (**Figure 3C**) that forms a complex neural circuit in the myenteric plexus (Jakob et al., 2020; Kenney und Ganta, 2014). The parasympathetic and sympathetic nervous systems are anatomically distinct branches of the ANS. While sympathetic neurons induce a fight or flight reaction, the neurons of the parasympathetic nervous system elicit a rest and digest response. On the other hand, the ENS forms a dense network together with glial cells and neurons and contributes to maintaining homeostasis by regulating blood flow and peristalsis (Jakob et al., 2020). It is well described that both sensory and autonomic neurons of the PNS interact with the immune system to drive inflammation. Thus, the nervous and the immune system are capable of influencing each other in tissue homeostasis as well as during inflammatory conditions (Gabanyi et al., 2016; Matheis et al., 2020; Muller et al., 2014; Willemze et al., 2018)

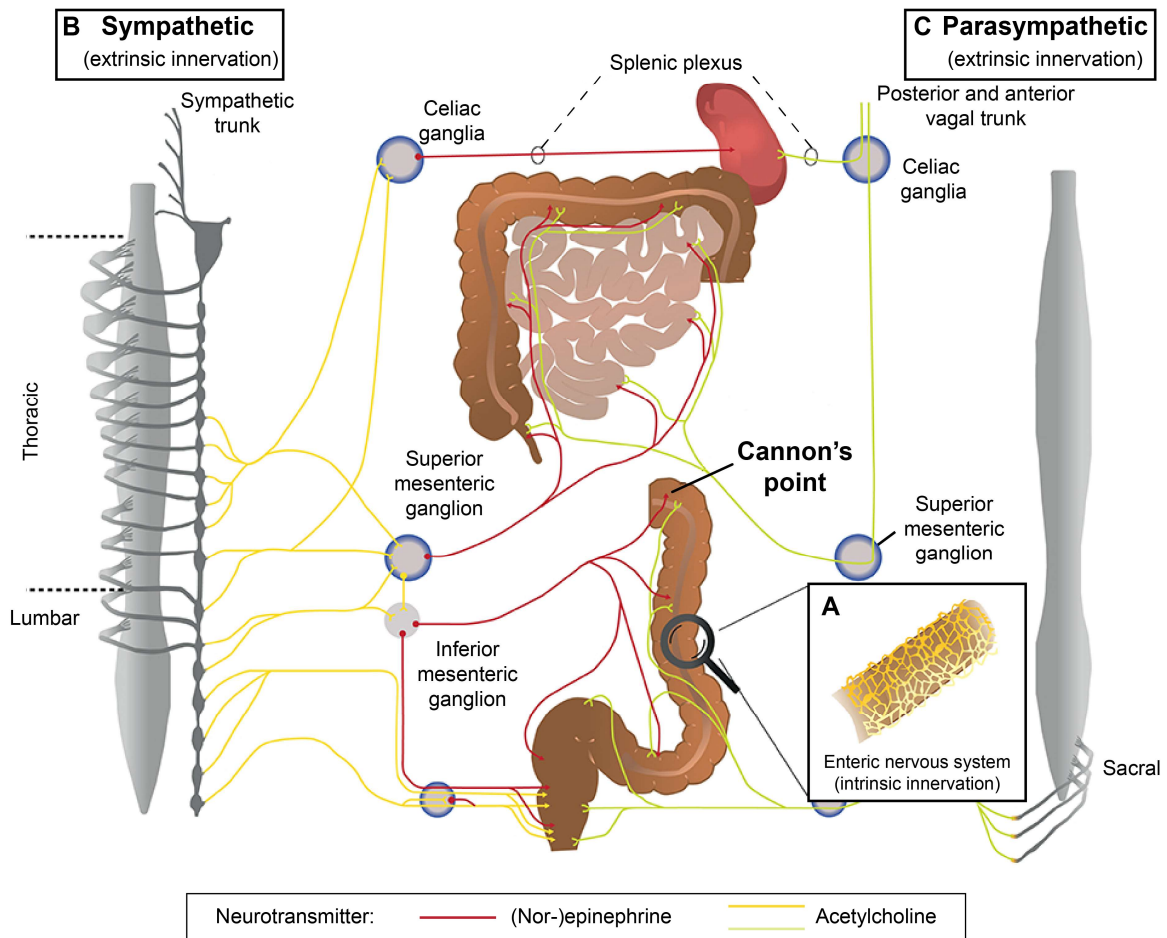


**Figure 3: Organization of the three anatomical branches of the peripheral autonomous nervous system.**

(A) The enteric nervous system is organized in Meissner and Auerbach plexus throughout the intestine (bottom right). Innervation is intrinsic if the cell bodies of the neuron are located within the intestinal tissue and extrinsic if they are outside. (B) The preganglionic cell bodies of the sympathetic nervous system located in the thoracolumbar region receive the signal from the hypothalamus and the brain stem. These preganglionic cell bodies synapse with postganglionic neurons in the sympathetic trunk and following signal transmission, the GI tract is innervated by the postganglionic sympathetic neurons (red). (C) The preganglionic parasympathetic neuron cell bodies are in the brainstem and pelvic sacral nerves. The GI tract is innervated by the vagal nerve that includes preganglionic parasympathetic fibers (green). This innervation ends at the cannon's point of the transverse colon and after this point, the pelvic sacral nerves innervate the colon. The neurotransmitter of the sympathetic nervous system (norepinephrine) is shown in red while that of the parasympathetic and enteric nervous system (acetylcholine) is indicated in green and yellow. The image is adapted from Jakob et al. 2020. Copyright (2020) Jakob, Murugan and Klose. This figure is licensed under a Creative Commons Attribution 4.0 International License <https://creativecommons.org/licenses/by/4.0/>.

### 1.3.1 The Enteric Nervous System

The GI tract functions are regulated by the ANS by intrinsic as well as extrinsic innervation (Uesaka et al., 2016). Being the largest component of ANS, the ENS is composed of thousands of neurons and ganglia (Furness et al., 2014). The extrinsic component of the ENS is made of sympathetic and parasympathetic divisions, while the intrinsic component consists of the myenteric plexus (Auerbach's plexus), the outer submucous plexus (Schabadasch's plexus), and the inner submucous plexus (Meissner's plexus). The ENS originates from vagal neural crest cells and colonizes the GI tract in the early postnatal life (Altaf und Sood, 2008; Uesaka et al., 2016; Wang et al., 2011). The ENS is often referred to as the "abdominal or second brain" as it contains more than 100 million neurons outside of the CNS. Excitatory and inhibitory enteric neurons innervate circular and longitudinal muscles in the GI tract and modulate their spatiotemporal contractions (Furness, 2012; Veiga-Fernandes und Pachnis, 2017). The crucial role of ENS has been described in Hirschsprung's disease- a congenital disorder that lacks enteric neurons in the distal bowel. In this disease, the colon propulsive motility pattern modulated by enteric neurons is disturbed leading to high morbidity and death (Heuckeroth, 2018).

### 1.3.2 The Parasympathetic Nervous System

The motor function of the upper GI tract is regulated by parasympathetic innervation via the vagus nerve. This nervous system is cholinergic in nature and its primary neurotransmitter is acetylcholine (Brinkman et al., 2019b). The vagus nerve has 80% afferent and 20% efferent fibers. The afferent fibers control taste, somatic and visceral information while the efferent fibers regulate GI motility and secretion. The vagus nerve interacts with enteric neurons expressing choline acetyltransferase (ChAT), Vasoactive intestinal polypeptide (VIP) nitric oxide synthase (nNOS), and is in proximity to  $\alpha 7$  nicotinic receptor-expressing ( $\alpha 7$ nAChR) expressing macrophages within the muscularis (Bonaz et al., 2017; Cailotto et al., 2014; Johnson et al., 2018). In response to ingested food, enterocytes and enteroendocrine cells secrete gut peptides such as cholecystokinin (CCK), ghrelin, and leptin. The receptors for these gut peptides are expressed on most nodose neurons (Moran, 2009; Raybould, 2007). Through lamina propria, these signals diffuse and activate the nearby myenteric, vagal, and spinal afferent neurons. These peptides can also distantly function as hormones by entering the bloodstream (Cummings

und Overduin, 2007). During fasting, the level of circulating CCK is relatively lower, and the receptors expressed on vagal afferents are increased. However, increased CCK levels upon feeding act to reduce vagal afferent receptor expression that in turn signals CNS to mediate satiety (Raybould, 2007; Strader und Woods, 2005). Subsequently, rats administered with CCK intraperitoneally showed reduced food intake (Ghia et al., 2007). The parasympathetic nervous system exerts both inhibitory and excitatory control over GI motility. The preganglionic neurons contracted by the vagal efferent fibers regulate GI motility in two distinct pathways. Activation of muscarinic cholinergic receptors allows the contraction of GI smooth muscles by an excitatory cholinergic pathway, whereas the release of nitric oxide and/or vasoactive intestinal polypeptide allows the relaxation of GI smooth muscles by a non-cholinergic and non-adrenergic pathway (Browning und Travagli, 2014).

### 1.3.3 The Sympathetic Nervous System

The sympathetic nervous system (SNS) is another part of ANS, that governs the “fight or flight” response. The sympathetic preganglionic neurons arise from the thoracic and lumbar spinal cord and activate postganglionic neurons. The sympathetic postganglionic neurons innervating the small intestine are contained in the superior mesenteric ganglion, the neurons innervating the colon reside in the inferior mesenteric ganglion, and those innervating the stomach are within the celiac ganglion (Simmons, 1985). Regulation of electrolyte secretion of epithelial cells, gut motility, and blood flow is modulated by sympathetic neurons innervating the GI tract (Lomax et al., 2010). In addition, they regulate GI inflammation by communicating with innate (McCafferty et al., 1997; Straub et al., 2006) as well as the adaptive immune systems (Sanders, 2012). Several investigations have described increased sympathetic innervation in IBD (Birch et al., 2008; Kyösola et al., 1977) suggesting an altered response of SNS in disease conditions. The sympathetic fibers innervate the submucosal and myenteric plexus and regulate the activity of enteric neurons by inhibiting the release of neurotransmitters (Tack und Wood, 1992; Straub et al., 2006). Additionally, the sympathetic neurons densely innervate the GI vascular bed which helps in regulating the blood pressure. Norepinephrine (NE) is an important and primary neurotransmitter of the SNS, however, it is also shown to release Galanin, somatostatin, neuropeptide Y (NPY), and other neuropeptides (Tan et al., 2018).

#### 1.4 Neuro-immune interactions

The gut innervating neurons rapidly communicate with the resident immune cells and modulate homeostatic functions of the intestine. A study showed that the neuronal signals modulate resident macrophage functions while macrophages on the other hand regulate neuronal survival. This bi-directional communication plays a crucial role in health and disease (Muller et al., 2014). GI macrophages perform various homeostatic functions such as tissue remodeling and clearance of apoptotic cells (Cummings et al., 2016). In addition, these resident GI macrophages support and protect enteric neurons (Schepper et al., 2018c). The mechanism underlying this neuron-macrophage crosstalk relies on Bone morphogenic protein-2 (*BMP-2*) secreted by resident macrophages that orchestrate muscle contraction by acting on BMP receptors expressed on enteric neurons. In turn, colony-stimulating factor - 1 (*CSF-1*) required for macrophage survival is secreted by enteric neurons (Muller et al., 2014). Subsequently, neuro-immune interactions have gained particular focus in intestinal research.

At the beginning of the 21<sup>st</sup> century, Kevin Tracey and colleagues described the novel concept “inflammatory reflex” (Tracey, 2002). This reflex demonstrated the role of parasympathetic or sympathetic neurons in modulating immune responses in bacterial sepsis. Activation of the vagus nerve inhibits systemic inflammation by modulating *TNF- $\alpha$*  production in the spleen. Upon lipopolysaccharide (LPS) injection, splenic and vagus nerves are activated and lead to subsequent release of NE in the spleen. In response to NE, CD4<sup>+</sup> T cells induce acetylcholine that acts on  $\alpha$ 7nAChR macrophages to suppress *TNF- $\alpha$*  production (Borovikova et al., 2000; Andersson und Tracey, 2012; Tracey, 2009). Interestingly, in the spleen, the innervation of adrenergic neurons is more abundant compared to vagal innervation (Berthoud und Powley, 1993). Therefore, it was hypothesized that acetylcholine-producing T cells were activated by adrenergic rather than cholinergic neurons and subsequently modulates macrophage cytokine production (Rosas-Ballina et al., 2011). This data led to the key discovery that the immune system is not completely autonomous and gained increasing interest in parasympathetic and sympathoimmune studies.

Sympathetic neurons via catecholamines such as epinephrine, NE, or dopamine, signal to  $\alpha$ - or  $\beta$ -adrenergic receptors that are present on almost all immune cell types (Brinkman

et al., 2019b; Marino und Cosentino, 2013).  $\beta_2$  adrenergic receptor ( $\beta_2AR$ ) activation on bone marrow-derived dendritic cells *in vitro* stimulated with LPS, suppressed the release of pro-inflammatory cytokines indicating an anti-inflammatory role of sympathetic neurotransmitters (Nijhuis et al., 2014). Similarly, *Adrb2* signaling induced IL-10 secretion and suppressed inflammation while *Adrb2*<sup>-/-</sup> mice were more susceptible to DSS-induced intestinal inflammation (Ağaç et al., 2018b). Recently, transcriptomics data revealed that high levels of the  $\beta_2AR$  are expressed on resident macrophages (Gabanyi et al., 2016). During infection, sympathetic neurons are activated and release NE that acts on macrophage  $\beta_2AR$ . This NE-adrenergic signaling provides enteric neuroprotection by the release of polyamines and maintains neuronal homeostasis in the gut (Gabanyi et al., 2016; Matheis et al., 2020). Consequently, SNS has been recognized as a mediator in modulating inflammation. However, the question arises as to their role in modulating macrophage functions during a GI inflammation and the consequences of these neuro-immune interactions *in vivo*.

### 1.5 Intestinal tissue-resident macrophages

GI macrophages are a specialized population of phagocytes that perform diverse functions in host defense and homeostasis (Schepper et al., 2018b). They promote tissue homeostasis under healthy conditions while their function changes during noxious challenges thereby inducing inflammation and host defense mechanisms (Amit et al., 2016). By using the FITC-dextran tracer, Mikkelsen and colleagues first identified macrophage-like cells in different layers of the intestine that were capable of dextran uptake (Mikkelsen et al., 1985). These tissue-resident macrophages are observed in the myenteric plexus between circular and longitudinal cells, mucosal, submucosal, and serosal regions (**Figure 4**) (Wehner und Engel, 2017).

Recently, a study revealed the distribution and morphology of these macrophages by deep tissue and intravital imaging techniques (Gabanyi et al., 2016). The mucosal lamina propria populates a dense network of CD11b<sup>+</sup>CX<sub>3</sub>CR1<sup>+</sup>CD103<sup>-</sup> and CD11b<sup>+</sup>CX<sub>3</sub>CR1<sup>-</sup>CD103<sup>+</sup> cells (Muller et al., 2014) and have a short half-life of 3 weeks (Jaensson et al., 2008) that requires constant replenishment by myeloid bone marrow-derived progenitors (Bain et al., 2014). The lamina propria macrophages (LPMs) are found close to the epithelium layer and express pro-inflammatory genes like *IL-1 $\beta$*  and *IL-12b*

(Gabanyi et al., 2016; Bain und Mowat, 2014). They are in constant motion sensing for harmful pathogens and have a pivotal role in maintaining intestinal immunity (Wynn et al., 2013). Muscularis macrophages found between the longitudinal and circular muscle layers are identified as one of the primary innate immune cells involved in maintaining intestinal homeostasis. These  $CD11b^+ CX3CR1^{hi} MHCII^{hi} CD11c^{lo} CD103^-$  macrophages (Muller et al., 2014) exhibit a tissue-protective phenotype under steady-state and express *Arg1*, *CD163*, and *YM1* anti-inflammatory genes (Gabanyi et al., 2016). Compared to LPMs, these macrophages are mostly static showing no cellular displacement. Two phenotypically distinct-shaped populations: Bipolar and stellate shape are observed in the muscularis externa. Of note, the morphology of the stellate-shaped macrophages is similar to that of microglia in the brain (Schepper et al., 2018a).

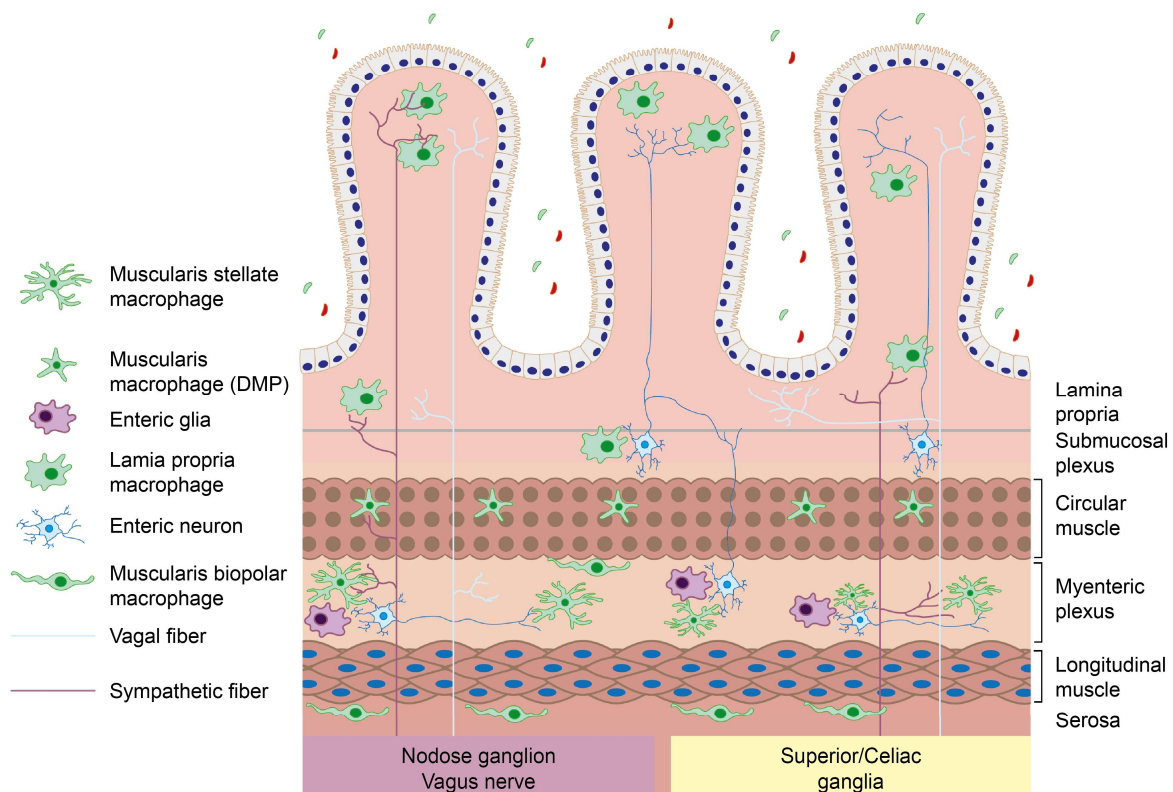


**Figure 4: Distribution of macrophages in different layers of the intestine**

Intestinal macrophages are predominantly found in mucosal, submucosal, serosal, and myenteric plexus. In muscularis externa, between circular and longitudinal muscle layers, these macrophages form dense networks and appear as stellate-shaped cells. In the serosal layer, the macrophages are mostly bipolar. Both extrinsic parasympathetic and sympathetic neurons as well as intrinsic enteric neurons innervate the GI tract and are shown to modulate these macrophage functions. The image was adapted from Wehner, Engel, *J Physiol*, 2017 under license number 5095910274829.

In steady-state, intestinal macrophages are constantly replenished by circulating Ly6C<sup>+</sup> monocytes (Bain et al., 2014). These monocytes possess a tolerogenic phenotype towards commensal microbiota in the healthy tissue context (Zigmond und Jung, 2013; Varol et al., 2009). However, in acute inflammation, the tolerogenic signature is altered differentiating these cells into a pro-inflammatory phenotype that induces intestinal disorders (Engel et al., 2010; Zigmond et al., 2012). Notably,  $\beta_2AR$  activation on muscularis macrophages promotes a tissue-protective anti-inflammatory phenotype, while treatment with  $\beta_2AR$  antagonist impaired the upregulation of *Ag1* and other anti-inflammatory genes during bacterial infection (Gabanyi et al., 2016). In addition, this neuro-immune axis is crucial in preventing infection-induced neuronal cell death and maintaining homeostasis (Matheis et al., 2020). Although adrenergic mechanisms have been clearly described in bacterial infections, the regulatory role of SNS on muscularis macrophages in inflammatory conditions has not been analyzed so far.

## 1.6 The postoperative ileus

Surgical handling of the intestine is shown to trigger inflammation leading to a transient dysmotility of the gastrointestinal tract clinically known as postoperative ileus (POI) (Mueller et al., 2011; Jonge et al., 2003; Wehner et al., 2007; Stein et al., 2018). The symptoms of POI include postoperative discomfort, nausea, abdominal pain, vomiting, delayed stool passage, prolonged hospital stay, and increased patient morbidity (Kreis et al., 2003; Vather et al., 2014).

### 1.6.1 Pathophysiology of POI

Although the surgical procedure itself is the principal cause, other factors also contribute to the pathophysiology of POI. It is a complex process involving neural, pharmacological, and immune-mediated mechanisms (Stakenborg et al., 2017). Mechanoreceptors and/or nociceptors are activated upon a surgical insult subsequently leading to afferent fiber stimulation. This triggers supraspinal and spinal reflexes causing temporary inhibition of GI motility (Jonge et al., 2003; Boeckxstaens et al., 1999). Surgeries often use opioids as analgesics that activates  $\mu$ -opioid receptors expressed on the myenteric fibers. The activation of these receptors inhibits the release of acetylcholine from myenteric neurons and reduces the GI transit time (Holte und Kehlet, 2002). Alvimopan, a selective opioid

antagonist improves the postoperative GI motility to a minor extent (Vaughan-Shaw et al., 2012).

#### 1.6.1.1 Neurogenic phase- the early or effector phase of POI

Two important phases of POI triggered by abdominal surgeries are proposed to be the significant cause of this disease (**Figure 5**). The first phase is neurally mediated involving adrenergic neurons since inhibition of normal motility is prevented when adrenergic nerves are depleted (Plourde et al., 1993; Zittel et al., 1994). Laparotomy activates a neural pathway involving a spinal loop that synapses afferent splanchnic nerves in the spinal cord and travels efferent nerves back to the gut (Boeckxstaens und Jonge, 2009). Some acute studies have identified the involvement of supraspinal pathways 30-90 minutes after surgery with corticotrophin-releasing factor (CRF) playing a key role. Supraoptic neurons of the hypothalamus are stimulated upon CRF release that sends projections to spinal and thoracic glands.

Activation of sympathetic preganglionic neurons located on the inter-mediolateral column of the thoracic cord eventually inhibits the entire GI motility (Barquist et al., 1996; Stengel und Taché, 2009). In addition, intense stimulation of afferent splanchnic nerves is also shown to trigger non-adrenergic vagal pathways (Boeckxstaens et al., 1999). The activation of mechanoreceptors and/or nociceptors during abdominal surgery ends after the closure of the abdomen, therefore, the factors involved in the late, inflammatory phase could play a role in the extended nature of POI.

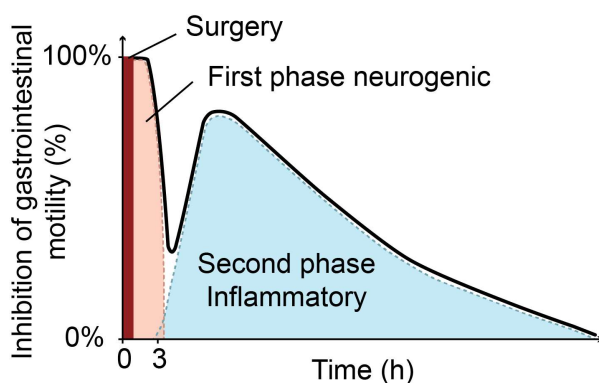


**Figure 5: The two phases of POI triggered by abdominal surgery**

The first phase of POI is induced during the abdominal surgery but ends soon after the closure of the abdomen. Three to four hours after the surgery, the second, inflammatory, and prolonged phase of POI begins thus making it clinically more relevant.

### 1.6.1.2 Inflammatory phase- the late and clinically relevant phase of POI

In 1978, dogs implanted with intestinal electrodes showed inhibition of electrical spiking activity during incision of muscle and peritoneum (Bueno et al., 1978). However, at the end of the surgery, this primary inhibition phase was transiently ceased. 3-4 hours after surgery, a secondary inhibition phase was observed that resulted in a prolonged reduction of electrical spiking activity. Nevertheless, the recovery of this electric activity was observed after 94 hours (Bueno et al., 1978). Although they described inhibitory neuronal pathways to be involved in the first phase, the mechanisms underlying the second phase remained elusive. 20 years later, studies in rats described inflammation of the muscularis externa to be the principal mechanism involved in the prolonged second phase of POI (Kalff et al., 1998; Kalff et al., 1999b; Kalff et al., 1999a). The inflamed tissue from the animals that underwent manipulation showed the impaired contractile activity of muscle strips (Kalff et al., 1999b). In line, extravasation of leukocytes and the normal muscle strip functions were conserved when animals were treated with antibodies against intercellular adhesion molecule 1 (ICAM-1), further confirming that intestinal manipulation induced

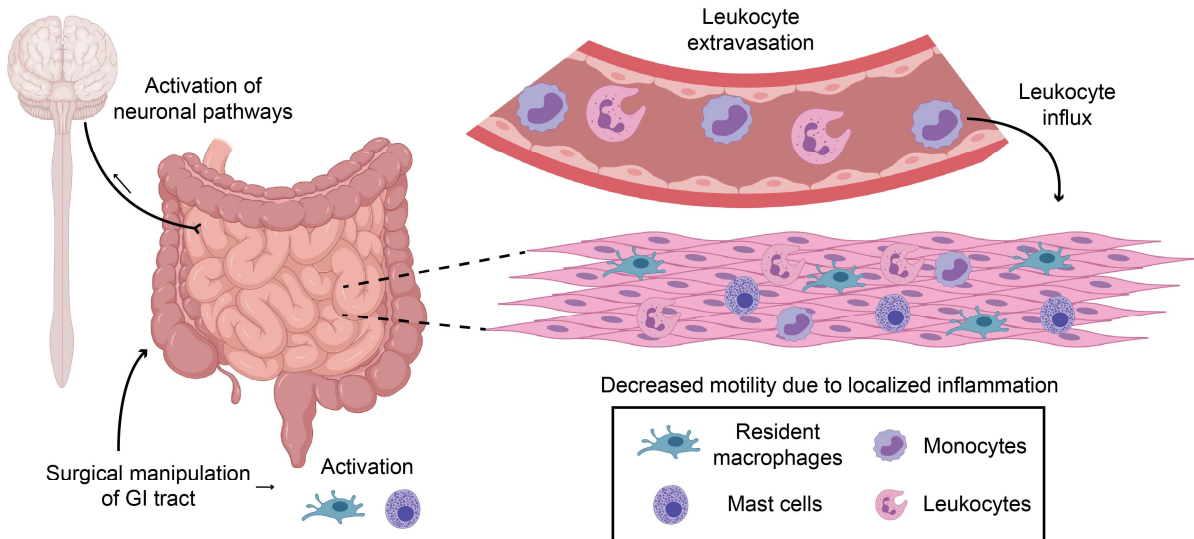


**Figure 6: Schematic representation of inflammatory cascade after intestinal manipulation**

In the first phase of POI, abdominal surgery triggers adrenergic and non-adrenergic pathways that inhibit GI motility. Tissue-resident muscularis macrophages and mast cells (in humans) are activated upon intestinal manipulation that initiates the inflammatory cascade. Upon activation, cytokines and chemokines are released by these resident cells followed by the extravasation of monocytes and neutrophils into the muscularis externa. This leads to a disturbed GI motility and worsened symptoms of POI.

inflammation contributing to the severity of POI (The et al., 2005). It is shown that mast cells found in proximity to the afferent nerve fibers as well as blood vessels are released upon surgical interventions (Coldwell et al., 2007). Although the exact mechanism involved in the activation of mast cells is still not clear, it is hypothesized that calcitonin gene-related peptide or substance P released by activated afferent nerves could trigger mast cell release (Bueno et al., 1997). Fundamentally, the activation of mast cells could be a primary event that leads to increased intestinal permeability and translocation of luminal contents, followed by the activation of resident muscularis macrophages and glia cells (Wehner und Engel, 2017; Stoffels et al., 2014; Schneider et al., 2020; Boeckxstaens und Jonge, 2009). Upon activation, the resident macrophages mediate the release of pro-inflammatory cytokines followed by the infiltration of blood-derived leukocytes characterized as CD45<sup>+</sup> Ly6C<sup>+</sup> Ly6G<sup>-</sup> monocytes and CD45<sup>+</sup> Ly6C<sup>+</sup> Ly6G<sup>+</sup> neutrophils (**Figure 6**) (Farro et al., 2017; Stein et al., 2018). Genetic depletion of these macrophages in op/op mice showed reduced inflammatory mediators and attenuated the number of infiltrating leukocytes in the muscularis (Wehner et al., 2007).

#### 1.6.2 Activation of resident macrophages in the early phase of POI

Resident macrophages are activated by damage-associated molecular pattern (DAMP) such as ATP that is released upon damage due to intestinal manipulation (Ozaki et al., 2004) or by LPS and other cytokines entering the systemic circulation (Hori et al., 2001; Torihashi et al., 2000). Within one hour after intestinal manipulation, p38, ERK(1/2), JNK/SAP, and other intracellular signaling pathways are shown to be activated (Wehner et al., 2009; Backer et al., 2009). Following the phosphorylation of these transcription factors, pro-inflammatory cytokines such as *IL1 $\beta$* , *TNF $\alpha$* , *IL6*, enzymes *iNOS*, *COX2*, and chemokines including *MIP1-a* and *MCP1* are released by the activated resident macrophages. Notably, ICAM-1 is increased in the endothelium and leads to extravasation of blood-derived leukocytes (Kalff et al., 1999b; Kalff et al., 1998; The et al., 2005; Türler et al., 2007). Together, all this phenomenon contributes to the impaired and prolonged GI motility.

### 1.6.3 Generalized impairment of GI motility

Although local inflammation occurring at the manipulated areas leads to impaired smooth muscle contractility, the generalized hypomotility including the untouched areas by the surgeon might explain the involvement of other mechanisms. It is proposed that neural pathways are triggered by inflammation also in the distant non-manipulated areas leading to the inhibition of GI motility (Boeckxstaens und Jonge, 2009). Even without the signs of gastric inflammation, delayed gastric emptying was observed in mice that underwent small intestinal manipulation. To this end, normal gastric emptying was observed when neuronal inhibitory input to the stomach was prevented with ganglion blockers hexamethonium and guanethidine suggesting activation of the inhibitory adrenergic pathway in the distant untouched areas upon manipulation (Jonge et al., 2003). Further, increased spinal nerve activity, and c-fos expression in the brainstem and spinal cord was observed 24 hours after intestinal manipulation (Kreiss et al., 2003; Mueller et al., 2008). Taken together, intestinal manipulation triggers a series of events involving both neural and inflammatory mechanisms leading to an impaired muscle function in the entire GI tract.

## 1.7 Objectives

Peripheral neuro-immune and neuro-epithelial interactions play a crucial role in modulating intestinal immune and antimicrobial responses, respectively. In the muscularis externa, the outermost layer of the intestine, TH<sup>+</sup> sympathetic neurons manage immune modulation by controlling resident macrophages in their proximity. In the mucosa, the innermost layer of the intestine, sympathetic neurons lay close to the epithelium that suggests a modulating role of the SNS in epithelial biology, e.g barrier function or antimicrobial peptide production. We hypothesized that the SNS regulates macrophage as well as epithelial function *in vivo* during homeostasis. Based on previous findings, we anticipated a particular role of SNS- macrophage interactions in acute postoperative bowel wall inflammation occurring during POI, a non-infectious, neuro-inflammatory motility disorder affecting mainly the muscularis externa. To prove our hypothesis, we established the following objectives:

Objective 1: To establish an appropriate STX model to study the role of SNS *in vivo*

Objective 2: To analyse the immune status of resident muscularis macrophages upon STX under baseline conditions

Objective 3: To investigate the transcriptional changes after STX in the muscularis externa, and resident muscularis macrophages as well as the cellular and functional alterations during POI.

Given that SNS is also related to submucosal and epithelial integrity, we additionally aimed to understand the effects of STX on the epithelial function during gut homeostasis. We focused on the mucosa where IECs release antimicrobial proteins that act as a protective barrier against harmful luminal content. Altered levels of antimicrobial proteins contribute to the development of inflammatory bowel disorders. Several studies have described SNS involvement in mucosal immunity, however, their role in modulating antimicrobial responses has never been addressed, yet. In this thesis, we aimed to answer the following question:

Objective 4: To study the impact of the SNS on mucosal epithelial antimicrobial defense.

## 2. Material and Methods

### 2.1 Material

#### 2.1.1 Devices

Device	Company
Flow cytometry	Canto I, Becton, Dickinson, and company (BD), Heidelberg, Germany
Fine balance	Mettler Toledo, Gissen, Germany
Fluorescence microscope (TE2000)	Nikon, Düsseldorf, Germany
Freezer -20°C	Bosch, Stuttgart, Germany
Freezer -80°C	Sanyo, Hamburg, Germany
Homogenizer (Precellys)	Bertin, Montigny-le-Bretonneux, France
Refrigerator 4°C	Leibherr, Ochsenhausen, Germany
Light microscope	Leica, Wetlar, Germany
Magnetic stirrer	IKA laboratory technology, Staufen, Germany
Nanodrop spectrophotometer	Thermo-scientific, Schwerte, Germany
Anesthesia machine	Drägerwerk AG Lübeck, Lübeck, Germany
Taqman PCR machine	C1000™ Thermal Cycler, Bio Rad, München, Germany
Water bath (shaking)	Society for laboratory technology, GFL, Burgwedel, Germany
Thermomixer	Type 5355, Eppendorf, Germany
cDNA synthesis thermocycler	MJ research, Watertown, Massachusetts, USA
Centrifuge (Galaxy mini benchtop)	VWR, Darmstadt, Germany/ 5415D+5415R, Eppendorf, Hamburg, Germany
Vortex	MS3 basic, IKA, Staufen, Germany
Western blotting system	Bio-rad, Hercules, CA, USA

Device	Company
Protein Detection and Imaging	Bio-rad, Hercules, CA, USA
Flow cytometry cell sorter	Diva, Becton, Dickinson, and company (BD), Heidelberg, Germany

### 2.1.2 Consumable materials

Device	Company
FACS-tubes	Sarstedt, Nümbrecht, Germany
Falcon tubes (15, 50 ml)	Greiner Bio-one cellstar, Frickenhausen, Germany
Filter tips	Thermo Scientific, Schwerte, Germany
Microscope slide	Engbrecht, Edermünde, Germany
Suture thread (natural silk 5.0)	Catgut, Markneukirchen, Germany
Pipettes (5, 25 ml)	Corning Incorporated, NY, USA
Pipette (10 ml)	Greiner Bio-One Cellstar, Frickenhausen, Germany
Pipette tips (Blue, yellow)	Greiner Bio-One Cellstar, Frickenhausen, Germany
Pipette tips (white)	Corning Life science, Amsterdam, The Netherlands
PCR reaction tube (0.2, 0.6 ml)	Corning Life science, Amsterdam, The Netherlands
Cotton swab	MaiMed, Billerica, MA, United states of America
Cell culture plates (24 well)	Trasadingen, Switzerland

## 2.1.3 Reagents

Device	Company
6-hydroxydopamine	Sigma Aldrich, Saint Louis, MO, USA
Bovine Serum Albumin (BSA)	Applicher, Darmstadt, Germany
Cholecystokinin-8	Sigma Aldrich, Saint Louis, MO, USA
Collagenase II	Worthington, Lakewood, NJ, USA
Dispase II	Roche, Mannheim, Germany
Deoxyribonuclease Roche	Mannheim, Germany
Mounting medium Aquatex	Merck, Darmstadt, Germany
Ethylenediaminetetraacetic acid (EDTA)	Applicher, Darmstadt, Germany
Ethanol absolute	Applicher, Darmstadt, Germany
Fetal Calf serum (FCS)	PAN Biotech, Aidenbach, Germany
Hanker Yates	PAN Biotech, Aidenbach, Germany
Histofix	Carl Roth, Karlsruhe, Germany
Hoechst 33342	Life Technologies, Darmstadt, Germany
Isoflurane	AbbVie, Wiesbaden, Germany
Sodium chloride	Applichem, Darmstadt, Germany
NuPAGE MES Running Buffer 20x	Bio-rad, Hercules, CA, USA
NuPAGE Transfer Buffer 20x	Bio-rad, Hercules, CA, USA
PBS tablets	Life Technologies, Darmstadt, Germany
Penicillin/Streptomycin	Life Technologies, Darmstadt, Germany
Protease Inhibitor Cocktail	Sigma, Munich, Germany
SYBR Green PCR Master Mix	Life Technologies, Darmstadt, Germany
Sodium Dodecyl sulfate	Sigma, Munich, Germany
Triton-X 100	Sigma, Munich, Germany
Trizol	Life Technologies, Darmstadt, Germany
Trypsin-Inhibitor	Applichem, Darmstadt, Germany
Tween-20	Sigma, Munich, Germany
FITC-dextran70 kDa	Sigma, München, Germany

## 2.1.4 Buffers and solutions

Solution	Composition
2 x RIPA Buffer	50 mM Tris-HCl pH 8 3 mM Glycerolphosphate 150 mM NaCl 1% Sodiumdeoxycholate 1% NP-40 0.2% SDS 2 mM $\beta$ -Na <sub>3</sub> VO <sub>4</sub> Protease Inhibitor Cocktail
10x TAE Buffer	40 mM Tris-HCl pH 8 40mM Acetic acid 1mM EDTA-Na <sub>2</sub> -Salt
10x TBST	0.2 M Tris-HCl pH 7.6 1.37 M NaCl 80,06 g
Blocking Buffer (IFC)	3% BSA in PBS P/S 1 ml
Blocking buffer (Western blot)	5% Milk powder in TBST
FACS buffer	1% FCS in PBS 2 mM EDTA
Tissue lysis buffer (Per 1 mg tissue)	10 $\mu$ l PBS 2 mM EGTA 2 mM EDTA, Protein inhibitor Cocktail

Solution	Composition
Tissue enzyme digestion mix	1 mg/ml Collagenase II 1 mg/ml DNase 2.4 mg/ml Dispase II 1 mg/ml BSA 0.7 mg/ml Trypsin Inhibitor in PBS
Krebs-Ringer-Buffer	H <sub>2</sub> O 1000 ml 5.9 mM KCl 120 mM NaCl 11.5 mM Glucose 15.5 mM NaHCO <sub>3</sub> 6(H <sub>2</sub> O) MgCl <sub>2</sub> 0,97 ml 2(H <sub>2</sub> O) CaCl <sub>2</sub> 1,47 ml 1.4 mM NaH <sub>2</sub> PO <sub>4</sub>
Western blot running buffer	1 X running buffer (Bio-rad)
Western blot washing buffer	1 ml Tween-20 in TBST

## 2.1.5 Kits

Device	Company
BCA Assay	Thermo Scientific, MA, USA
cDNA	Life Technologies, Darmstadt, Germany
Reverse-Transcription Kit	Life Technologies, Darmstadt, Germany
RNA isolation kit	Thermo Scientific, MA, USA
Western Blot kit	Thermo Scientific, MA, USA

## 2.1.6 Antibodies

Application	Antigen	Conjugate	Isotype	Company
Flow cytometry	CD45	FITC	Mouse IgG1, $\kappa$	Biolegend
Flow cytometry	F4 / 80	PE	Rat IgG2a, $\kappa$	eBioscience
Flow cytometry	Ly6C	PE-Cy7	Rat IgG2c, $\kappa$	Biolegend
Flow cytometry	Ly6G	APC	Rat IgG2a	Miltenyi
IHC	MHCII	Unconjugated	Rat IgG2b, $\kappa$	Biolegend
IHC	TH	Unconjugated	IgG1 $\kappa$	Millipore
IHC	GFP	Unconjugated	IgY	Novus biologicals
Western blot	TH	Unconjugated	IgG1 $\kappa$	Millipore
Western blot	$\beta$ -actin	Unconjugated	IgG2a	Sigma

## 2.1.7 Primers for qPCR

Gene		Sequence
Adra1a	Fwd	TTGAAATTCGGGAAGAAGGA
	Rev	GAGAAGAAAGCCGCCAAGAC
Adra1b	Fwd	AGGCAGCTGTTGAAGTAGCC
	Rev	TCTTCATCGCTCTCCCACTT
Adra1c	Fwd	ATTGAAGTAGCCCAGCCAGA
	Rev	GCTGGTTCCCCTTTTTCTTC
Adra2a	Fwd	TCTGGTCGTTGATCTTG CAG
	Rev	CATCTCGGCTGTCATCTCCT
Adrab1	Fwd	AAGTCCAGAGCTCGCAGAAG
	Rev	GCTGATCTGGTCATGGGATT
Adrab2	Fwd	TAGCGATCCACTGCAATCAC
	Rev	ATTTTGGCAACTTCTGGTGC
Adrab3	Fwd	GGGAAGGTAGAAGGAGACG
	Rev	ACAGGAATGCCACTCCAATC

Gene		Sequence
β3 defensin	Fwd	GTTTGCATTTCTCCTGGTGC
	Rev	GCCTCCTTTCCTCAAACAAC
BMP-2	Fwd	AGACCACCGGCTGGAGAG
	Rev	TTTTCCCACTCATCTCTGGAA
CD163	Fwd	GTGCTGGATCTCCTGGTTGT
	Rev	CGTTAGTGACAGCAGAGGCA
CLD3	Fwd	GCAAGCAGACTGTGTGTCGT
	Rev	TACCGTCACCACTACCAGCA
Cldn2	Fwd	CCACAAGCAGGCTCAAGAAG
	Rev	TTCGCCTTCTCTGGACCTA
CSF-1R	Fwd	CTCTGCTGGTGCTACTGCTG
	Rev	TTGCCTTCGTATCTCTCGATG
Defa1	Fwd	CAGGCCGTATCTGTCTCCTT
	Rev	ATGACCCTTCTGCAGGTTT
IL-10	Fwd	GATGCCCCAGGCAGAGAA
	Rev	CACCCAGGGAATTCAAATGC
Lyz1	Fwd	GAGACCGAAGCACCGACTATG
	Rev	CGGTTTTGACATTGTGTTTCGC
Muc2	Fwd	TGCCCAGAGAGTTTGGAGAGG
	Rev	CCTCACATGTGGTCTGGTTG
Ocln	Fwd	CATAGTCAGATGGGGGTGGA
	Rev	ATTTATGATGAACAGCCCCC
Reg3g	Fwd	TTCCTGTCCTCCATGATCAAAA
	Rev	CATCCACCTCTGTTGGGTTCA
TFF3	Fwd	CTCTGTCACATCGGAGCAGTGT
	Rev	TGAAGCACCAGGGCACATT

## 2.1.8 Primers (Quantitect)

Gene	Assay ID
Arg-1	QT00134288
YM1/ Chi3l3	QT02241722
IL-1b	QT01048355
Retnla1/Fizz1	QT00254359

## 2.1.9 Primers (Taqman)

Gene	Assay ID
IL-6	Mm00446190_m1
GAPDH	Mm99999915_g1
iNOS	Mm00440485_m1
TNF-a	Mm00443258_m1

## 2.1.10 Mouse lines

Mouse line	Description
C57BL/6j	Janvier
CX3CR1 <sup>GFP/+</sup>	Jackson

## 2.1.11 Software applications

Software	Company
Citavi	Swiss Academic Software GmbH
FACS Diva	Canto II BD Bioscience
FlowJo 7.6.5	Tree star Inc.
Illustrator CS6	Adobe

Software	Company
Multigauge	Fujifilm
Office 2010	Microsoft
Prism 8.4.3	Graphpad
SDS2.2	Applied Biosystems
ImageJ	Open Source
Partek	Partek

## 2.2 Methods

### 2.2.1 Animals

8-10 weeks old C57BL6/J mice were used for surgical & chemical denervation, sham, and intestinal manipulation experiments. 8 weeks old CX3CR1<sup>GFP/+</sup> mice were used for cell sorting experiments. The intestinal tissue samples from TrkA<sup>ff</sup> control and TH-Cre;TrkA<sup>ff</sup> mutant mice were fixed and generously provided by Prof. Rejji Kuruvilla. The animal experiments were approved by the Ethics committee of the University Hospital of Bonn, under the animal proposal number AZ 81-02.04.2018.A221, 2018.04.02. The animal room was maintained on a 12 hour light/ dark illumination cycle, humidity (45-65%), temperature (20- 25 °C). All animals were maintained under pathogen-free conditions and the experiments were carried out according to the animal care protection federal law.

### 2.2.2 The surgical denervation procedure (sSTX)

This is an intestine-specific denervation technique to deplete sympathetic neurons (Olivier et al., 2016). By inhalation of isoflurane (3-5%, 3-5 l/min flow), mice were anesthetized and 100 µl of tramadol (85 µl NaCl, 15 µl 10 mg/kg tramadol) was subcutaneously injected few minutes before sSTX. The skin and the peritoneum were opened by making a midline incision of approximately 1 cm. The entire small bowel was taken out with the help of two sterile moist cotton swabs and placed on sterile gauze. The sympathetic plexus runs along the superior mesenteric artery (SMA), and SMA is located on the posterior end of the ganglia. The sympathetic plexus was surgically destroyed without damaging the surrounding blood vessels. This procedure takes approximately five minutes. Sham-operated mice were used as controls. For sham operation, the small bowel was taken out and rested on the sterile gauze for five minutes without destroying the sympathetic plexus. After sSTX/ sham operation, the small bowel is placed back into the abdominal cavity. By using 5.0 silk threads, the abdomen was closed by two layers of continuous sutures. Both sSTX and sham-operated mice received 1 mg/kg tramadol in the drinking water for 3 days. Two weeks after the surgery, mice were sacrificed by cervical dislocation for further analysis.

### 2.2.3 The chemical denervation procedure (cSTX)

6-Hydroxydopamine (6-OHDA) is a neurotoxin that selectively targets catecholaminergic nerve terminals (Glinka et al., 1997). Mice were randomly divided into two groups: vehicle and 6-OHDA treatment. 6-OHDA was dissolved in 0.1% L-ascorbic acid-containing sterile saline and 250  $\mu$ l of this solution was intraperitoneally (i.p) injected to mice at the dosage of (A) one-time 200 mg/kg, (B) two-times 100 mg/kg, (C) two-times 50 mg/kg or (D) three-times 80 mg/kg 6-OHDA respectively. The vehicle group was treated with sterile saline alone. Two weeks after cSTX, mice were sacrificed by cervical dislocation, and further analysis was carried out.

### 2.2.4 Cholecystokinin (CCK) test

Fine bundles of the vagal fibers run along the superior mesenteric artery, a site where we performed sSTX (Berthoud und Powley, 1996). Hence, we carried out a functional CCK test to assess vagal integrity. Animals that underwent sSTX and cSTX were used for the CCK test. cSTX/vehicle and sSTX/sham-operated mice were starved for twenty hours and were supplied with only drinking water. After twenty hours, 8  $\mu$ g/kg CCK dissolved in 0.1% L-ascorbic acid-containing sterile saline and was injected i.p. The control groups were treated with only sterile saline. All mice were caged alone and pre-weighed food was provided without the supply of drinking water. Two hours after the CCK/saline treatment, the amount of food consumed by these mice was measured.

### 2.2.5 The mouse model of non-infectious postoperative ileus

Intestinal manipulation (IM) is a standardized technique carried out as previously described (Vilz et al., 2012). This technique is used to imitate the trauma that is unavoidable during abdominal surgeries. Acute inflammation of the intestinal bowel wall is induced predominantly in the muscularis externa that peaks twenty- four hours after IM. By inhalation of isoflurane (3-5%, 3-5 l/min flow), mice were anesthetized and 100  $\mu$ l of tramadol (85  $\mu$ l NaCl, 15  $\mu$ l 10 mg/kg tramadol) was subcutaneously injected few minutes before IM. Approximately 1 cm of a midline incision was made to open the skin followed by the peritoneum. With the help of two sterile moist cotton swabs, the entire small bowel was taken out and positioned on sterile gauze. By applying moderate compression, the cotton swabs are rolled over the intestine from the duodenum to the terminal ileum. This

procedure was avoided on the mesentery to prevent intestinal bleeding. The IM was carried out two times, then the small bowel was carefully placed back into the abdominal cavity. By using 5.0 silk threads, both the peritoneum and the skin were closed by two layers of continuous sutures. The operated mice were placed under the red lamp until they are fully awake. 1 mg/kg tramadol was supplied in the drinking water for 3 days.

#### 2.2.6 Isolation of primary leukocytes from the muscularis externa

Mice were sacrificed by cervical dislocation and the small bowel was removed from the abdomen. The small bowel was approximately divided into a segment of 2-3 cms long. Each segment of the bowel is placed over a thin glass rod and the mesentery is pulled out with the tweezer. With a moist cotton swab, the muscularis externa is carefully stripped from the underlying mucosal layer. The procedure is repeated for all the segments of the small bowel. The isolated muscularis externa tissue was mechanically cut with a sharp razor blade. The cut tissue is washed off with PBS buffer and enzymatically digested for 40 minutes at 37 °C and 130 rpm in a shaking water bath. The digested cell suspension is resuspended several times and poured over a 45 µm sterile gauze. Sterile ice-cold PBS is added to the cell suspension and washed at 500 g, at 4 °C for 5 minutes. The cell pellet was resuspended in fluorescent activated cell sorting (FACS) buffer for subsequent staining procedures. The single-cell suspension was stained with CD16/32 and fluorochrome-labeled monoclonal antibodies against Ly6G, CD45, Ly6C, PE. Hoechst-33342<sup>+</sup> was used to exclude dead cells. The FACS analysis was carried out on canto I at the FACS core facility of University Hospital, Bonn, Germany. The filters used are 530/30 (FITC), 585/42 (PE), 780/60 (PE-Cy7), 660/20 (APC), and 450/50 (Hoechst).

#### 2.2.7 Gastrointestinal transit time measurement

The animals that underwent sham operation or IM (24 hours) were used to measure the GI transit time. Mice were gavaged with 100 µL of non-absorbable 70 kDa FITC-labelled dextran (6.25 mg/mL). 90 minutes after the gavage, mice were sacrificed by cervical dislocation, and the complete GI tract is taken out from the abdomen. The GI tract from the stomach to the colon was divided into 15 segments. The contents in each segment were collected separately into Eppendorf tubes containing 1 mL cold PBS. The distribution of FITC dextran in the stomach and small intestine is measured by the means of

fluorescence spectrometry at a wavelength of 488 nm. The GI transit time was calculated as the geometric center (GC) of distribution of FITC-labeled dextran with the formula:  $GC = \Sigma(\% \text{ of total fluorescent signal per segment} * \text{segment number})/100$

#### 2.2.8 Whole mounts preparation and Immunofluorescence staining

The whole-mount was prepared from segment number eight of the small bowel under a light microscope. The intestine is transferred onto a petri dish containing dissecting wax. The mesentery is pinned to this mounting plate and the bowel segment is opened exposing the lumen. The intestine is stretched, pinned in the bottom, and fixed in 4% histofix for 20 minutes. After fixing, the intestine is washed vigorously with ice-cold PBS. The mucosal layer is then carefully removed with the help of fine forceps without damaging the bottom muscle layer. After preparing the whole-mounts, they are incubated in Triton-X for 15 minutes at room temperature to facilitate the antibody penetration to the underlying cellular components. The whole-mounts are subsequently washed three times with cold PBS and blocked in buffer containing 3% BSA for 1 hour with shaking at room temperature. The whole-mounts are incubated with primary antibodies (TH and MHCII) overnight at 4 °C. The following day, the whole-mounts are washed three times with cold PBS and incubated with respective secondary antibodies for 1 hour at room temperature. The whole-mounts are washed again and mounted onto to slide and embedded with few drops of a mounting agent. The slides are allowed to dry in the dark for two days and then the images were taken on a fluorescence microscope.

#### 2.2.9 Hanker yates staining

To detect myeloperoxidase (MPO)-positive neutrophils and monocytes in the muscularis externa after an IM, Hanker Yates staining was performed. Segment number eight of the small bowel is pinned and fixed in absolute ethanol for 10 minutes at room temperature. Mucosa and submucosa were stripped, and the muscle layer was washed three times with cold PBS. Hanker Yates staining solution (1 mg/ml in 10 ml PBS and 100 µl hydrogen peroxide) was added onto the fixed muscle layer and incubated for 10 minutes at room temperature. The staining solution is poured off and washed with cold PBS. The whole-mounts are embedded with an aqueous mounting agent and coverslipped. The slides were allowed to dry for two days and MPO<sup>+</sup> cells were counted under the light microscope

at 200 X magnification in five randomly chosen areas. The calibration factor in cells per mm<sup>2</sup> (0,22 µm/px) was used for calculations.

#### 2.2.10 Flow cytometry-based cell sorting

To check the effects of STX on resident CX3CR1<sup>+</sup> muscularis macrophages, these cells were FACS-sorted and gene expression analysis was carried out. The muscularis externa tissue of three CX3CR1<sup>GFP/+</sup> mice was pooled together to achieve a higher cell yield. To exclude blood monocytes, we performed heart perfusion. Single-cell suspension was obtained from the pooled muscularis tissue. Cells were sorted based on high GFP expression with a 488 nm laser and 530/30 BP filter on the FACS Aria flow cytometer. Forward scatter area (FSC-A) versus side scatter area (SSC-A) gating was used to eliminate aggregated cell debris. Hoechst-33342<sup>+</sup> was used to exclude dead cells. The cells were sorted into FACS buffer containing 1% FCS.

#### 2.2.11 RNA isolation from sorted cells

PicoPure™ RNA Isolation Kit was used for isolating RNA from the sorted cells. The GFP<sup>+</sup> cells from CX3CR1<sup>GFP/+</sup> reporter mice were FACS-sorted into FACS buffer containing 1% FCS. The sorted cells were centrifuged at 300 g for 5 minutes and the supernatant was discarded. 100 µl of PicoPure extraction buffer was added to the cell pellet and RNA isolation procedure was carried out according to the instructions from the manufacturer. RNA concentration was measured using a nanodrop and cDNA was isolated by a High-Capacity cDNA Reverse Transcription Kit.

#### 2.2.12 RNA isolation of the complete tissue

RNA from the complete tissue was isolated by a trizol based approach. 1000 µl trizol was added to 20 mg tissue (muscularis externa or mucosa) and homogenized with the ceramic beads. Following 5 minutes of incubation at room temperature, the tissue suspension was added to 200 µl of cold chloroform. The samples were incubated for 15 minutes at room temperature and then centrifuged for 15 minutes at maximum speed. The upper transparent phase was transferred to new tubes, 500 µl Isopropanol was added and incubated for 15 minutes on ice. The samples are centrifuged for 15 minutes at maximum speed and the supernatant is discarded. The pellet is washed with 1000 µl of 70% ethanol

and centrifuged for 10 minutes at maximum speed. The washing step is repeated and the samples were vacuum dried. 30  $\mu$ l of RNase free water is added to the pellet and incubated on a thermocycler for 5 minutes at 37 °C and 550 rpm speed. RNA concentration was measured using a nanodrop and cDNA was isolated by a High-Capacity cDNA Reverse Transcription Kit.

#### 2.2.13 *Ex vivo* stimulation assay

The muscularis externa tissue of three CX3CR1<sup>GFP/+</sup> mice was pooled together and single-cell suspension was isolated as explained before. Cells were sorted on the FACS Aria flow cytometer, based on high GFP expression into FACS buffer containing 1% FCS. The sorted cells were centrifuged at 300 g for 5 minutes and the supernatant was discarded. The cell pellet was resuspended in DMEM with 10% FCS and co-cultured with either 100 ng/ $\mu$ L LPS or 100 ng/ $\mu$ L M-CSF in a 12-well plate for 3 hours at 37 °C. 1 mL sterile PBS was added to the plate and the cells were gently scraped to detach from the surface. The entire content was collected into a 50 mL falcon tube together with the media. An additional 9 mL of sterile PBS was added to the falcon tubes and the samples were centrifuged at 500 g for 5 minutes. Cell lysis and total RNA extraction of *ex vivo* LPS/M-CSF stimulated samples were carried out using PicoPure™ RNA Isolation Kit.

#### 2.2.14 Reverse transcription and quantitative real-time polymerase chain reaction (PCR)

The RNA isolated from the sorted cells or the complete muscularis tissue was reverse transcribed to cDNA by a High-Capacity cDNA Reverse Transcription Kit according to the instructions from the manufacturer. Subsequently, the cDNA synthesis was carried out in the following steps: Denaturation by heating to 110 °C, binding of the primers for 10 minutes at 25 °C, elongation for 2 hours at 37 °C, denaturation for 5 seconds at 85 °C, Cooling to 4 °C.

The real-time PCR was performed in a 384 well plate using Power SYBR green PCR master mix. Reactions were prepared as follows: 1  $\mu$ L of DNA with 5  $\mu$ L SYBR green master mix, 1  $\mu$ L quantitect primer assay (containing forward and reverse primer), and 3  $\mu$ L water. All the reactions were performed in technical triplicates. GAPDH house-keeping gene was used due to its constant expression in the muscularis. The quantification was

carried out using the  $\Delta\Delta\text{CT}$  method. Replicates that differed with more than one cycle from the other two were excluded from the analysis.

#### 2.2.15 RNA sequencing

The RNA from the muscularis externa tissue was isolated using a trizol based isolation protocol and was subjected to bulk 3' mRNA sequencing. RNA quality from each sample was checked using RNA tape-station analysis software 3.2 and the following variables were considered: RIN, 28S/18S (area), peak molarity (nmol/l), % integrated area, and concentration. The sample purity was measured using a nanodrop and the ratio was between 1.8-2.1 for A260/A280 and 2.0-2.2 for the A260/A230 for all the samples. For 3' mRNA sequencing, the expression analysis was performed with the same input concentration from all samples. Using Smart-seq2 technology, RNA-seq libraries were prepared and subjected to reverse transcription. cDNAs were amplified by HiFi DNA polymerase and quantified using Qubit. The samples were sequenced in an Illumina HiSeq 2500 at the Next Generation Sequencing Facility, University Hospital of Bonn. Using the lexogen pipeline on the Partek software, the sequencing data was analyzed. Approximately, 13 million reads were generated with an average read length of 50 base pairs. After aligning the sequences with STAR 2.5.3a and quantifying to mm 10- ensemble transcripts release, 10.5-12.5 million reads were generated of which 82% were fully within an exon.

#### 2.2.16 Western blot

Protein was isolated from the muscularis externa tissue for western blot analysis. Tissue lysis buffer was added to 20 mg muscularis tissue, and homogenized with the ceramic beads. The homogenate was diluted in 1 X RIPA buffer (10  $\mu\text{l}$  per 1 mg tissue), sonicated for 10 seconds, and placed on ice for 15 minutes. After centrifuging for 15 minutes at 4 °C, maximum speed, the supernatant was collected for BCA assay to determine the protein concentration. Before loading the samples onto the gel, they were heated with SDS loading buffer at 72 °C for 10 minutes. For gel electrophoresis, 30  $\mu\text{g}$  protein and 5  $\mu\text{l}$  protein ladder (Biorad) were loaded onto 4-20% gradient gels and run for 36 minutes at 180 V. The gel was transferred onto PVDF membrane using the fast transfer system 25 V, 1.3 A, 7 minutes. The membrane was blocked with 5% milk powder dissolved in TBST

and 1% Penicillin/Streptomycin for 1 hour at room temperature. After blocking, the membranes were incubated with primary rabbit TH antibody (1:1000 dilution in 5% skimmed milk), and mouse actin antibody (1:10000 dilution in 5% skimmed milk) overnight at 4 °C. The following day, the membrane was washed three times with TBST and incubated with horse-radish peroxidase (HRP) coupled secondary antibody for 1 hour at room temperature. After washing, the chemiluminescent substrate was added onto the membrane and incubated for 5 minutes in the dark. The TH and actin bands were detected on the Bio-rad protein imaging system.

#### 2.2.17 Fluorescence microscopy

Images were acquired using a Nikon (TE2000) fluorescence microscope and analyzed with ImageJ 1.47 v.

#### 2.2.18 Statistical analysis

The statistical analysis was performed with Graphpad Prism version 8.4.3 software. The values are expressed as mean  $\pm$  SEM (standard error of mean) and the significance was assessed using an unpaired t-test, one-way or a two-way multiple comparison ANOVA test. The significance levels were indicated as  $p \leq 0.05$  (\*),  $p \leq 0.01$  (\*\*), and  $p \leq 0.001$  (\*\*\*).

### 3. Results

3.1 Sympathetic denervation modulates resident muscularis macrophage inflammatory response upon intestinal manipulation and reduces postoperative symptoms in mice

The majority part of this thesis is already published as a paper titled “Sympathetic Denervation Alters the Inflammatory Response of Resident Muscularis Macrophages upon Surgical Trauma and Ameliorates Postoperative Ileus in Mice” in the International Journal of Molecular Sciences.

#### 3.1.1 Selection of the sympathetic denervation approach

To address the role of SNS in homeostasis and intestinal inflammation, we aimed to abolish SNS functions in the gut. To this end, we validated the effectiveness of three different STX procedures to deplete tyrosine hydroxylase (TH)<sup>+</sup> sympathetic neurons in the gut.

##### 3.1.1.1 The genetic approach (gSTX)

We first tested a genetic approach by using TH-Cre;TrkA<sup>ff</sup> mutant mice. The genotyping of these mice was performed by PCR analysis (**Figure 7A**) and fixed intestinal tissue from these mice was generously provided by the group of Rejji Kuruvilla. This approach targets *TrkA*, an essential gene that supports the survival of sympathetic neurons. Crossbreeding of TrkA floxed with TH-Cre recombinase expressing mice resulted in TH-Cre;TrkA<sup>ff</sup> mutant mice lacking the TrkA protein in sympathetic neurons. These mice were previously shown to have a complete loss of sympathetic neurons in the pancreas (Borden et al., 2013). To check for successful STX, we performed intestinal whole-mount immunofluorescence stainings for TH, an exclusive marker for sympathetic neurons. We used three months old TrkA<sup>ff</sup> control and TH-Cre;TrkA<sup>ff</sup> mutant mice to compare the expression of TH<sup>+</sup> neurons in the small intestinal muscularis externa whole mounts. Interestingly, we did not observe any difference in the TH expression between *TrkA*<sup>ff</sup> and TH-Cre;TrkA<sup>ff</sup> mutant mice in these whole mounts (**Figure 7B**). This shows that the genetic approach with TH-Cre;TrkA<sup>ff</sup> mutant mice is not efficient in eliminating TH<sup>+</sup> sympathetic neurons in the small bowel muscularis externa.

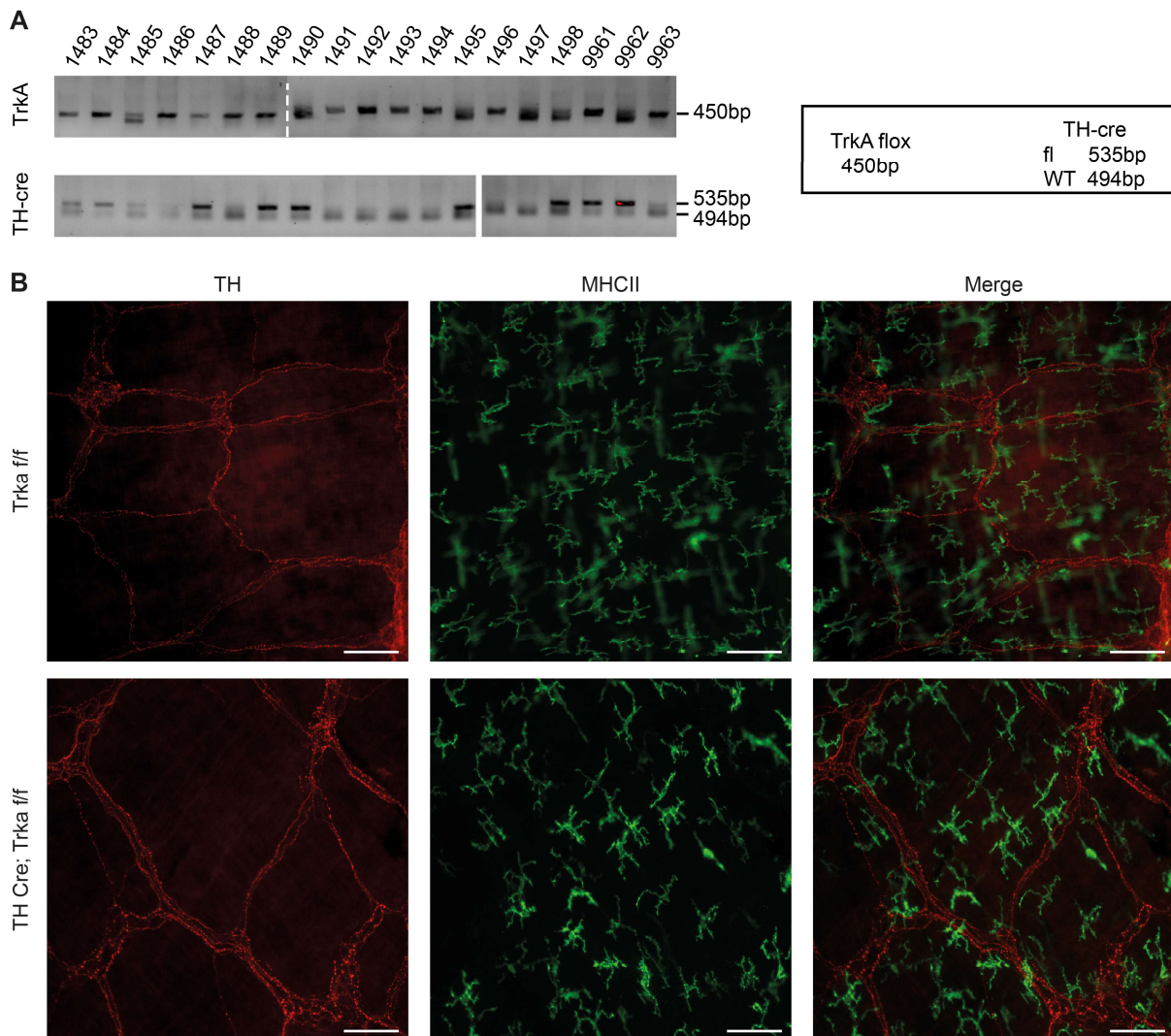


**Figure 7: A genetic SNS denervation approach relied on a TH-Cre driver line**

(A) The DNA gel showing genotyping of TH-Cre (450bp) and TrkA flox (fl- 535bp, wt- 494bp) mice. (B) Immunofluorescence of TH (red) and MHCII (green) showing no difference in the TH<sup>+</sup> fibers between TH-Cre;TrkA<sup>fl/fl</sup> mutant and control TrkA<sup>fl/fl</sup> mice in the ileal muscularis externa. Selective depletion of TrkA did not abolish TH<sup>+</sup> fibers in the small bowel muscularis whole-mount specimens. Scale bars, 100  $\mu$ m

### 3.1.1.2 The surgical approach (sSTX)

The second tested STX approach is intestine-specific, surgically applied, and was performed in C57BL/6j mice. The SNS innervating the small bowel runs along the superior mesenteric artery and was surgically destroyed as described before (Olivier et al., 2016; Willemze et al., 2019). Two weeks after this sSTX procedure, we performed immunofluorescence stainings for TH from ileal whole mounts (**Figure 8A**).

We observed an effective ablation of TH expressing nerve fibers in sSTX mice as compared to sham-operated mice (**Figure 8B**). In conclusion, sSTX was shown to be efficient in eliminating small bowel SNS innervation in the GI tract.

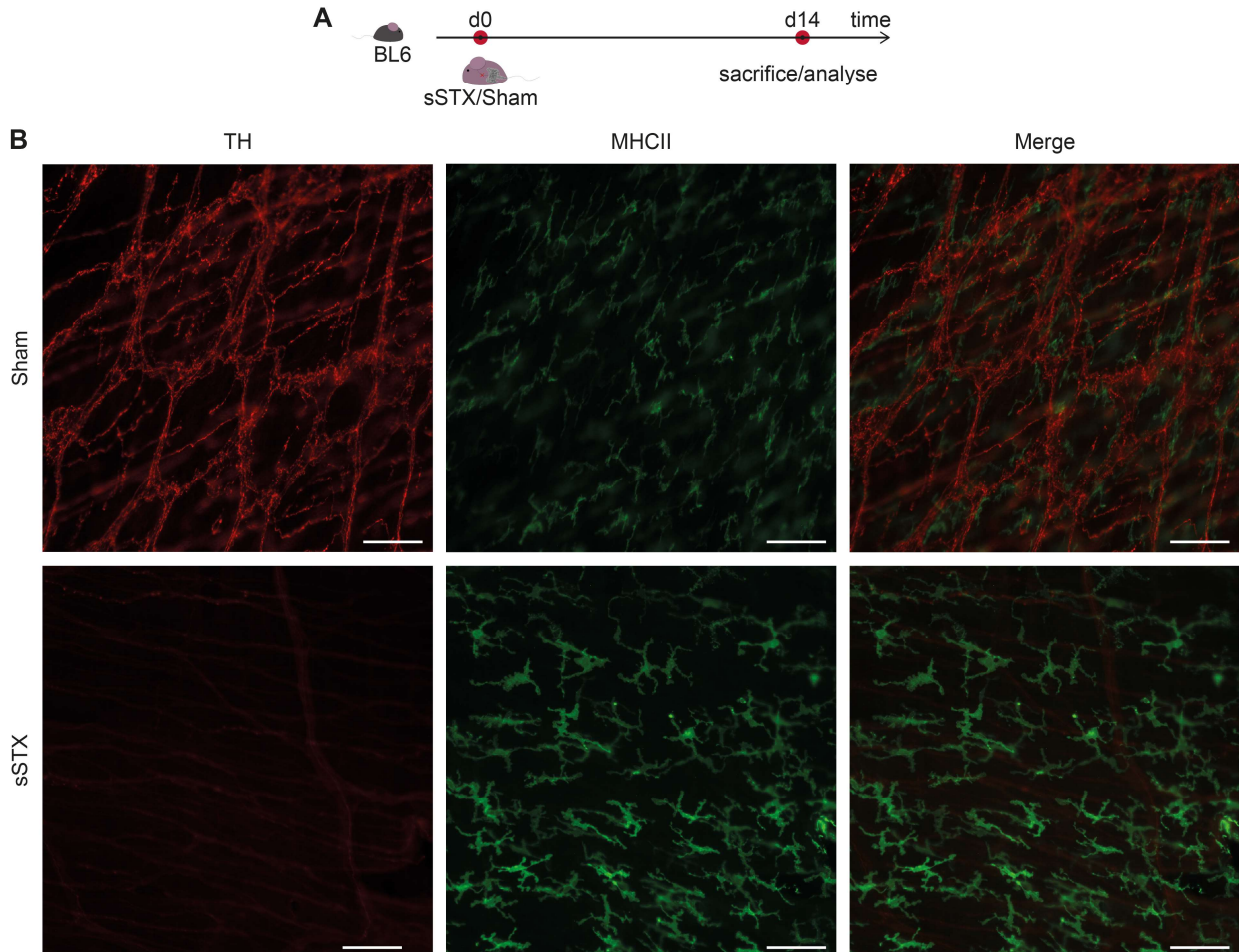


**Figure 8: A surgical SNS denervation approach that is intestine-specific.**

(A) The experimental setting for the surgical approach (sSTX). Animals underwent sSTX or sham operation and were allowed to recover for two weeks. Whole-mount immunofluorescence staining was carried out for TH (red) and MHCII (green). (B) Profound loss of TH<sup>+</sup> fibers in the ileum whole mounts of mice that underwent sSTX at the level of superior mesenteric artery compared to the sham-operated mice. Scale bars, 100  $\mu$ m

### 3.1.1.3 The chemical approach (cSTX)

As a third approach, we used the neurotoxin 6-hydroxydopamine hydrobromide (6-OHDA) that selectively degenerates noradrenergic nerve terminals (Eaker et al., 1988; Cohen et al., 1976). Several studies have already used different concentrations of 6-OHDA to deplete sympathetic neurons in their animal models (Willemze et al., 2019; Zheng et al., 2017; Pellegrini et al., 2020). To find the most effective concentration for our studies, we

tested four different dosages of (A) two-times 50 mg/kg or (B) two-times 100 mg/kg during two consecutive days or (C) one-time 200 mg/kg, or (D) three-times 80 mg/kg 6OHDA. We speculated that injecting a single high dose of 6-OHDA might be harmful to the animals or cause systemic side effects. Therefore, we gave a repetitive injection of low dosages. 6-OHDA was injected intraperitoneally in C57BL/6j mice and two weeks after this treatment, we performed TH immunofluorescence staining from ileal muscularis whole-

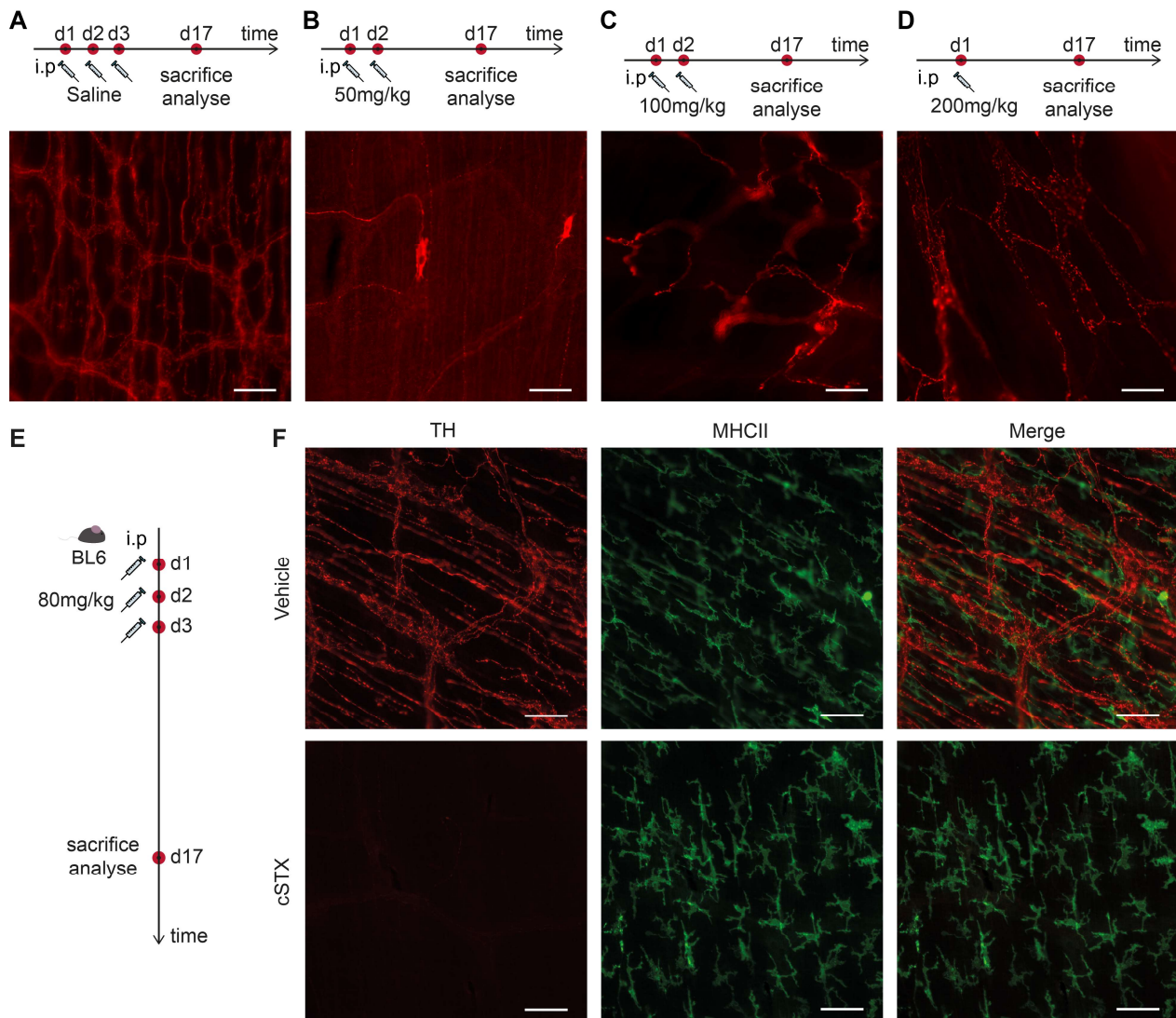


**Figure 9: Selection of the right dosage for the chemical SNS denervation approach**

(A-D) Immunofluorescence of ileal muscularis externa whole mounts showing some positive TH+ fibers two weeks after treating mice with two-times 50 mg/kg (B), two-times with 100 mg/kg (C), and a single dose of 200 mg/kg 6-OHDA (D) compared to the vehicle-treated mice (A). (E) The experimental setting for the chemical approach (cSTX) with 80mg/kg 6-OHDA for three consecutive days. (F) Representative whole mounts images showing profound loss of TH+ fibers in the ileum whole mounts of mice two weeks after cSTX as compared to the vehicle-treated mice. Scale bars, 100  $\mu$ m

mounts. The dosage of 50, 100, or 200 mg/kg was ineffective in ablating all TH<sup>+</sup> neurons (Figure 9B-D), as we still observed some positive fibers for TH in the muscularis whole-mounts compared to vehicle-treated mice (Figure 9A). However, two weeks after the three-times 80 mg/kg 6-OHDA treatment (Figure 9E), we observed a profound loss of TH<sup>+</sup>

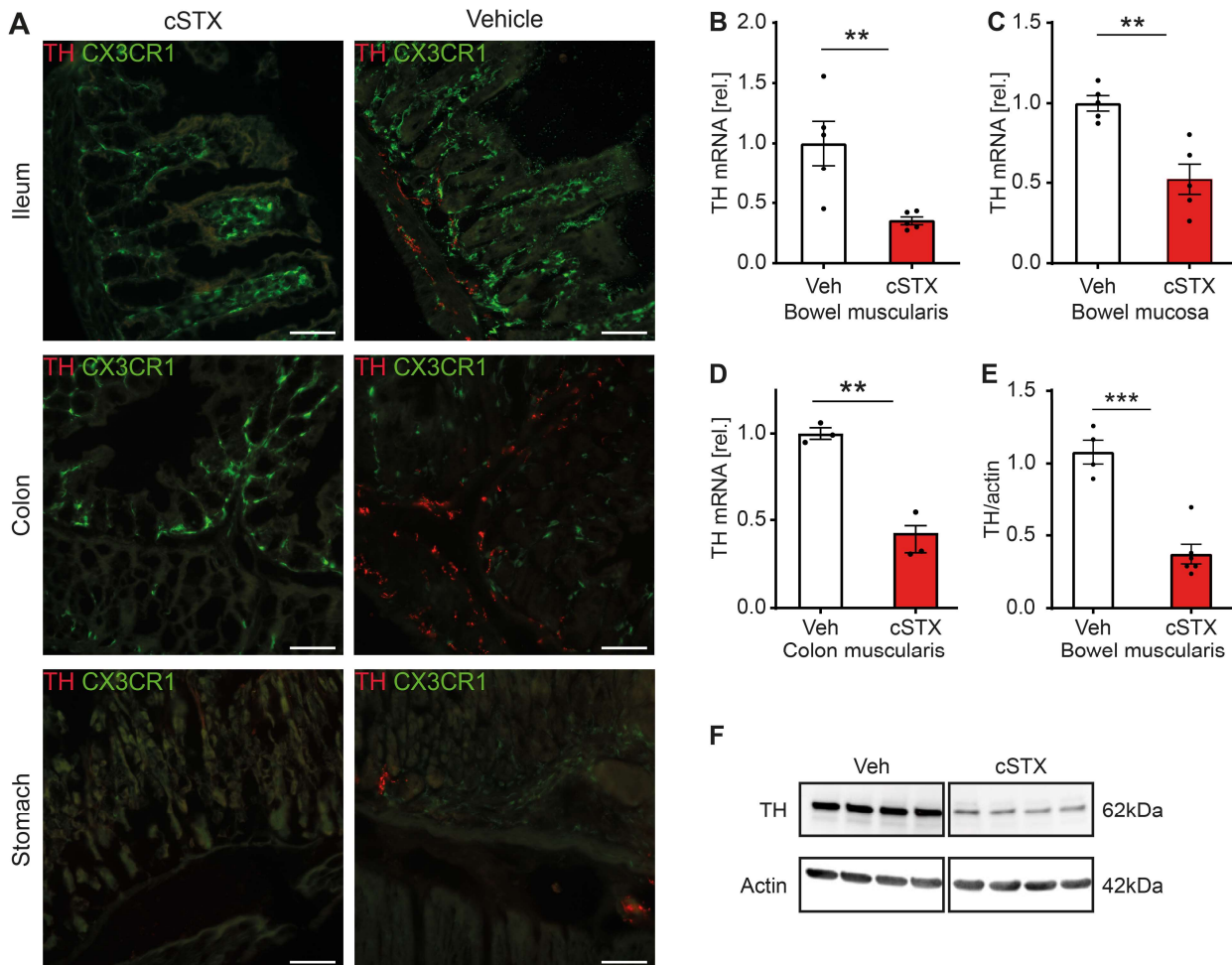


**Figure 10: 6-OHDA approach depletes TH<sup>+</sup> neurons in the GI tract**

(A) Representative histological sections of 6-OHDA-treated mice showing profound loss of TH<sup>+</sup> sympathetic neurons in the terminal ileum (bottom left), terminal colon (bottom middle), and stomach (bottom right) compared to the vehicle-treated mice. Scale bars, 100  $\mu$ m. (B-D) qPCR analysis of small intestinal muscularis externa (B), small intestinal lamina propria (C), and colon muscularis (D) of cSTX-treated mice showing the downregulation of TH (red bar) as compared to the vehicle-treated mice (white bar). (E) Representative western blot image of cSTX-treated mice showing a reduction in TH protein bands compared to vehicle-treated mice. (F) Quantification of the TH protein in cSTX-treated mice showing reduced protein levels (red bar) compared to the vehicle-treated mice (white bar). The graphs are normalized to actin protein bands and are plotted as mean  $\pm$  SEM. The statistical analysis was carried out by unpaired t-test (\* $p$ <0.05, \*\* $p$ <0.01, and \*\*\* $p$ <0.001).

sympathetic fibers in the ileal muscularis whole mounts compared to vehicle-treated mice (**Figure 9F**). Histological sections of the stomach, terminal ileum, and colon also showed a complete loss of these TH<sup>+</sup> neurons in 6OHDA-treated mice (**Figure 10A**).

Consistently, the TH mRNA levels in the small intestinal muscularis externa (**Figure 10B**), lamina propria mucosa (**Figure 10C**), and colon muscularis (**Figure 10D**) specimens were reduced in 6-OHDA treated mice. The TH protein levels were also reduced in small intestinal muscularis further confirming the elimination of TH<sup>+</sup> sympathetic neurons in 6-OHDA treated mice (**Figure 10E-F**). Together, chemical denervation with a dosage of three times 80 mg/kg was shown to be efficient in eliminating all TH<sup>+</sup> sympathetic neurons in the GI tract.

In addition, we also checked if it was possible to maintain a long-term STX. Subsequently, we injected mice with a triple dosage of 80 mg/kg 6-OHDA and two weeks later, a single dose of 80 mg/kg 6-OHDA was injected for every ten days after that. Two months after 6-OHDA treatment, we performed immunofluorescence staining for TH from ileal whole mounts. We observed a complete loss of TH<sup>+</sup> nerve fibers in cSTX-treated (**Figure 11B**) compared to vehicle-treated mice (**Figure 11A**). This shows that 80 mg/kg 6-OHDA for three consecutive days is efficient in depleting all TH<sup>+</sup> sympathetic neurons and the denervation lasts at least two months after this treatment.

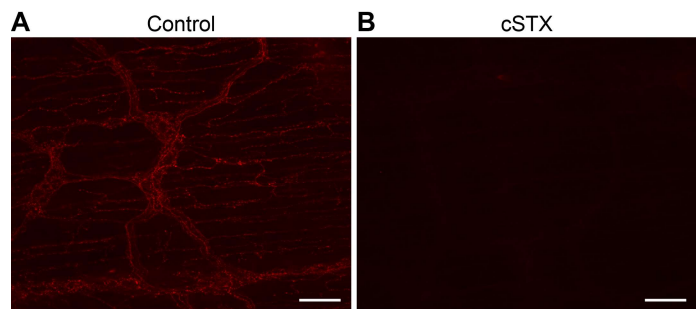


**Figure 11: cSTX of TH<sup>+</sup> sympathetic neurons in the gut 60 days after 6-OHDA treatment**

(A-B) Representative images of TH immunofluorescence showing complete loss of TH<sup>+</sup> sympathetic neurons in ileum muscularis whole mounts of cSTX-treated (B) compared to the vehicle-treated mice (A). Scale bars, 100  $\mu$ m

3.1.2 Selection of the STX approach targeting only sympathetic but not parasympathetic neurons.

Surgical and chemical STX were both efficient in depleting TH<sup>+</sup> sympathetic neurons in the GI tract. We next asked, if these two STX models only target sympathetic and/or also parasympathetic vagal neurons. Some vagal nerve fibers run as fine bundles of vagal

afferents along the superior mesenteric ganglion where we performed the sSTX procedure (Berthoud und Powley, 1996).

To test this hypothesis, we performed a functional indirect test based on the induction of satiety via cholecystokinin (CCK) as there are no direct markers, i.e. exclusive histological markers available to detect the vagus nerve integrity. Known as the peptide hormone of the GI tract, CCK, has a stimulatory effect on the vagus nerve and induces satiety when administered intraperitoneally to mice (Ghia et al., 2007). Consequently, mice with intact vagus nerve signaling will eat less food after CCK injection, while mice with disturbed vagus nerve signaling will eat significantly more food. Therefore, we analyzed the effect of CCK on both surgically and chemically sympathectomized mice. We divided the groups into vehicle/6-OHDA, or Surgery/sham-operated mice treated with NaCl/CCK (**Figure 12A**).

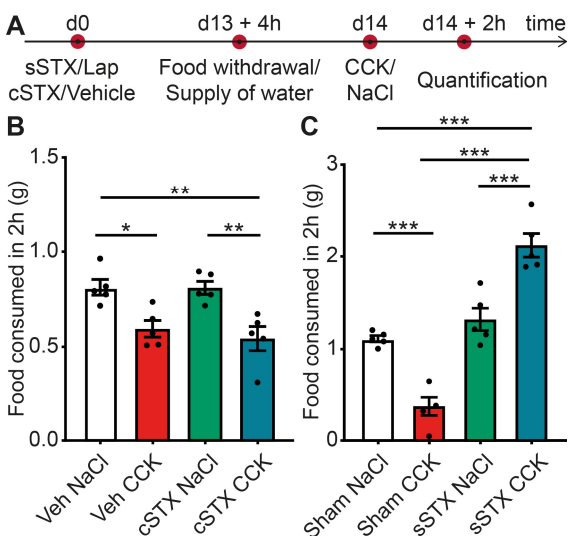


**Figure 12: Selection of the denervation approach targeting only sympathetic neurons.**

(A) The experimental setting for the CCK test. (B) cSTX-treated mice injected with CCK showing a significant reduction in food intake indicating intact vagus nerve signaling. (C) Surgically denervated mice injected with CCK showed a significant increase in food uptake as compared to sham-operated mice. Values in each column (B) and (C) are shown as mean  $\pm$  SEM and statistical analysis was carried out by two-way ANOVA (\* $p < 0.05$ , \*\* $p < 0.01$ , and \*\*\* $p < 0.001$ ).

The vehicle-treated mice injected with 8  $\mu\text{g}/\text{kg}$  CCK showed a reduced food intake (-40%) compared to the NaCl-treated mice. Similarly, cSTX-treated mice injected with CCK also showed a decreased food intake (-40%) compared to the vehicle-treated mice (**Figure 12B**) indicating that upon chemical denervation, the vagal signaling is still intact. In the sSTX experiment, sham-operated mice injected with CCK consumed less food (-70%) than NaCl-treated mice (**Figure 12C**). However, in the surgically-denervated group, the effect of CCK was attenuated as displayed by the increased food intake (+50%) showing disturbed vagal signaling. Together, we conclude that sSTX disturbs the vagal innervation whereas the cSTX with 6-OHDA only targets sympathetic neurons. Consequently, during

all subsequent experiments, we used the chemical approach to deplete the sympathetic neurons.

The first objective of this thesis was to find a suitable STX model. Of all the models we tested, three times 80 mg/kg 6-OHDA was the most appropriate.

### 3.1.3 Selection of the treatment time point

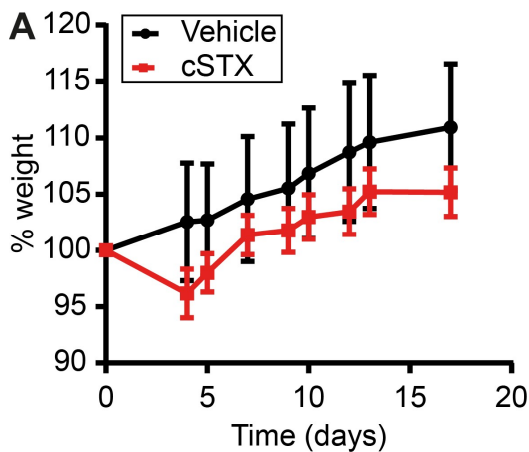


**Figure 13: Bodyweight measurement after the treatment with 6-OHDA**

(A) Weight curve of 6-OHDA (cSTX group) and vehicle-treated mice. No weight loss was observed upon 6-OHDA treatment

After selecting 6-OHDA as the procedure to deplete sympathetic neurons, we confirmed whether the treatment time point was suitable for further analysis. First, we measured the body weight of the cSTX-treated mice to check if cSTX induces weight loss or any other clinical signs as this could have a crucial impact on further analysis. cSTX-treated mice did not show weight loss after the i.p injection of 6-OHDA compared to the vehicle-treated mice (**Figure 13A**). An overall assessment of cSTX-treated mice to check if they were in pain or distress identified no signs of hunched back, squinted

eyes, restlessness, agitation, not drinking, not eating, violent reaction, or sizeable abdominal mass in the cSTX-treated animals indicating all these animals were well-conditioned.

Since 6-OHDA induces cell death of sympathetic neurons, we hypothesized that this treatment might recruit immune cells into the muscularis for clearance of dying neurons. To answer this, we treated mice with either 6-OHDA or saline and analyzed the infiltrating CD45<sup>+</sup> leukocyte cell population at multiple time points by flow cytometry (**Figure 14A**). We identified three distinct subpopulations of CD45<sup>+</sup> cells by Ly6C<sup>+</sup>, F4/80<sup>+</sup>, and Ly6G<sup>+</sup> staining. These CD45<sup>+</sup> leukocytes were defined as F4/80<sup>+</sup> macrophages, Ly6C<sup>+</sup> Ly6G<sup>-</sup> monocytes, and Ly6C<sup>+</sup> Ly6G<sup>+</sup> neutrophils. The gating strategy is based on singlets and living CD45<sup>+</sup> cells (**Figure 14B**). Hoechst was used to exclude dead cells.

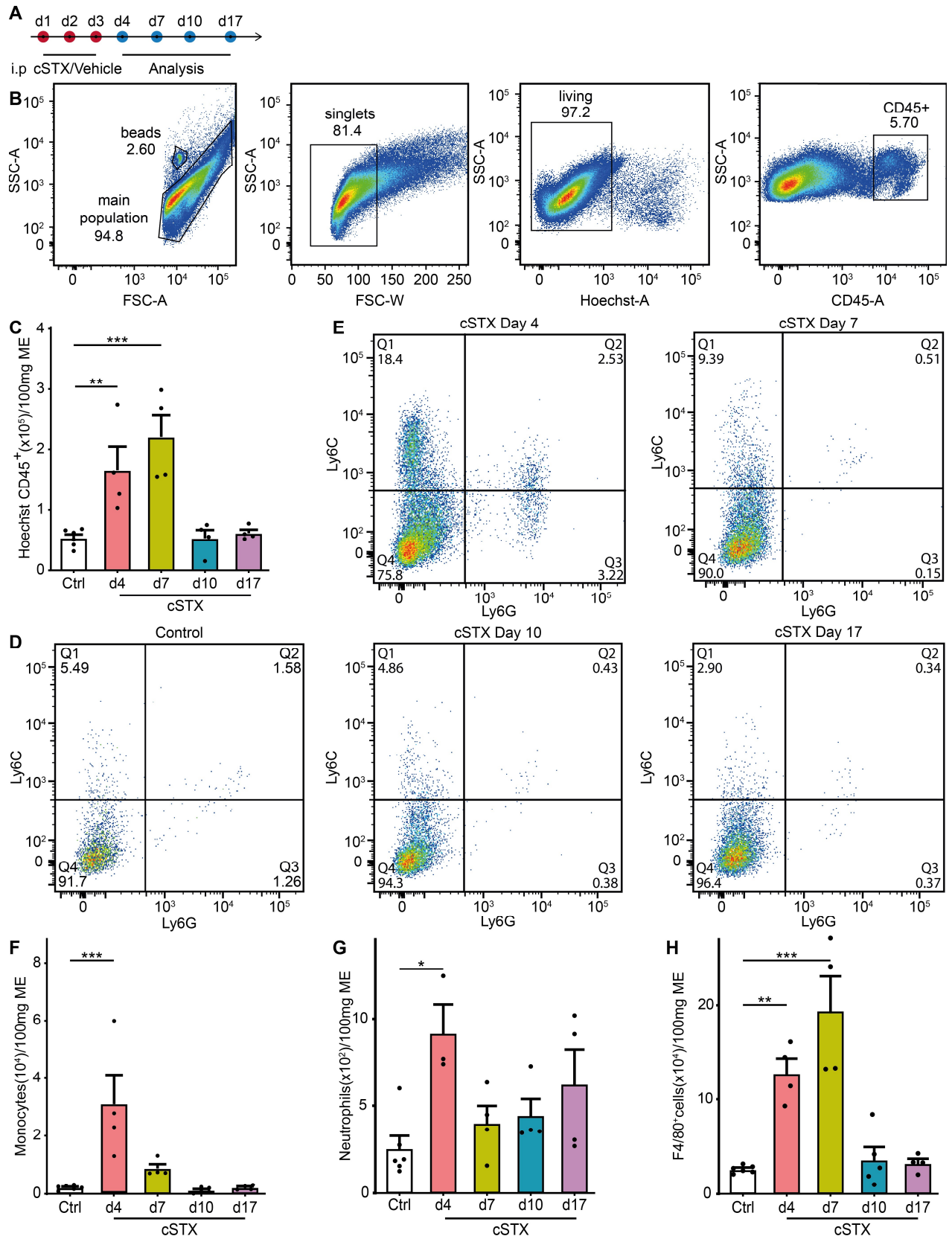


### Figure 14: Leukocyte immune cell infiltration into muscularis upon cSTX-treatment

(A) Timeline for analyzing leukocyte immune cell infiltration into muscularis externa at multiple time points after the treatment with 6-OHDA. (B) Representative FACS dot plots showing the gating strategy of the main population, singlets, living dead exclusion, and CD45<sup>+</sup> cells in the muscularis externa. (C) Quantification of Hoechst- CD45<sup>+</sup> leukocytes upon cSTX-treatment as compared to vehicle-treated mice. (D-E) Representative FACS dot plots showing the ratio of Ly6C<sup>+</sup> Ly6G<sup>-</sup> monocytes, Ly6C<sup>+</sup> Ly6G<sup>+</sup> neutrophils of control (D) and cSTX-treated mice (E) at day 4, 7, 10 and 17. (F-H) Quantification of bar graphs showing the absolute numbers of total Ly6C<sup>+</sup> Ly6G<sup>-</sup> monocytes (F), Ly6C<sup>+</sup> Ly6G<sup>+</sup> neutrophils (G) and F4/80<sup>+</sup> macrophages (H) isolated from muscularis externa upon cSTX as compared to vehicle-treated mice at day 4, 7, 10 and 17. Values in each column is shown as mean  $\pm$  SEM and statistical analysis was carried out by ordinary one-way ANOVA test (\* $p < 0.05$ , \*\* $p < 0.01$  and \*\*\* $p < 0.001$ ) comparing vehicle-sorted macrophages versus indicated groups.

On day four, upon 6-OHDA treatment, the total numbers of CD45<sup>+</sup> leukocytes in the muscularis were significantly higher (3-fold) (**Figure 14C**), indicating that immune cells infiltrate into the muscularis. At this time point, compared to vehicle-treated mice (**Figure 14D**), we detected significantly higher levels of Ly6C<sup>+</sup> Ly6G<sup>-</sup> monocytes (12-fold) (**Figure 14E, F**), Ly6C<sup>+</sup> Ly6G<sup>+</sup> neutrophils (3.5-fold) (**Figure 14E, G**), and F4/80<sup>+</sup> macrophages (5-fold) (**Figure 14H**). On day seven, we also observed an increase in the total numbers of CD45<sup>+</sup> leukocytes upon cSTX-treatment. However, the level of monocytes and neutrophils already decreased, while F4/80<sup>+</sup> cells (8-fold) slightly increased. On days 10 and 17 upon cSTX-treatment, the numbers of neutrophils, monocytes, and F4/80<sup>+</sup> macrophages all completely returned to control levels. Subsumed, cSTX treatment induces a transient inflammation in the intestinal muscularis that is self-limiting and resolves within ten days. Due to this transient inflammation, we waited for 17 days after cSTX to avoid any side effects that might affect the further analysis.

#### 3.1.4 Changes in the muscularis externa upon cSTX

After selecting a suitable time point for the STX approach, we next aimed to check general changes in the muscularis externa upon cSTX. For this, we first established a transcriptional profile by 3' bulk RNA sequencing to describe the molecular effects of the cSTX in the intestinal muscularis. This analysis was carried out on day 17 when the transient peri-interventional inflammation in the muscularis externa was resolved for at least seven days after 6-OHDA or saline treatment. 23681 genes were obtained after

normalization with the standard CPM method and principal component analysis (PCA) was plotted. Further filtering using p-value ( $\geq 0.05$ ) and false-discovery rate (FDR) fold change ( $\pm 2$ ) gave a total of 1740 genes which were then used for gene enrichment pathway analysis. PCA showed that the vehicle and cSTX-treated samples clustered into two different axes (**Figure 15A**). The functional enrichment analysis on 1740 differentially expressed genes for immune-related gene ontology (GO) terms showed “*defense response, inflammatory response, immune response, positive regulation of inflammatory*

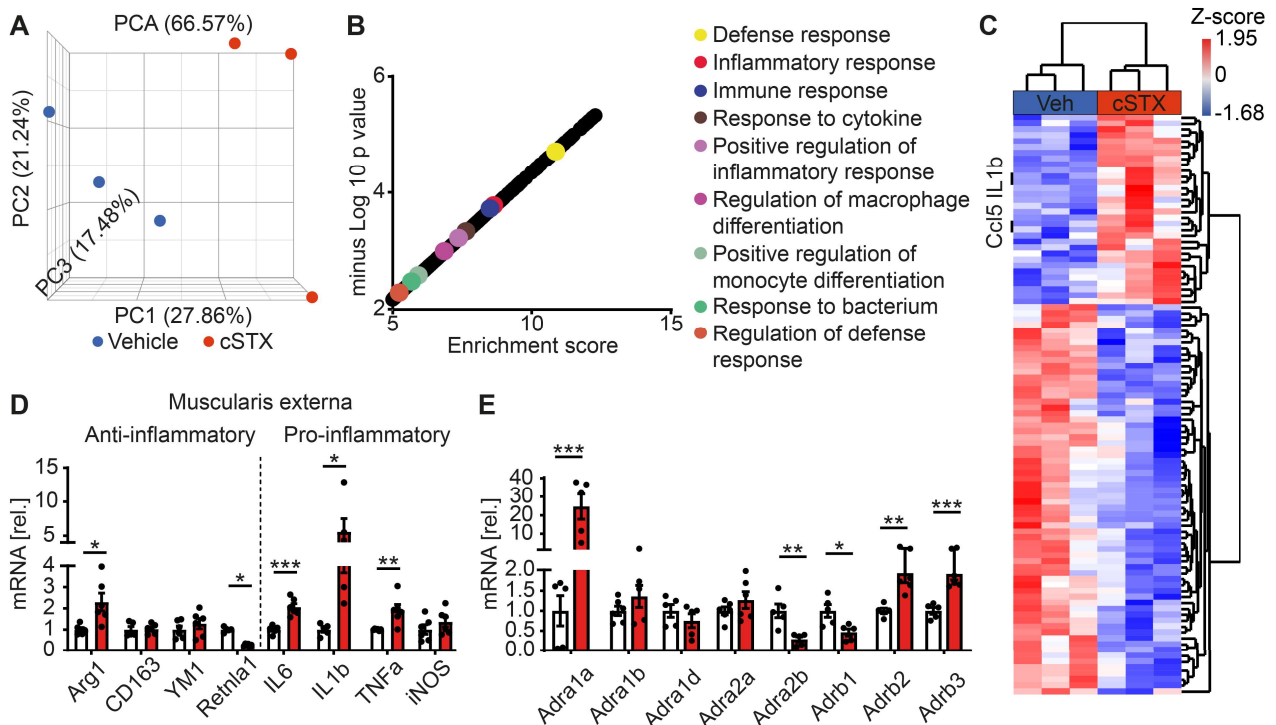


**Figure 15: RNA sequencing of the vehicle and cSTX-treated muscularis externa samples**

Mice underwent cSTX/vehicle treatment and two weeks later RNA was isolated from the whole muscularis externa tissue, and subjected to 3' bulk RNA sequencing. (A) PCA plot showing the clustering of bulk RNA sequencing specimens from muscularis externa of the vehicle and cSTX-treated mice. (B) Functional enrichment of differentially expressed genes ( $p < 0.05$ , fold change  $\pm 2$ ) showing immune-related GO terms upon cSTX. (C) Hierarchical clustering of the GO term “*inflammatory response*” between vehicle and cSTX-treated mice showing an increase in *IL-1b* upon cSTX. (D) qPCR analysis of cSTX-treated mice (red) showing the levels of pro and anti-inflammatory genes in the muscularis externa as compared to vehicle-treated mice (white). (E) qPCR analysis showing the expression of different adrenergic receptors in the muscularis externa of vehicle (white) and cSTX-treated mice (red). Values in each column are shown as mean  $\pm$  SEM and statistical analysis was carried out by unpaired t-test (\* $p < 0.05$ , \*\* $p < 0.01$  and \*\*\* $p < 0.001$ ) comparing vehicle-treated groups versus indicated groups.

*response and response to cytokines*” enriched upon cSTX (**Figure 15B**). This shows that the basic immune state of the muscularis is altered after cSTX. Notably, the hierarchical clustering of the GO term “*inflammatory response*” showed an increase in Interleukin 1 beta (*IL-1 $\beta$* ) and other inflammatory markers upon cSTX (**Figure 15C**). Therefore, by qPCR, we analyzed the expression of classical pro-inflammatory genes that were shown to be modulated during acute inflammation of the muscularis externa (Stein et al., 2018). In cSTX-treated mice, we detected higher expression of pro-inflammatory genes such as Interleukin-6 [*IL6* (2-fold)], *IL-1 $\beta$*  (10-fold), and Tumor necrosis factor-  $\alpha$  [*TNF- $\alpha$*  (2-fold)] compared to the vehicle-treated mice (**Figure 15D**). Furthermore, the anti-inflammatory genes Cluster of Differentiation 163 (*CD163*) and chitinase-like protein 3 (*Chil3/YM1*) levels were comparable between both groups. The Resistin-like alpha precursor (*Retnla1*) level (-75%) was downregulated while Arginase-1 [*Arg1* (1.2-fold)] was upregulated in the cSTX-treated mice. In addition, mRNA levels of a set of adrenergic receptor expression genes alpha-1A adrenergic receptor (*Adra1a*), alpha-1B adrenergic receptor (*Adra1b*), alpha-1D adrenergic receptor (*Adra1d*), alpha-2A adrenergic receptor (*Adra2a*), alpha-2B adrenergic receptor (*Adra2b*), beta-1 adrenergic receptor (*AdrB1*), beta-2 adrenergic receptor (*AdrB2*), and beta-3 adrenergic receptor (*AdrB3*) were also altered (**Figure 15E**) indicating that cSTX affects intestine also on the receptor level expression of NE, its principal neurotransmitter. The broad changes in adrenoceptor gene expression indicate that several cell types are affected by cSTX. Taken together, these data suggest that upon cSTX, the basal immunological gene expression profile of the muscularis externa is shaped towards a pro-inflammatory rather than anti-inflammatory pattern and a missing innervation by the SNS distinctly affects adrenergic receptor expression.

### 3.1.5 Distinct changes in CX3CR1<sup>+</sup> muscularis macrophages upon cSTX

Tissue-resident CX3CR1<sup>+</sup> macrophages lay in proximity to the TH<sup>+</sup> sympathetic neurons in the muscularis externa, and some studies have reported the involvement of adrenergic signaling on the macrophage differentiation stage (Gabanyi et al., 2016). Therefore, we hypothesized that the altered basal muscularis immune state after sympathetic denervation could be due to the altered activation state of macrophages. To test this hypothesis, we used CX3CR1<sup>GFP/+</sup> reporter mice and FACS-sorted all Hoechst<sup>+</sup> CX3CR1<sup>+</sup>

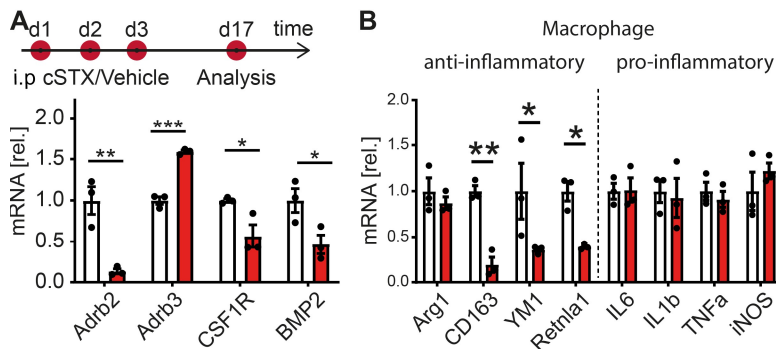


**Figure 16: Changes on resident CX3CR1<sup>+</sup> macrophages upon cSTX**

(A) Timeline showing the experimental setup for sorting CX3CR1<sup>+</sup> muscularis macrophages upon cSTX. (B-C) qPCR analysis of sorted macrophages from cSTX-treated mice (red) showing the levels of macrophage receptors and cytokines (B) and the mRNA expression of different pro and anti-inflammatory genes (C) in the muscularis externa compared to the vehicle-treated mice (white). Values in each column are shown as mean  $\pm$  SEM and statistical analysis was carried out by unpaired t-test (\* $p < 0.05$ , \*\* $p < 0.01$  and \*\*\* $p < 0.001$ ) comparing vehicle-sorted macrophages versus indicated groups.

75%), *YM1* (-50%), and *Retnla1* (-60%) and no changes in *Arg1* upon cSTX on this individual cellular level (**Figure 16C**). However, the pro-inflammatory genes *IL6*, *IL-1 $\beta$* , *TNF- $\alpha$* , and inducible nitric oxide synthase (*iNOS*) did not change upon cSTX. This shows that cSTX dampens the expression of macrophage anti-inflammatory genes while their pro-inflammatory cytokine profile remains unaltered.

### 3.1.6 *Ex vivo* stimulation of CX3CR1<sup>+</sup> muscularis macrophages with LPS/M-CSF

Since we observed an altered macrophage anti-inflammatory profile upon cSTX, we speculated that sympathetic neuronal loss might dampen the ability of intestinal CX3CR1<sup>+</sup> muscularis macrophages to induce anti-inflammatory genes. We tested this hypothesis using an *ex vivo* setup wherein we FACS-sorted CX3CR1<sup>+</sup> muscularis macrophages 17 days after saline or 6-OHDA treatment and stimulated these sorted cells with either M-CSF or LPS for three hours at 37 °C (**Figure 17A**). This assay shows alterations in the CX3CR1<sup>+</sup> macrophage anti- or pro-inflammatory responses induced by M-CSF or LPS. However, our preliminary experiments showed that due to the extreme digestion and

cells 17 days after saline or 6-OHDA treatment (**Figure 16A**). The sorted CX3CR1<sup>+</sup> muscularis macrophages from cSTX-treated mice showed significantly lower levels (-80%) of *Adrb2* ( $\beta_2$  adrenergic receptor), *CSF-1R* (-40%, macrophage colony receptor-1), *BMP-2* (-50%, bone morphogenetic protein-2) and higher levels (1.5-fold) of *Adrb3* ( $\beta_3$  adrenergic receptor) (**Figure 16B**).

Notably, we also observed a reduction in the anti-inflammatory genes *CD163* (-

FACS-sorting procedures, the unstimulated cells were unable to survive for three hours. Hence, we excluded the groups that were stimulated neither with LPS nor with M-CSF from our analysis.

Upon LPS stimulation, we detected comparable levels of *IL-1 $\beta$*  and *TNF- $\alpha$*  in sorted macrophages of the vehicle and cSTX-treated groups. We observed a slight increase in

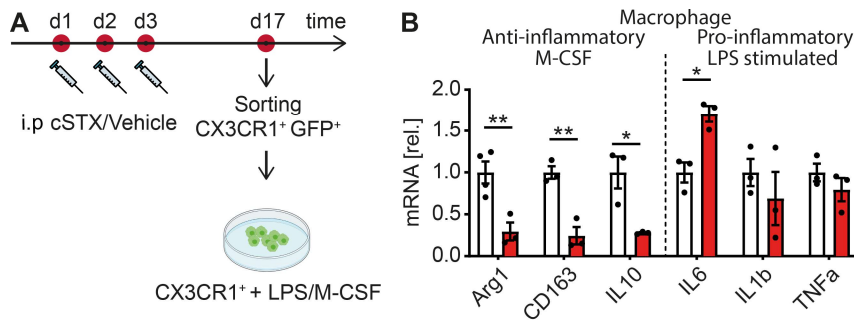


**Figure 17: Resident CX3CR1<sup>+</sup> macrophage anti- and pro-inflammatory gene response upon stimulation with M-CSF/LPS**

(A) Timeline showing the experimental setup for *ex vivo* M-CSF or LPS stimulation of sorted CX3CR1<sup>+</sup> muscularis macrophages from the vehicle and cSTX-treated mice. (B) qPCR analysis of sorted CX3CR1<sup>+</sup> macrophages from vehicle (white) and cSTX-treated mice (red) stimulated with M-CSF/LPS showing the levels of anti- and pro-inflammatory genes. Values in each column are shown as mean  $\pm$  SEM and statistical analysis was carried out by unpaired t-test (\* $p < 0.05$ , \*\* $p < 0.01$  and \*\*\* $p < 0.001$ ).

*IL6* gene expression in the cSTX sorted macrophages. In contrast, upon stimulation with M-CSF, the anti-inflammatory genes *Arg1*, *CD163*, and Interleukin 10 (*IL-10*) were dominantly reduced in cSTX-sorted macrophages (Figure 17B). Taken together, our findings show that genes associated with an anti-

inflammatory status of CX3CR1<sup>+</sup> macrophages were less reduced while the macrophage pro-inflammatory profile was only slightly affected upon sympathetic denervation.

The second objective was to investigate the immune status of the resident muscularis macrophages upon cSTX. While cSTX did not affect pro-inflammatory gene expression in macrophages, their anti-inflammatory genes were reduced. This indicates an immunomodulatory role of SNS on resident macrophages under homeostasis.

### 3.1.7 Effects of cSTX in the early phase of non-infectious acute POI

As the transcriptional programs of CX3CR1<sup>+</sup> muscularis macrophages at the basal level are shaped towards a pro-inflammatory signature by the SNS, we next questioned if it also plays a role in acute intestinal inflammation. To answer this, we took advantage of a well-described surgical intestinal manipulation (IM) model that results in a clinically relevant transient motility disorder, known as postoperative ileus (POI) (**Figure 18A**). POI is a common consequence of abdominal surgery, resulting in sterile inflammation of the muscularis externa which induces transient disturbances of regular gastrointestinal motility (Wehner et al., 2007; Mueller et al., 2011). We treated mice with saline or 6-OHDA 17 days before subjecting them to either surgical IM or a sham operation (**Figure 18B**). Three hours after surgery, many inflammatory cytokines are known to be upregulated in POI. Therefore, we performed a quantitative PCR for prototypical inflammatory markers shown to be regulated in the muscularis during POI (Stein et al., 2018). The mRNA

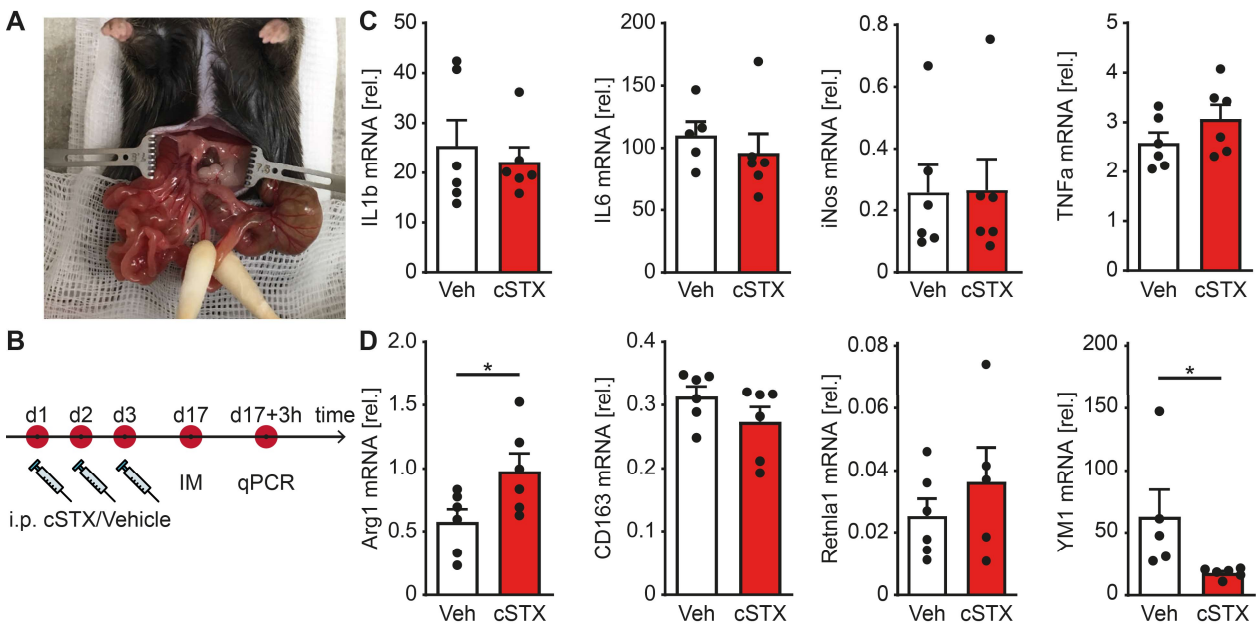


**Figure 18: Changes in the muscularis externa upon cSTX in the early phase of POI**

(A) An image of intestinal manipulation (IM) showing the procedure to induce postoperative ileus as a model to study the role of SNS in a non-infectious, acute muscularis inflammation. (B) The experimental setting for vehicle and cSTX-treated mice followed by IM. (C-D) qPCR analysis of vehicle (white) and cSTX-treated mice (red) showing fold change mRNA expression of different pro (C) and anti-inflammatory genes (D) in the muscularis externa three hours after IM. Expression levels are normalized to vehicle-treated mice without IM. Values in each column are shown as mean  $\pm$  SEM and statistical analysis was carried out by unpaired t-test (\* $p < 0.05$ , \*\* $p < 0.01$  and \*\*\* $p < 0.001$ ).

expression of pro-and anti-inflammatory genes is normalized to the GAPDH house-keeping gene expression of vehicle-treated mice without IM. Pro-inflammatory cytokines *IL-1 $\beta$*  and *IL6* were strongly induced in the muscularis of cSTX-treated mice. However, there was no difference between the vehicle and cSTX-treated animals three hours after IM (**Figure 18C**). In contrast, the level of the anti-inflammatory gene *YM1* was increased (50-fold) in vehicle-treated mice, but it was reduced (-60%) in the cSTX group. Although *CD163* and *Retnla1* were reduced after IM, no difference was observed between the vehicle and cSTX-treated groups (**Figure 18D**). *Arg1* expression decreased in vehicle-treated mice (-50%), while this drop was not observed in the cSTX group upon IM. This indicates that cSTX did not affect the overall immunological tissue response upon IM.

### 3.1.8 CX3CR1<sup>+</sup> muscularis macrophage anti-inflammatory genes are reduced upon cSTX in the early phase of POI

Activation of resident macrophages is shown to be crucial in POI (Wehner et al., 2007) and recently, our group investigated macrophage polarization and plasticity in the course of POI (Stein et al., 2018). Although we observed distinct immune changes in the muscularis externa three hours after IM, the functional changes of CX3CR1<sup>+</sup> resident muscularis macrophages remained unclear. Therefore, we FACS-sorted intestinal CX3CR1<sup>+</sup> cells three hours after IM from the vehicle and cSTX-treated mice (**Figure 19A**). The mRNA expression of pro-and anti-inflammatory genes is normalized to the GAPDH house-keeping gene expression of sorted macrophages from the vehicle-treated mice without IM. In general, only *IL6* was upregulated three hours after IM in sorted macrophages in both the vehicle and cSTX-treated groups but no differences were observed between the two groups. Further, the levels of *IL1 $\beta$* , *TNF $\alpha$* , and *iNOS* were also comparable in the vehicle and cSTX-treated sorted macrophages (**Figure 19B**). In contrast, the postoperative anti-inflammatory genes *Arg1* (-60%), *CD163* (-30%), and *YM1* (-60%) were significantly reduced in cSTX-sorted-macrophages compared to vehicle-sorted-macrophages three hours after IM with the only exception in *Retnla1* levels (**Figure 19C**). Taken together, these findings show that cSTX reduced the expression of several

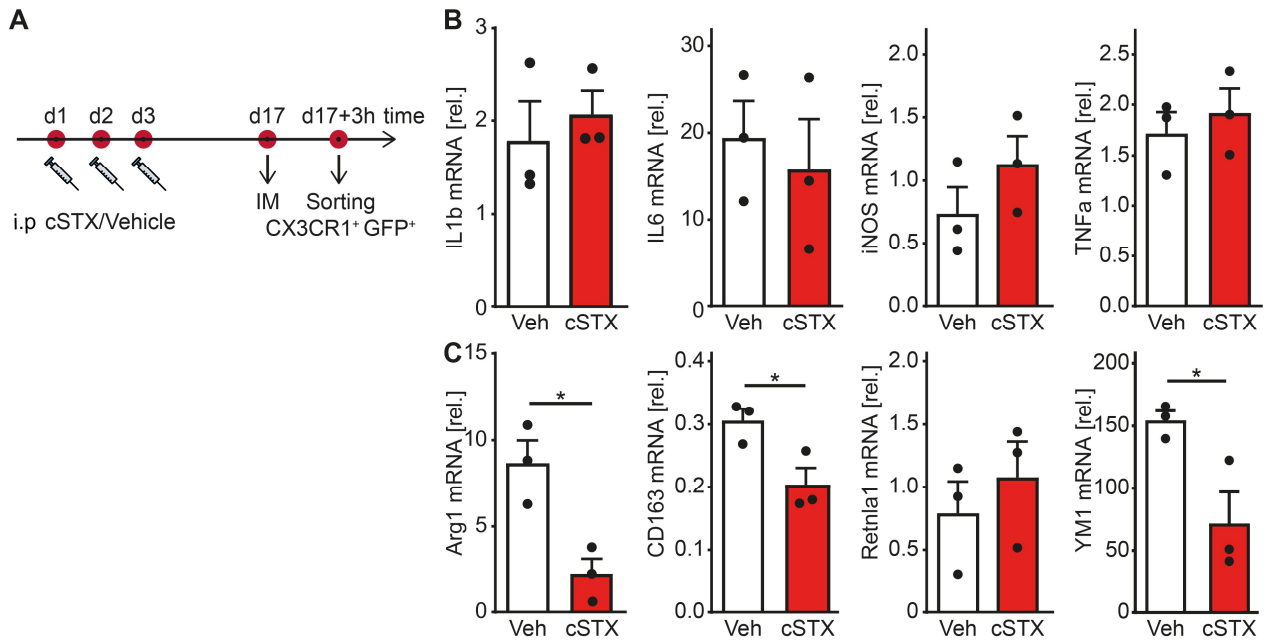


**Figure 19: Resident CX3CR1<sup>+</sup> macrophage anti- and pro-inflammatory gene response upon cSTX in the early phase of POI**

(A) Timeline showing the experimental setup for sorting resident CX3CR1<sup>+</sup> macrophages from the vehicle and cSTX-treated mice three hours after IM. (B-C) qPCR analysis of sorted CX3CR1<sup>+</sup> macrophages from vehicle (white) and cSTX-treated mice (red) showing fold-change mRNA expression of pro (B) and anti-inflammatory genes (C). Values in each column are shown as mean  $\pm$  SEM and statistical analysis was carried out by unpaired t test (\* $p < 0.05$ , \*\* $p < 0.01$  and \*\*\* $p < 0.001$ ). Expression of mRNA for IL-1 $\beta$ , IL-6, TNF $\alpha$ , iNos, Arg1, CD163, Retnla1, and YM1 determined by qPCR, presented relative to house-keeping gene GAPDH expression of sorted macrophages from the vehicle-treated mice without IM.

postoperative anti-inflammatory genes in the early phase of POI. We speculate that this might affect the postoperative inflammation of the muscularis and consequently impact the functional outcome of POI.

### 3.1.9 Sympathetic neuronal loss results in reduced symptoms of postoperative ileus.

To measure the effects of sympathetic denervation in the late or clinically relevant effector phase of POI, we analyzed the outcome of mice subjected to the vehicle or cSTX-treatment. This phase manifests around twenty-four hours after IM in the POI mouse model when inflammation and functional disturbances peak. According to the analyses performed at the three hours time-point, we also analysed *IL-1 $\beta$*  and *IL6* that are upregulated at the late phase of POI. Vehicle-treated mice showed an upregulation of *IL-1 $\beta$*  and *IL6* upon IM (**Figure 20A**). However, cSTX-treated mice showed a moderate increase in *IL-1 $\beta$*  (2.5-fold) and *IL6* (3.5-fold), compared to the corresponding vehicle-

treated mice. Simultaneously, anti-inflammatory genes such as *CD163* (-65%) and *YM1* (-30%) were downregulated but no changes were observed in the expression of *Arg1* and *Retn1a1* twenty-four hours after IM (**Figure 20B**).

Together, our data show that the effect of sympathetic neuronal loss on the postoperative immune response lasts for hours and might also affect the functional outcome of POI. To investigate this outcome after denervation, we measured the cellular infiltration and motility disturbances. As a readout to determine the extent of motility disturbances during POI, the gastrointestinal (GI) transit time was measured twenty-four hours after IM. Vehicle-treated animals showed a reduced GI transit ( $3.3 \pm 0.26$ ) upon IM compared to the corresponding sham-operated mice ( $10.8 \pm 0.45$ ). In contrast, cSTX-treated mice showed an accelerated GI transit ( $5.7 \pm 0.75$ ) (**Figure 20C**) twenty-four hours after IM. Notably, the postoperative MPO<sup>+</sup> immune cell infiltration into the muscularis externa was

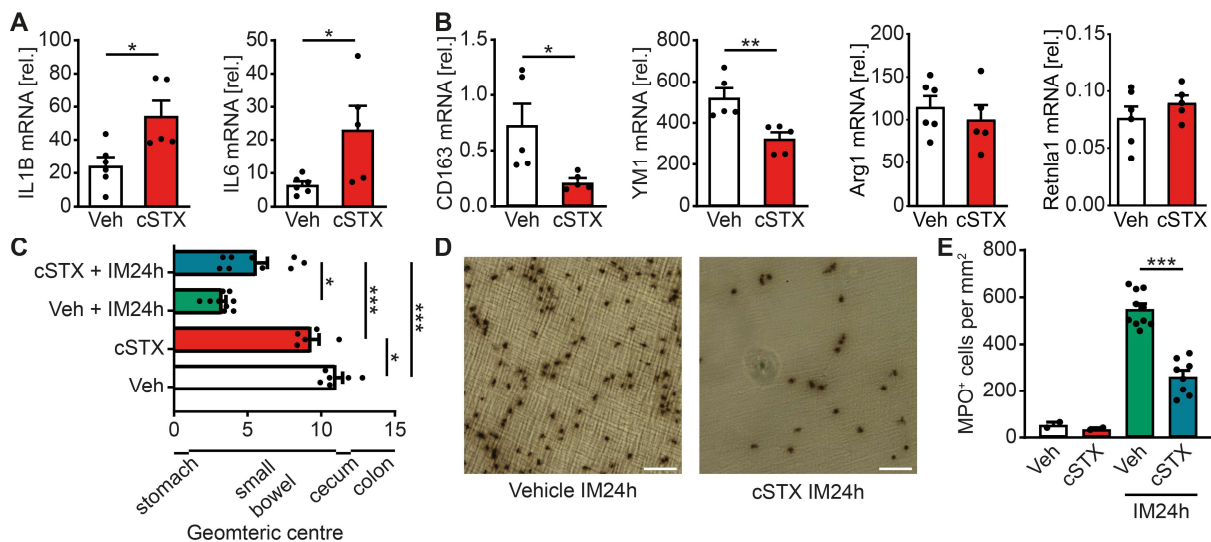


**Figure 20: Functional outcome upon cSTX in the late or effector phase of POI**

(A-B) qPCR analysis from vehicle (white) and cSTX-treated mice (red) showing the expression of pro (A) and anti-inflammatory genes (B) in the muscularis twenty-four hours after intestinal manipulation. Values in each column are shown as mean  $\pm$  SEM and statistical analysis was carried out by unpaired t test (\* $p < 0.05$ , \*\* $p < 0.01$  and \*\*\* $p < 0.001$ ) comparing vehicle-treated mice without IM versus indicated groups. (C) GI transit time shown as the geometric center of distribution of FITC dextran in the stomach (st), small intestine, cecum (c) and colon calculated twenty-four hours after intestinal manipulation. (D) Ileum muscularis whole mounts of vehicle (left) and cSTX-treated (right) mice showing myeloperoxidase-staining (MPO) for polymorphonuclear neutrophils (PMNs) twenty-four hours after intestinal manipulation. (E) Quantification of MPO<sup>+</sup> leukocytes upon intestinal manipulation in cSTX compared to the vehicle-treated mice. The graphs are plotted as mean  $\pm$  SEM and statistical analysis was carried out by a two-way ANOVA (\* $p < 0.05$ , \*\* $p < 0.01$ , and \*\*\* $p < 0.001$ ).

also reduced (-55%) (**Figure 20D, E**).

Further, by FACS staining, we characterized the postoperative muscularis externa immune cells twenty-four hours after IM (**Figure 21A**). We observed a reduction in living CD45<sup>+</sup> cells, Ly6C<sup>+</sup> Ly6G<sup>-</sup> monocytes (**Figure 21B**), Ly6G<sup>+</sup> Ly6C<sup>+</sup> neutrophils, and F4/80<sup>+</sup> macrophages (**Figure 21C**) in cSTX-treated compared to vehicle-treated animals upon IM.

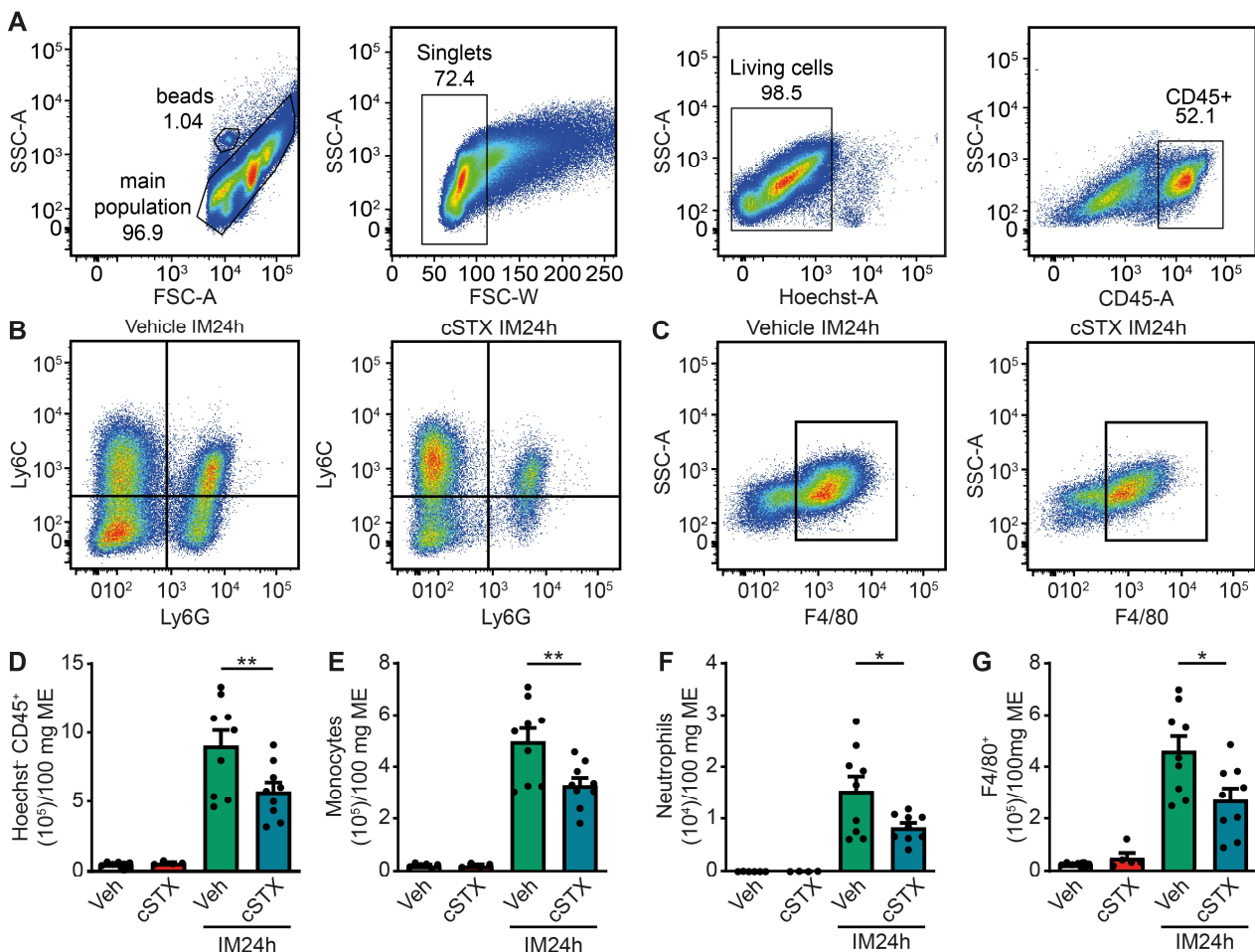


**Figure 21: Effects of cSTX at the late phase of POI**

(A-C) Representative FACS images showing the gating strategy of the main population, singlets, and Hoechst- CD45<sup>+</sup> cells (A), the ratio of Ly6C<sup>+</sup> Ly6G<sup>-</sup> monocytes and Ly6C<sup>+</sup> Ly6G<sup>+</sup> neutrophils (B), and monocyte-derived F4/80<sup>+</sup> macrophages (C) isolated from small bowel muscularis externa of vehicle and cSTX-treated mice twenty-four hours after IM. (D-G) Bar graphs showing the quantification of total Hoechst CD45<sup>+</sup> leukocytes (D), Ly6C<sup>+</sup> Ly6G<sup>-</sup> monocytes (E), Ly6C<sup>+</sup> Ly6G<sup>+</sup> neutrophils (F) and monocyte derived F4/80<sup>+</sup> macrophages (G) of the vehicle and cSTX-treated mice twenty-four hours after IM. The graphs are plotted as mean  $\pm$  SEM and statistical analysis was carried out by two-way ANOVA (\* $p < 0.05$ , \*\* $p < 0.01$  and \*\*\* $p < 0.001$ ).

Quantification revealed more than 37% reduction in living CD45<sup>+</sup> leukocytes (**Figure 21D**), 34% reduction in Ly6C<sup>+</sup> Ly6G<sup>-</sup> monocytes (**Figure 21E**), 46% reduction in Ly6G<sup>+</sup> Ly6C<sup>+</sup> neutrophils (**Figure 21F**), and 41% reduction in F4/80<sup>+</sup> macrophages (**Figure 21G**) twenty-four hours after IM in cSTX-treated compared to vehicle-treated animals. Together, the cSTX resulted in the reduced number of infiltrating leukocytes twenty-four hours after IM and consequently led to an improved GI transit.

The third objective was to investigate the effect of cSTX on the muscularis externa and resident macrophages in the disease model of POI. cSTX reduced macrophage anti-inflammatory genes also in the early phase of POI. In the late phase, leukocyte infiltration into muscularis was reduced with a quicker recovery of bowel motility.

In subsumption of the muscularis externa related effects of the SNS, we observed an elevated pro-inflammatory status in the tissue upon cSTX. A particular perspective on the resident CX3CR1<sup>+</sup> macrophages within this tissue revealed an anti-inflammatory state of this cell population. In the early phase of POI, some of the anti-inflammatory genes were reduced CX3CR1<sup>+</sup> macrophages while in the late phase, infiltrating leukocyte numbers dropped and GI transit time was accelerated. Together, this indicated an altered immune response in surgery-induced inflammation by cSTX. These findings may suggest sympathetic interventions as a possible approach to treat or prevent POI and this might be also of interest for other acute intestinal inflammatory disorders.

### 3.2 Effects of sympathetic denervation on mucosal antibacterial defense

The last part of this thesis exclusively focussed on the effects of cSTX in the mucosa. POI, the disease that we were predominantly interested in, mainly affects the tunica muscularis externa but not the mucosa. Therefore, we analysed mucosal changes after cSTX under homeostasis.

#### 3.2.1 Changes in the mucosa after cSTX

After having shown that the baseline muscularis immune response is altered upon cSTX, we next aimed to investigate whether cSTX also affected the release of pro-inflammatory cytokines and adrenergic receptors in the mucosa which we partially also checked in the muscularis externa. By quantitative PCR, we measured increased *IL-1 $\beta$*  (2.5-fold) and *TNF- $\alpha$*  (75-fold) cSTX-treated compared to vehicle-treated mice (**Figure 22A**).

Notably, the anti-inflammatory genes *Arg1* and *CD163* were also reduced in the mucosa of cSTX-treated compared to the vehicle-treated mice (**Figure 22B**) pointing towards common immune shaping mechanisms of the SNS in the tunica muscularis and the mucosa. This shows that distinct changes occur upon cSTX shaping the mucosal profile to a more pro-inflammatory and simultaneously less anti-inflammatory pattern. Further, the series of additional adrenergic receptors including *Adra1b*, *Adra1d*, *Adra2a*, *Adra2b*, *Adrb1*, *Adrb2*, and *Adrb3* but not *Adra1a* were also prominently reduced indicating changes on several cell types expressing these receptors in the mucosa (**Figure 22C**).

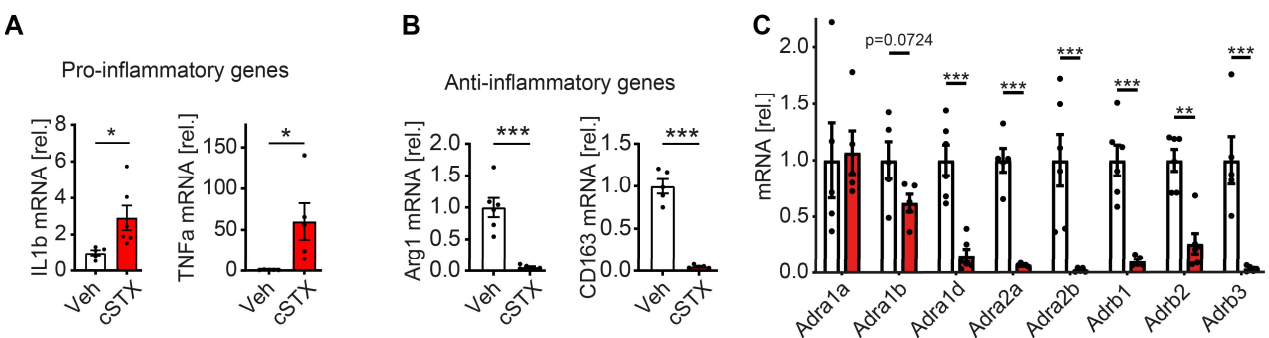


**Figure 22: Effects of cSTX in the mucosa**

(A-C) qPCR analysis from vehicle (white) and cSTX-treated mice (red) showing the expression of pro-inflammatory genes (A) anti-inflammatory genes (B) and adrenergic receptors (C), in the mucosa. Values in each column are shown as mean  $\pm$  SEM and statistical analysis was carried out by unpaired t-test (\* $p < 0.05$ , \*\* $p < 0.01$  and \*\*\* $p < 0.001$ ) comparing vehicle-treated mice versus indicated groups.

These cells include but are not limited exclusively to macrophages, epithelial cells, innate lymphoid cells, B and T-cells (Jacobson et al., 2021).

### 3.2.2 Increased epithelial tight junction genes after cSTX

After having observed these pronounced changes, we aimed to achieve a more comprehensive view on the alteration of molecular pathways after cSTX within the mucosa and we performed a bulk 3' mRNA sequencing from the muscularis-free mucosal samples of vehicle and cSTX-treated mice. 17541 genes were obtained after normalization with the standard CPM method and PCA graph was plotted. Further filtering using p-value ( $\geq 0.05$ ) and FDR fold change ( $\pm 2$ ) gave a total of 456 genes which were then used for gene enrichment pathway analysis. PCA showed that the vehicle and cSTX-treated samples clustered into two different axes (**Figure 23A**).

The volcano plot of 26346 differentially expressed genes showing the upregulation of antimicrobial defense genes upon cSTX (**Figure 23B**). The functional enrichment analysis on these differentially expressed genes for immune-related gene ontology (GO) terms revealed “*defense response to gram-positive bacterium, antibacterial humoral response, mucosal immune response, response to the bacterium, and tight junction*” to be significantly enriched upon cSTX-treatment. This shows that the basic immune state of the mucosa is indeed altered upon sympathetic denervation (**Figure 23C**).

As we observed an enrichment in genes connected to the GO term “*tight junctions*” upon cSTX, we speculated that sympathetic denervation might affect epithelial tight junction responses (**Figure 23D**). By quantitative PCR, we confirmed increased mRNA levels of tight junctions claudin-3 [cld3 (9-fold)], claudin-2 [cldn2 (4-fold)], and occludin [ocldn (2.5)] in cSTX-treated mice suggesting a role of sympathetic neurons in regulating epithelium tight junctions and thereby barrier functions (**Figure 23E-G**).

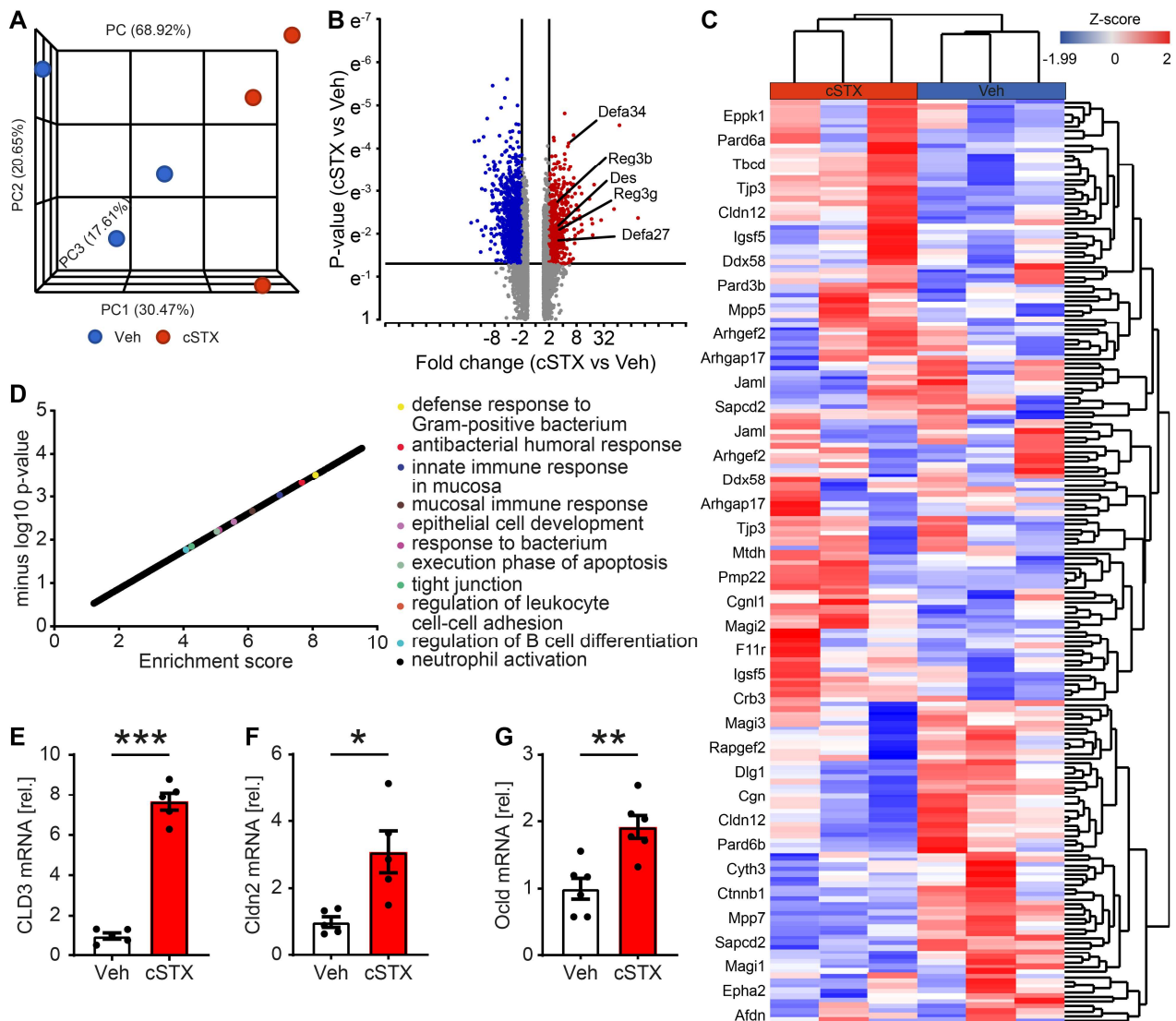


**Figure 23: Effects of cSTX on epithelium tight junctions**

(A) PCA plot showing the clustering of bulk RNA sequencing specimens from the intestinal mucosa of the vehicle and cSTX-treated mice. (B) The distribution of 26346 differentially expressed genes on the volcano plot. (C) Functional enrichment of differentially expressed genes ( $p < 0.05$ , fold change  $\pm 2$ ) in the mucosa showing immune-related GO terms upon cSTX. Enrichment of 3-fold or higher was expected to be biologically relevant (D) Heatmaps showing the clustering of differentially expressed genes of the GO term tight junction. (E-G) qPCR analysis showing the expression of various tight junction genes CLD3, Cldn2, ocldn in the mucosa of vehicle (white) and cSTX-treated mice (red). Values in each column are shown as mean  $\pm$  SEM and statistical analysis was carried out by unpaired t-test (\* $p < 0.05$ , \*\* $p < 0.01$  and \*\*\* $p < 0.001$ ) comparing vehicle-treated mice versus indicated groups.

### 3.2.3 cSTX increased antimicrobial defense genes

Another major function of the epithelium is to provide a proper antimicrobial defense as the intestinal mucosa is continuously exposed to the luminal microbial content. In this line, we observed an enrichment of genes for the GO term “antibacterial humoral response” (Figure 24A) in cSTX animals, and we quantified some distinct antimicrobial defense also by qPCR. Trefoil factor 3 [*TFF3* (16-fold)] was increased in the mucosa of cSTX-treated mice as compared to vehicle-treated mice (Figure 24B). We also observed an increase in bacterial defense genes such as Neutrophil defensin 1 precursor [*Defa1* (6-fold)], Regenerating islet-derived protein 3-gamma [*Reg3g* (4-fold)], Defensin-B3 precursor [ $\beta$ 3 defensin (3.5-fold)], Lysozyme C-1 precursor [*Lyz1* (3.5-fold)], and mucin-2 [*Muc2* (3-fold)]

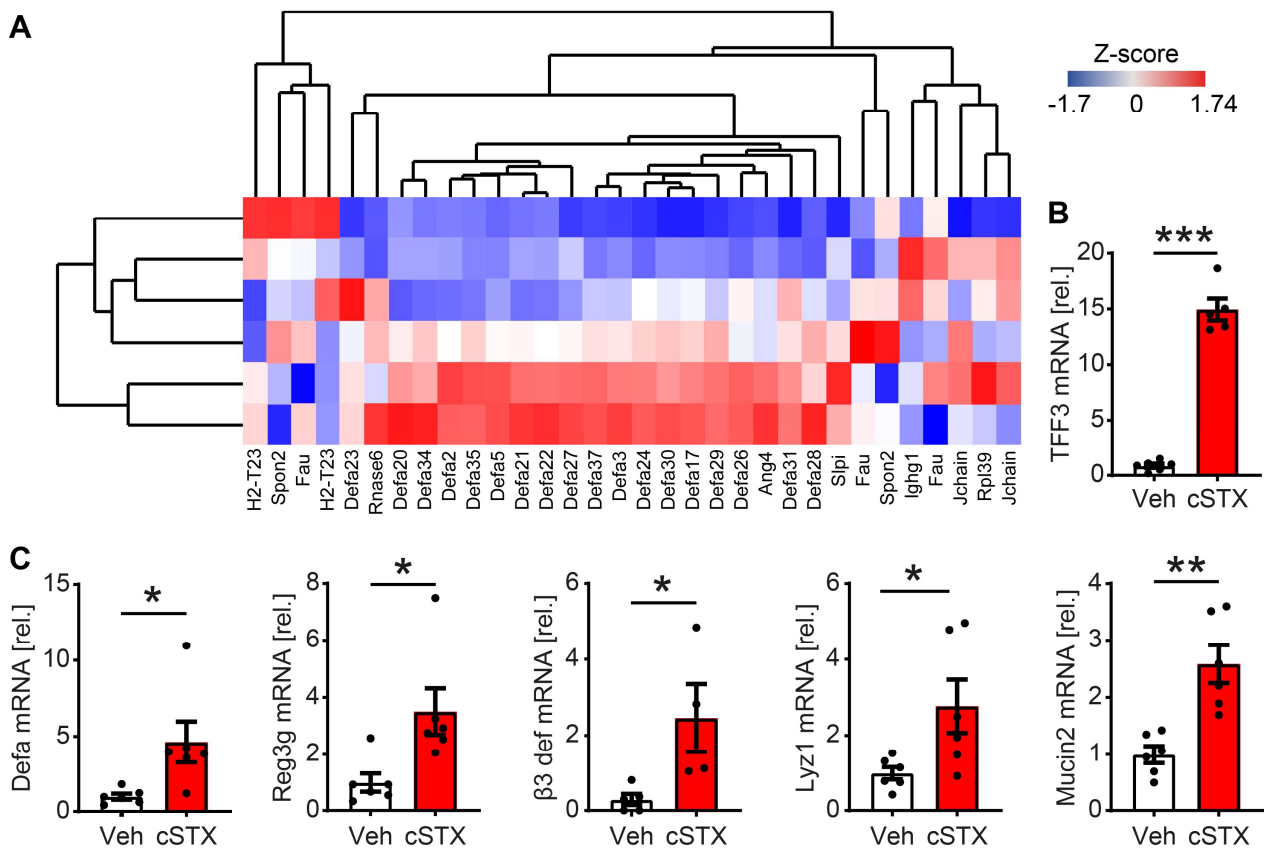


**Figure 24: Antibacterial humoral response in the mucosa upon cSTX**

(A) Heatmaps showing the clustering of differentially expressed genes of the GO terms antibacterial humoral response. (B) qPCR analysis showing an increase in TFF3 (C) genes and various microbial defense genes *defa1*, *Reg3g*,  $\beta$ 3 def, *lyz1*, *muc2* (D) in the mucosa of vehicle (white) and cSTX-treated mice (red). Values in each column are shown as mean  $\pm$  SEM and statistical analysis was carried out by unpaired t-test (\* $p < 0.05$ , \*\* $p < 0.01$  and \*\*\* $p < 0.001$ ).

in cSTX-treated mice (**Figure 24C**) confirming an increased mucosal antibacterial activity after cSTX. These findings add to the previously described role of sympathetic neurons in regulating epithelial cell functions and underline the important role of the SNS in affecting epithelial barrier integrity and function.

The fourth objective was to investigate the effect of cSTX in the mucosa. The pro-inflammatory status of the mucosa under baseline was also affected by cSTX as shown by increased *IL-1 $\beta$*  and *TNF- $\alpha$*  gene expression. Additionally, as levels of tight junctions and antimicrobial defense genes were also elevated, the SNS comprehensively controls epithelial biology under homeostasis.

Subsumed, our mucosal-related studies describe the role of SNS in modulating the antimicrobial gene responses of epithelial cells. cSTX led to an increase in pro-inflammatory genes as well as elevated levels of tight junctions and antimicrobial defense genes under homeostasis. Considering the profound changes after cSTX in the muscularis externa, our findings await future confirmation on a potential mechanistic role of the SNS also in immune-driven mucosal disorders. We speculate that sympathetic intervention may serve as a possible therapeutic approach to modify mucosal immune and antimicrobial response and barrier integrity during immune-driven intestinal disorders.

## 4. Discussion

### 4.1 Effects of cSTX on the muscularis externa and resident CX3CR1<sup>+</sup> Macrophages in health and disease

Neuro-immune interactions between the SNS and immune cells play an essential role in maintaining intestinal homeostasis and modulating inflammatory insults. In line, recent works highlighted a specific function of the SNS and its neurotransmitters and described the neuronal modulation of resident CX3CR1<sup>+</sup> muscularis macrophages (Gabanyi et al., 2016; Matheis et al., 2020). These macrophages are closely associated with the enteric neurons (Muller et al., 2014) but also with the extrinsic TH<sup>+</sup> sympathetic nerves (Verheijden und Boeckxstaens, 2018; Kolter et al., 2020). Hence, in the muscularis externa, innervation of these sympathetic neurons might also affect the resident macrophages. Furthermore,  $\beta_2$ -adrenergic receptor signaling is shown to upregulate neuroprotective programs in muscularis macrophages upon luminal infection and mediate protection to neurons via the arginase 1- polyamine axis (Matheis et al., 2020). Interestingly, these resident macrophages are shown to be involved in several GI disorders such as intestinal ischemia-reperfusion (Liu et al., 2015; Schaefer et al., 2008), gastroparesis (Choi et al., 2010), and as the basis of the present thesis in POI (Kalff et al., 1998; Wehner et al., 2007; Stein et al., 2018). As sympathetic overactivity occurs upon abdominal surgery and disturbs bowel motility patterns resulting in POI (Jonge et al., 2003), we hypothesized that the SNS can modulate muscularis macrophage function in acute, surgically induced inflammation. Consequently, in this study, we focused to investigate the immunomodulation of muscularis macrophages by the SNS under homeostasis and during POI in mice.

Sympathetic neurons are characterized by the expression of the enzymes TH and dopamine beta-hydroxylase that innervate all layers of the bowel wall (Lomax et al., 2010; Schank et al., 2006). In addition, TH is an essential enzyme in a biosynthetic pathway of dopamine and NE (Savitt et al., 2005). To address the role of SNS, and understand their impact on homeostasis and intestinal diseases, it was essential to abolish SNS function in the gut. Therefore, to successfully eliminate these gut extrinsic TH<sup>+</sup> sympathetic innervations particularly within the muscularis externa *in vivo*, we opted to employ three

distinct methods possessing all experimental advantages and disadvantages. Consequently, we used a genetic (Borden et al., 2013), a surgical (Olivier et al., 2016; Willemze et al., 2019) and, a chemical approach (Pellegrini et al., 2020).

#### 4.1.1 cSTX targets sympathetic neurons without affecting vagal innervation

In the genetic approach, we used a TH-Cre mouse line that has been used before successfully in GI research (Yoo et al., 2021). This approach has an enhanced cellular specificity although it does not exclusively target sympathetic but also dopaminergic neurons (Savitt et al., 2005). Further, it has the advantage to precisely target a particular gene and/or cell population without possible side effects of drugs or a surgical intervention that might influence further analysis. For gSTX, we used *TrkA*, a nerve growth factor promoting pancreatic sympathetic innervation. *TrkA* is necessary to establish pancreatic islet shapes, and their innervation is absent in the pancreas of mice lacking NGF (Glebova und Ginty, 2004). Accordingly, the genetic depletion of *TrkA*, in TH-Cre;*TrkA*<sup>ff</sup> mutant mice, was effective in abolishing sympathetic neurons in the pancreas (Borden et al., 2013). However, in the intestinal muscularis externa of TH-Cre;*TrkA*<sup>ff</sup> mutant mice, we did not observe this reduction in TH<sup>+</sup> fibers. We speculate that *TrkA* might not be crucial for the survival of sympathetic neurons innervating the GI tract. Therefore, TH-Cre mouse driver line lacking *TrkA* was not effective in ablating gut projecting sympathetic neurons.

Since the 1950s, surgical ganglionectomy and vagotomy have been used and validated in animal studies as selective but invasive denervation approaches that target sympathetic and parasympathetic intestinal innervation, respectively (Shingleton et al., 1952). The herein used intestine-specific sSTX approach (Olivier et al., 2016) was effective in abolishing extrinsic sympathetic neurons in the muscularis externa. However, fine bundles of vagal afferent fibers divide and reassemble along the SMA, the surgical site where sSTX is performed (Wang und Powley, 2007). Therefore, sSTX is at risk of simultaneously at least partially disturbing the parasympathetic intestinal innervation by surgical transection. To determine the integrity of the vagal fibers, we performed an indirect functional CCK approach by assessing food intake. CCK induces the effect of satiety while vagotomy blocks this effect (Bucinskaite et al., 2000). Injection of CCK to the sham-operated mice showed reduced food consumption indicating intact vagal signaling. However, sSTX mice displayed an increase in the amount of food consumed. This

indicates that sSTX not only destroys the sympathetic neurons but also disturbs the vagal signaling. Nevertheless, the CCK test is an indirect approach and there is no direct evidence for disturbed vagus nerve activity due to the missing vagal markers and scarcely detectable vagal fibers at the quantitative levels. A limitation of the CCK test, however, is that CCK receptors are not only expressed on vagal afferents, but also, neurons of the midbrain, and the myenteric plexus (Honda et al., 1993; Rehfeld, 2017). Therefore, the effect of satiety might still be induced in the absence of intact vagal signaling. Alternative approaches like retro- or anterograde tracing of the nerve fibers (Niu et al., 2020; Han et al., 2018) would be an alternative option, although, not a perfect option as they don't target all vagal fibers.

As a third approach, we tested the application of a neurotoxin 6-OHDA in the peritoneum that destroys catecholaminergic pathways (Hernandez-Baltazar et al., 2017). Although it is the most broadly used approach to deplete sympathetic neurons, it has two limitations. First, it targets both dopaminergic and noradrenergic neurons (Tieu, 2011). Secondly, due to the peritoneal application route, it might also act at distant sites and targets sympathetic innervation in other visceral organs. Nevertheless, it is broadly accepted and we expected that it also does target the vagal nerves. Insufficient dosing could affect further analysis and excessive drug dosage might lead to undesirable side effects. Therefore, we first tested different amounts of 6-OHDA to accomplish complete loss of TH<sup>+</sup> neurons in the bowel muscularis externa. Three times 80 mg/kg 6-OHDA showed complete ablation of sympathetic fibers along the GI tract- in the stomach, small bowel, and colon two weeks after the treatment. In addition, this model did not disturb vagal signaling as measured by the decreased food intake upon CCK administration proving intact vagal afferent fibers. Furthermore, our data showed increased CD45<sup>+</sup> leukocytes in the muscularis externa precisely characterized as Ly6C<sup>+</sup> Ly6G<sup>+</sup> neutrophils, Ly6C<sup>+</sup> Ly6G<sup>-</sup> monocytes, and F4/80<sup>+</sup> bone marrow-derived macrophages within four days after 6-OHDA treatment. We defined this as a sterile inflammatory response in the muscularis externa necessary for the rapid clearance of debris from dying sympathetic neurons after 6-OHDA treatment (Zhang et al., 2015). However, as shown by flow cytometry analysis, it was a transient cellular inflammation that was utterly resolved a week before we carried out our analyses. Consequently, cSTX with three times 80 mg/kg 6-OHDA was proven to be the most

reliable approach in eliminating TH<sup>+</sup> sympathetic neurons in the GI tract without disturbing vagal innervation.

Although cSTX-induced inflammation is transient, it might still have a long-lasting effect on the macrophages. For instance, LPS triggers a macrophage-mediated inflammatory response, leading to tissue damage and lethality. However, a state of tolerance is induced in prolonged exposure to LPS that results in reduced pro-inflammatory cytokine expression (O'Carroll et al., 2014; Seeley und Ghosh, 2017). Interestingly, peripheral whole blood from polytraumatized patients showed reduced pro-inflammatory cytokines after exposure to LPS indicating a tolerant immune status in these patients (Halbgebauer et al., 2020). Therefore, we can not completely exclude the possibility of a cSTX-induced lasting effect on macrophages. However, even with the sSTX approach, the denervation procedure triggers an inflammatory response and thus, any other potential options are still at the risk of inducing immune-tolerance effects. Notably, benzalkonium chloride (BAC)-induced denervation is also used in other intestinal inflammation models (Sanidad et al., 2018; Yang et al., 2020). This locally applied BAC treatment temporarily reduces extrinsic TH<sup>+</sup> sympathetic fibers; however, these fibers reappear between 2- 3 weeks after treatment while TH<sup>+</sup> neurons in the intestine are still absent 60 days after 6-OHDA treatment. Furthermore, besides extrinsic sympathetic neurons, BAC also targets intrinsic enteric neural cells, particularly GFAP<sup>+</sup> glial cells, and enteric neurons (Tamada und Kiyama, 2016). Therefore, this was not a suitable approach for our studies.

4.1.2 cSTX shapes the muscularis externa profile to a pro-inflammatory status and reduces resident CX3CR1<sup>+</sup> macrophage anti-inflammatory cytokines under baseline conditions.

After selecting the 6-OHDA-induced cSTX approach, we investigated the consequence of neuronal loss in the muscularis. A bulk 3' RNA sequencing upon cSTX, revealed enrichment of genes connected to the GO term "inflammatory response" and an increase in *IL-1 $\beta$*  in the muscularis externa of cSTX-treated mice. By performing qPCR analysis, we confirmed an increase in inflammatory genes *IL-6* and *IL-1 $\beta$*  that we recently identified to be regulated during acute muscularis inflammation (Wehner et al., 2005; Hupa et al., 2019; Stoffels et al., 2014). Furthermore, distinct noradrenergic receptors predominantly expressed in the GI tract that are known to play critical roles in immune and inflammatory

responses (Seiler et al., 2008; Zeng et al., 2020) were also altered. Potential cellular sites of adrenergic receptor signaling include resident cell types such as macrophages, dendritic cells, smooth muscle cells, enteric neurons, and glial cells (Nijhuis et al., 2014; Grubišić und Gulbransen, 2017; Gabanyi et al., 2016; Nasser et al., 2006). Enteric neurons and glia cells express  $\alpha 2$  adrenergic receptors, and norepinephrine-mediated  $\alpha 2$  adrenergic signaling modulates enteric gut motility (Scheibner et al., 2002; Nasser et al., 2006).  $\beta$  adrenergic receptor activation on smooth muscle cells initiate the relaxation of these cells (Manara et al., 2000; Seiler et al., 2008). Selective  $\beta_2$  adrenergic signaling in macrophages triggers an anti-inflammatory response (Gabanyi et al., 2016). Therefore, different immune and non-immune cells in the muscularis externa might be affected by absent adrenergic inputs from sympathetic neurons after cSTX.

Although the expression levels of several pro- and anti-inflammatory genes in the whole muscularis tissue were modified upon cSTX, it was still unclear whether these changes originate from the resident muscularis macrophages. The macrophage immune responses respond selectively to adrenergic signaling (Gabanyi et al. 2016; Matheis et al. 2020), and therefore, we investigated the response of cSTX on these cells. We used CX3CR1<sup>GFP/+</sup> reporter mice (Jung et al., 2000) and subjected them to the cSTX procedure. In the GI tract, *Adrb2* ( $\beta_2$ AR) and *Adrb3* ( $\beta_3$ AR) are predominantly expressed by several immune and non-immune cells (Calvani et al., 2020) and modulate intestinal inflammation by inhibiting the release of pro-inflammatory cytokines (Ağaç et al., 2018a; Vasina et al., 2008). While *Adrb2* was upregulated in the muscularis externa, it was strongly reduced in sorted CX3CR1<sup>+</sup> macrophages. This suggests that macrophages are a major target of SNS signaling. However, as the reduction in *Adrb2* gene is accompanied by a general upregulation in the overall muscularis tissue, other cells (Seiler et al., 2008; Nasser et al., 2006) might try to compensate for the macrophage-specific reduction of *Adrb2* signaling in the muscularis after cSTX. Reduced *Adrb2* levels in sorted CX3CR1<sup>+</sup> macrophages from cSTX-treated mice are in line with a previous study describing NE signaling to macrophage *Adrb2* receptors (Gabanyi et al., 2016). While *Adrb2* was decreased, another macrophage adrenergic receptor, *Adrb3*, was slightly increased in the sorted CX3CR1<sup>+</sup> macrophages, but, it remained unclear whether this is part of a compensatory mechanism triggered by the absence of sympathetic neurons.

Another important observation of this study was that the levels of *BMP-2* and *CSF1-R*, a receptor of *CX3CR1*<sup>+</sup> muscularis macrophages were reduced in macrophages sorted from cSTX-treated mice. *BMP-2* is secreted by muscularis macrophages and regulates GI motility through direct action on enteric neurons in a non-inflamed bowel. In turn, these neurons secrete *CSF-1* required for macrophage survival (Muller et al., 2014). Resident macrophages indeed strictly depend on *CSF-1* signaling as mice depleted of *CSF-1* (Muller et al., 2014) as well as a mouse line that developed spontaneous mutations in the *CSF-1* gene (Mikkelsen und Thuneberg, 1999) show strongly reduced numbers up to an almost complete absence of resident muscularis macrophages respectively. Therefore, the slightly but not significantly disturbed GI motility observed in our studies in cSTX-treated mice might be caused due to the reduced *BMP-2* levels in macrophages. Furthermore, several markers including *YM1*, *CD163*, and *Retnla* used to identify an alternatively activated macrophage state (Leopold Wager und Wormley, 2014), were strongly reduced indicating an altered anti-inflammatory phenotype of macrophages. This is in line with the detected enrichment of genes listed within the GO term "Regulation of macrophage differentiation" in cSTX mice. The alternatively activated macrophages are known to play a role in wound healing as well as in regulating immune responses (Mikkelsen, 2010; Kim und Nair, 2019; Bain und Schridde, 2018). Interestingly, the downregulation of anti-inflammatory genes was only observed in sorted macrophages isolated from cSTX-treated mice but not in the muscularis externa tissue suggesting distinct changes on macrophages after cSTX. We did not observe a reduction in *Arg1* upon cSTX in our *in vivo* study. *Arg1* is often used as an anti-inflammatory marker for alternatively activated macrophages and a recent study showed that stimulation of peritoneal macrophages with NE or salbutamol upregulated *Arg1 in vitro* that was prevented by butaxamine, a  $\beta_2$ AR blocker (Gabanyi et al., 2016). However, several other classical anti-inflammatory genes, of which some were tested in this thesis, were not examined in the Gabayani et al., study. Although none of these markers alone can provide evidence of an altered macrophage function, we believe that due to the reduction in some of these genes, we can conclude an immune-modulatory role of the SNS on *CX3CR1*<sup>+</sup> macrophages *in vivo*. In addition, pro-inflammatory markers *IL-6* and *IL-1 $\beta$*  were upregulated in the muscularis but not in the cSTX-sorted macrophages. This indicates that macrophage anti-inflammatory response is selectively affected by cSTX what in turn

triggers a pro-inflammatory reaction in the muscularis externa wherein these macrophages reside. Potential cellular sources for these cytokines could be enteric neurons and glia cells (Stoffels et al., 2014; Yan et al., 2021; Hupa et al., 2019).

These findings were further supported by our *ex vivo* M-CSF or LPS stimulation assay. M-CSF and LPS stimuli are known for inducing an anti-inflammatory or a pro-inflammatory cytokine profile of macrophages respectively (Hamilton et al., 2014; Orecchioni et al., 2019; Han et al., 2017). In the presence of M-CSF, bone marrow-derived macrophages differentiate into mature macrophages with a cell morphology similar to that of tissue macrophages (Nasser et al., 2020). Comparable levels of pro-inflammatory genes were expressed by both vehicle and cSTX-sorted macrophages after *ex vivo* LPS stimulation. However, cSTX-sorted macrophages failed to induce anti-inflammatory genes such as *Arg1*, *IL-10*, and *CD163* upon stimulation with M-CSF. This is in line with the reduced levels of *CSF-1R* observed in sorted macrophages of cSTX-treated mice (Figure 10B) and suggests that macrophages are resilient to anti-inflammatory M-CSF stimuli upon cSTX and continue to remain in a pro-inflammatory state *in vivo*. A shortcoming of this experimental part is that we have not checked other markers of alternative activation except for the ones mentioned above.

#### 4.1.3 cSTX alters macrophage anti-inflammatory profile also in the early phase of POI

Given that CX3CR1<sup>+</sup> muscularis macrophage immune functions are modulated by intestinal sympathetic innervation under baseline conditions, we next focused on exploring their relevance in an intestinal inflammation model. By mimicking the surgical trauma to the mice bowel wall, we induced POI and explored the role of SNS in modulating CX3CR1<sup>+</sup> muscularis macrophage functions. cSTX- treated mice showed reduced levels of anti-inflammatory marker *YM1* but not *CD163*, *Retnla1*, and *Arg1* in the muscularis externa tissue, three hours after IM. In addition, there were no changes in the early postoperative response of pro-inflammatory cytokines in the muscularis externa. Interestingly, these changes occurred in the early phase of POI when resident muscularis macrophages are activated and release inflammatory cytokines and chemokines but blood-derived leukocyte infiltration has not yet occurred. However, by FACS-sorting CX3CR1<sup>+</sup> muscularis macrophages three hours after IM, we observed a significant reduction in the levels of anti-inflammatory markers *YM1*, *Arg1*, and *CD163* while the macrophage pro-

inflammatory profile also was not altered. As the macrophage anti-inflammatory pattern was also reduced after the surgical trauma these data suggest a role of the SNS in CX3CR1<sup>+</sup> muscularis macrophage immunomodulation also in POI pathogenesis. Hence, we hypothesized that a dampened anti-inflammatory state of muscularis macrophages might impact the muscularis inflammation and finally bowel function in the clinically relevant late phase of POI.

In the late phase, we observed reduced anti-inflammatory genes *CD163* and *YM1* while pro-inflammatory genes *IL-1 $\beta$*  and *IL6* were noticeably increased in the muscularis externa of cSTX-treated mice twenty-four hours after IM. We interpret this increase in the pro-inflammatory cytokines as a compensatory mechanism upon cSTX that might occur to re-establish homeostasis upon surgical insult involving several resident cell types in the muscularis externa. Enteric glia cells that are activated upon IM (Stoffels et al., 2014; Schneider et al., 2020; Hupa et al., 2019), dendritic and T-cells (Engel et al., 2010), intestinal smooth muscle cells (Wehner et al., 2010), and enteric neurons (Yoo und Mazmanian, 2017; Burgueño et al., 2016) might also be the source of these pro-inflammatory genes in the muscularis externa. Nevertheless, the role of the SNS in modulating resident macrophage functions in the late phase of POI remained unaddressed as we were unable to perform gene expression profiling of CX3CR1<sup>+</sup> muscularis macrophages at this time-point due to the overlapping markers F4/80, MHCII, and Ly6C (Desalegn und Pabst, 2019) that are expressed on resident and infiltrating cells. Particularly, macrophages that derive from infiltrating monocytes can not be distinguished from the resident cells by these common markers. Further, infiltrating monocytes that are Ly6C<sup>+</sup> CX3CR1<sup>inter</sup> tremendously increase in the muscularis externa upon intestinal manipulation making it intricate to sort all the infiltrating cells. Alternatively, the resident CX3CR1<sup>high</sup> cell population could be sorted without any additional markers. However, in pathological conditions, Ly6C<sup>+</sup> CX3CR1<sup>inter</sup> are polarized to pro-inflammatory responses compared to Ly6C<sup>-</sup> CX3CR1<sup>high</sup> cell population that exhibit anti-inflammatory profile (Weber et al., 2011). Therefore, isolating only CX3CR1<sup>high</sup> cells might display a bias in the analysis as both the resident and infiltrating cells exhibit alternative differentiation outcomes. To overcome this, a highly multiplexed single-cell RNA sequencing (scRNAseq) that detects individual cell heterogeneity could be performed (Wen und Tang,

2018). scRNAseq can provide a broad perspective into changes in macrophage polarization states, and molecular programs co-expressed in macrophage subsets (Arlaukas et al., 2021). The use of this technique is yet limited by its high-cost need and required extensive training in single-cell bioinformatics and couldn't be performed within this thesis.

#### 4.1.4 Sympathetic neurons play a pro-inflammatory role in the late and clinically relevant phase of POI

As already known, monocytes and neutrophils are the major constituents of the immune infiltrate in the late phase of POI (Kalff et al., 1999b). Upon IM, we observed reduced numbers of Ly6C<sup>+</sup> Ly6G<sup>-</sup> monocytes, Ly6C<sup>+</sup> Ly6G<sup>+</sup> neutrophils, and MPO<sup>+</sup> cells in the muscularis externa of cSTX-treated mice. Although there was an increase in the

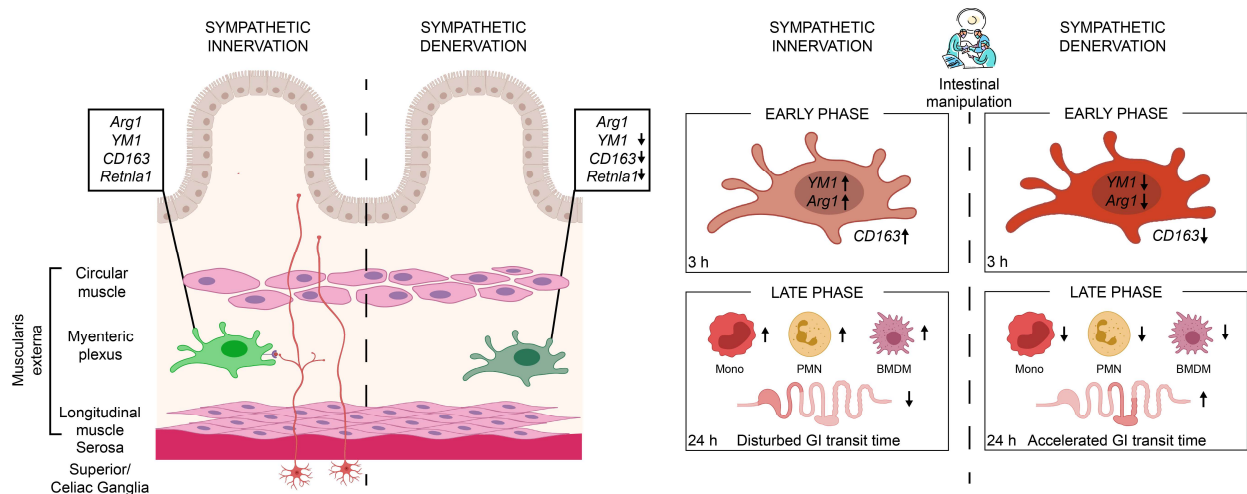


**Figure 25: Graphical abstract of the findings of this thesis in the muscularis externa.**

Resident muscularis macrophages play essential roles in homeostasis as well as in intestinal inflammation. These macrophages are the early responders in a mechanically triggered surgical trauma (intestinal manipulation), clinically known as POI. In steady-state, resident muscularis macrophages (light green macrophage) express anti-inflammatory genes YM1, CD163, Arg1, and Retnla1 in the presence of sympathetic neurons (red neurons). These muscularis macrophages (dark green macrophage) show reduced levels of these anti-inflammatory genes upon cSTX. The resident muscularis macrophages become activated (light red macrophage) following the intestinal manipulation and express high alternative activation markers YM1 and Arg1. However, preoperative cSTX reduced these macrophage anti-inflammatory genes (dark red macrophage) in the early phase, three hours after the intestinal manipulation. In the late, clinically relevant phase, cSTXs reduced blood-derived monocytes (mono), neutrophils (PMN), and monocyte-derived F4/80<sup>+</sup> macrophage (BMDM) numbers in the muscularis externa and finally leading to an accelerated transit time and improved symptoms of POI.

inflammatory genes in the muscularis, we unexpectedly observed reduced CD45<sup>+</sup> leukocytes infiltration and an overall improvement in terms of POI development. We further speculated that the dampened macrophage anti-inflammatory state at the early phase as well as the reduced leukocyte infiltration at the late phase of POI might affect the bowel motility measured by the GI transit. Indeed cSTX improved the postoperative GI transit time. These data suggest that IM might disturb sympathetic reflexes and interfere with the leukocyte infiltrates, leading to a prolonged postoperative ileus. To further confirm whether sympathetic neurons worsen POI symptoms, an SNS stimulation could be performed. This is done by stimulating the superior mesenteric nerve that mainly supplies GI sympathetic innervation (Willemze et al., 2018). Nevertheless, we could not perform SNS stimulation within this thesis and additional studies are required to confirm the pro-inflammatory role of SNS in postoperative ileus. Overall, this study underlines the importance of the SNS in modulating resident muscularis macrophage functions in health and inflammatory diseases (**Figure 25**).

#### 4.2 Effects of cSTX on the mucosal antimicrobial defense genes and insights into their role in immune driven disorders

Sympathetic and cholinergic nerves both innervate the GI wall but only sympathetic neurons extend to the mucosal layer (Brinkman et al., 2019a). In line, several studies highlighted the importance of the neuroimmune gut-brain axis in disease outcomes of IBD patients (Vanuytsel et al., 2014), in neurodegenerative diseases (Campos-Acuña et al., 2019), stroke mediated GI dysfunction (Huang et al., 2019), and in GI cancer (Zhang et al., 2020; Di et al., 2019). At the crypt base, intestinal stem cells differentiate to form various IECs, such as mucus-secreting goblet cells (Knoop und Newberry, 2018), antimicrobial-secreting paneth cells (Lueschow und McElroy, 2020), and peptide hormone-secreting enteroendocrine cells (Worthington et al., 2018). These IECs form a barrier between the host tissue and luminal microbes to maintain GI homeostasis (Peterson und Artis, 2014). The function of the intestinal epithelial barrier is modulated by protein complexes made of tight junctions, gap junctions, and desmosomes. Abnormal mucosal barrier function is associated with IBD (Alipour et al., 2016; Antoni et al., 2014). In addition, these IBD patients display dysfunction of ANS including enhanced sympathetic nerve function and attenuated vagal nerve function. Understanding the

immunomodulatory properties of the SNS provides a better understanding of their role in controlling excessive GI inflammatory responses. Although studies highlighted a specific role of SNS in regulating the mucosal immune responses (You et al., 2021; Willemze et al., 2019; Di Giovangiulio et al., 2015; González-Ariki und Husband, 1998), their impact on epithelial barrier integrity and defense responses are still evasive. To address this question, we abolished the SNS function in the gut by 6-OHDA induced STX and investigated its effect on epithelial barrier functions.

#### 4.2.1 cSTX affects epithelium barrier integrity and antimicrobial defense responses

As we interrupted SNS function in the gut, we speculated that it might affect  $\alpha$  and  $\beta$  receptor expression levels in the mucosa. In line with this, we observed reduced levels of these receptors indicating a direct effect of sympathetic depletion on various mucosal cells including macrophages, dendritic cells, and epithelial cells (Marino und Cosentino, 2013; Lundgren et al., 2011; Haber et al., 2017). Furthermore, altered levels of these receptors resulted in an increase in *IL-1 $\beta$* , and *TNF- $\alpha$*  response shaping the mucosal profile to a pro-inflammatory status. The intestinal epithelium acts as a protective barrier against the luminal environment with tight junctions playing a pivotal role. Several studies suggest the role of NE in modulating epithelial tight junction proteins (Luo et al. 2021; Geng et al. 2019). The hypothalamic–pituitary–adrenal axis is activated during psychological stress and releases NE into the circulatory system (Elenkov and Chrousos 2006). Tight junction protein levels of ZO-1, occludin, and claudin5 are decreased in the small intestine under psychological stress (Geng et al. 2019). In addition, an *in vitro* study showed that NE reduced the expression of tight junction protein occludin in Caco-2 cells (Luo et al. 2021). Whether SNS regulates epithelial tight junctions *in vivo* under healthy conditions was not previously investigated. By 3' bulk RNA sequencing, we found an enrichment of genes related to “*tight junctions*” in cSTX-treated mucosal samples and confirmed increased tight junction gene expression upon cSTX by qPCR, supporting a role of SNS in modulating epithelial tight junction gene responses *in vivo*. As the SNS plays a role in intestinal inflammation (Straub et al. 2006) and the loss of tight junction proteins and barrier integrity is part of IBD (Chelakkot et al. 2018), our data suggest a crucial role of the SNS in regulating inflammation at mucosal sites.

Interactions between neurons and IECs have been widely studied and the role of IECs in maintaining mucosal homeostasis is well documented (Sharkey et al. 2018). Goblet cells secrete TFF3, mucins, and antimicrobial peptides that protect the host against invading bacteria (Birchenough et al. 2015). Trefoil factors play a role in intestinal repair, wound healing, and restores mucosal homeostasis (Hoffmann 2005; Aihara et al. 2017). Interestingly, we observed increased levels of TFF3 in the mucosa of cSTX-treated mice. We speculate that loss of sympathetic neurons might cause disturbances in the epithelial cell homeostasis and therefore *TFF3* is enhanced to repair and restore homeostasis. Goblet cells form GAPs through muscarinic acetylcholine receptor (mAChR)- 4 signaling in the small intestine (Knoop et al. 2015). Through goblet-associated antigen passages (GAPs), goblet cells take up a variety of luminal antigens and deliver them to lamina propria dendritic cells (DCs) in the small intestine (McDole et al. 2012). This shows that cholinergic enteric and parasympathetic neurons might regulate luminal antigen sampling with goblet cells. Further, loss of goblet cells and reduced *Muc2* expression was observed

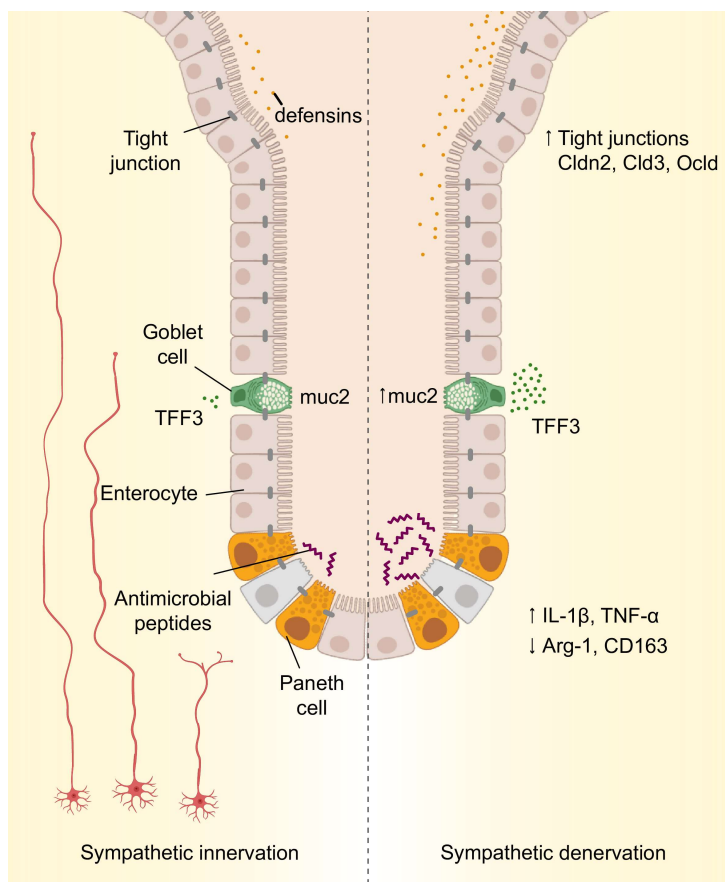


**Figure 26: Graphical abstract of the main findings in the mucosa**

In the presence of sympathetic innervation, the mucosal pro- and anti-inflammatory genes are regulated keeping the immune system under a balance to promote intestinal homeostasis. Upon sympathetic denervation, this regulatory balance is disturbed leading to increased levels of pro-inflammatory cytokines *IL-1 $\beta$* , and *TNF- $\alpha$* , and reduced levels of *Arg-1* and *CD163*. *TFF3*, a gene involved in mucosal repair is enhanced to restore homeostasis upon cSTX. Notably, the tight junction genes occludin (*ocld*), claudin-2 (*cld2*), and claudin-3 (*cldn3*), antimicrobial defense genes such as *Defa1*, *Reg3g*,  *$\beta$ 3 defensin*, *Muc2*, and *Lyz1* are elevated upon cSTX indicating a role of SNS in modulating epithelial biology under homeostasis.

in mice intraperitoneally treated with isoproterenol, a  $\beta$ -AR agonist. This study also described a pathological translocation of FITC dextran in mice treated with isoproterenol (Sorribas et al. 2020) indicating a negative effect of  $\beta$ -AR activation in modulating epithelial cell functions. Therefore, we hypothesized that enteric and parasympathetic neurons and SNS might play a role in modulating goblet cell functions. In line, 3' bulk RNA sequencing, revealed an enrichment of genes related to the GO immune term "*antibacterial humoral response*" upon cSTX indicating elevated levels of antimicrobial defense genes. By qPCR analysis, we also confirmed increased mRNA levels of *Muc2*, *Defa1*,  *$\beta$ 3-defensins*, *Lyz1*, and *Reg3g* upon denervation suggesting a role of SNS in modulating the epithelial defense responses (**Figure 26**). Dysregulation of IECs increases luminal translocation that activates an acute inflammatory response in the GI tract as observed in IBD (Ananthakrishnan et al. 2018). Although dysbiosis signatures of the gut microbiome largely contribute to mucosal inflammatory diseases, the underlying mechanism in IBD remains largely unknown. Further, other factors such as failed immune response against luminal agents (Smith et al. 2009), reduced defensins, and anti-microbial peptides (Wehkamp et al. 2005) are shown to play a significant role in the pathogenesis of IBD. Recently, a study showed a decrease in *Reg3 $\gamma$*  upon surgical STX in the ileum of an acute DSS-induced colitis mouse model, indicating a regulatory role of SNS in mucosal inflammation (Willemze et al. 2019). Based on these data, more studies on human material and clinical studies are now necessary to understand the role of SNS in mucosal inflammation in humans.

#### 4.3 Concluding remarks

In summary, in the muscularis externa, we show that SNS plays a distinct role in immune-modulation of resident CX3CR1<sup>+</sup> macrophage functions in health and disease. cSTX reduced macrophage anti-inflammatory genes under baseline conditions and shaped the muscularis externa profile to a pro-inflammatory pattern. Upon intestinal manipulation, sorted CX3CR1<sup>+</sup> resident macrophages from sympathectomized mice showed reduced anti-inflammatory genes favorable in diminishing leukocyte immune infiltration into the muscularis externa and simultaneously improving the bowel motility. Therefore, preoperative cSTX was beneficial in reducing muscularis inflammation symptoms during POI.

In the mucosa, sympathetic neurons play an essential role in regulating mucosal epithelial cell function. The SNS affects the integrity and antimicrobial capacity of the epithelium. After cSTX, the expression level of adrenergic receptors is altered and the mucosal profile is shaped towards a pro-inflammatory status. Elevated levels of tight junctions and antimicrobial defense genes are observed in the absence of sympathetic neurons. Finally, our study suggests the role of SNS in mucosal inflammatory disorders.

## 5. Abstract

**Introduction:** The sympathetic nervous system (SNS) innervates large parts of the gastrointestinal tract. Its projections are densely found in tunica muscularis externa and reach up to the mucosa, the innermost part of the bowel. In the muscularis externa, tyrosine hydroxylase-expressing (TH<sup>+</sup>) sympathetic neurons govern immune modulation by regulating the functions of resident macrophages in their proximity. These macrophages modulate muscularis inflammation during postoperative ileus (POI), a non-infectious, clinically relevant immune motility disorder. However, whether the SNS modulates macrophage functions *in vivo* during POI is unknown. Notably, the SNS projections are also found in the submucosa, close to the epithelium, where they regulate mucosal immunity. Due to its close association, the role of SNS in epithelial antimicrobial defense is highly likely but has not been elucidated so far.

**Methods:** We tested different sympathectomy (STX) models to ablate the intestinal sympathetic innervation. With the chemical STX (cSTX) approach using 6-OHDA treatment, we abolished TH<sup>+</sup> sympathetic neurons from the GI tract and interrupted both neuro-immune and neuro-epithelial sympathetic connections to investigate its impact on the gut inflammatory status in homeostasis and a mouse model of POI.

**Results:** In the muscularis externa, the resident CX3CR1<sup>+</sup> muscularis macrophages anti-inflammatory gene response was reduced after cSTX and the muscularis externa profile was shaped towards a pro-inflammatory status. The cSTX mediated reduction of macrophage anti-inflammatory genes was also observed in the early postoperative phase of POI. At the late and clinically relevant phase of POI, leukocyte infiltration into muscularis was reduced with a quicker recovery of bowel motility. On the mucosal level, cSTX affected the pro-inflammatory status and increased the expression of tight junctions and antimicrobial defense genes, indicating an influence of the SNS in modulating both epithelial cell and immune cell functions in intestinal homeostasis.

**Conclusion:** In summary, our data show that in the muscularis externa, the SNS plays a pivotal role in postoperative inflammation and highlights the role of resident CX3CR1<sup>+</sup> muscularis macrophages as mediators of sympathetic actions. In the mucosa, the SNS modulates tight epithelial junction and antimicrobial gene expression under homeostasis.

Keywords

CX3CR1+, Muscularis Macrophages, Muscularis externa, Sympathetic denervation, post-operative ileus.

## 6. List of Figures

Figure 1: Schematic view of the intestinal wall showing the organization of different layers. ....	11
Figure 2: Epithelial cells of the intestine .....	13
Figure 3: Organization of the three anatomical branches of the peripheral autonomous nervous system. ....	15
Figure 4: Distribution of macrophages in different layers of the intestine .....	20
Figure 5: The two phases of POI triggered by abdominal surgery .....	22
Figure 6: Schematic representation of inflammatory cascade after intestinal manipulation .....	23
Figure 7: A genetic SNS denervation approach relied on a TH-Cre driver line .....	45
Figure 8: A surgical SNS denervation approach that is intestine-specific. ....	46
Figure 9: Selection of the right dosage for the chemical SNS denervation approach ....	47
Figure 10: 6-OHDA approach depletes TH <sup>+</sup> neurons in the GI tract.....	48
Figure 11: cSTX of TH <sup>+</sup> sympathetic neurons in the gut 60 days after 6-OHDA treatment .....	49
Figure 12: Selection of the denervation approach targeting only sympathetic neurons. ....	50
Figure 13: Bodyweight measurement after the treatment with 6-OHDA.....	51
Figure 14: Leukocyte immune cell infiltration into muscularis upon cSTX-treatment.....	53
Figure 15: RNA sequencing of the vehicle and cSTX-treated muscularis externa samples.....	54
Figure 16: Changes on resident CX3CR1 <sup>+</sup> macrophages upon cSTX .....	56
Figure 17: Resident CX3CR1 <sup>+</sup> macrophage anti- and pro-inflammatory gene response upon stimulation with M-CSF/LPS .....	57
Figure 18: Changes in the muscularis externa upon cSTX in the early phase of POI....	58
Figure 19: Resident CX3CR1 <sup>+</sup> macrophage anti- and pro-inflammatory gene response upon cSTX in the early phase of POI.....	60
Figure 20: Functional outcome upon cSTX in the late or effector phase of POI.....	61
Figure 21: Effects of cSTX at the late phase of POI.....	62
Figure 22: Effects of cSTX in the mucosa .....	64
Figure 23: Effects of cSTX on epithelium tight junctions .....	66

Figure 24: Antibacterial humoral response in the mucosa upon cSTX..... 67  
Figure 25: Graphical abstract of the findings of this thesis in the muscuaris externa. .... 77  
Figure 26: Graphical abstract of the main findings in the mucosa..... 80

## 7. List of tables

Table 1	Devices
Table 2	Consumable materials
Table 3	Reagents
Table 4	Chemicals
Table 5	Buffers and solutions
Table 6	Kits
Table 7	Antibodies
Table 8	Primer sequences
Table 9	Mouse lines
Table 10	Softwares

## 8. References

- Ağaç D, Estrada LD, Maples R, Hooper LV, Farrar JD. The  $\beta$ 2-adrenergic receptor controls inflammation by driving rapid IL-10 secretion. *Brain, behavior, and immunity* 2018a; 74: 176–185
- Ağaç D, Estrada LD, Maples R, Hooper LV, Farrar JD. The  $\beta$ 2-adrenergic receptor controls inflammation by driving rapid IL-10 secretion. *Brain, behavior, and immunity* 2018b; 74: 176–185
- Alipour M, Zaidi D, Valcheva R, Jovel J, Martínez I, Sergi C, Walter J, Mason AL, Wong GK-S, Dieleman LA, Carroll MW, Huynh HQ, Wine E. Mucosal Barrier Depletion and Loss of Bacterial Diversity are Primary Abnormalities in Paediatric Ulcerative Colitis. *Journal of Crohn's & Colitis* 2016; 10: 462–471
- Altaf MA, Sood MR. The nervous system and gastrointestinal function. *Developmental disabilities research reviews* 2008; 14: 87–95
- Amit I, Winter DR, Jung S. The role of the local environment and epigenetics in shaping macrophage identity and their effect on tissue homeostasis. *Nat Immunol* 2016; 17: 18–25
- Andersson U, Tracey KJ. Reflex principles of immunological homeostasis. *Annual review of immunology* 2012; 30: 313–335
- Antoni L, Nuding S, Wehkamp J, Stange EF. Intestinal barrier in inflammatory bowel disease. *World Journal of Gastroenterology : WJG* 2014; 20: 1165–1179
- Arlaukas S, Oh N, Li R, Weissleder R, Miller MA. Macrophage imaging and subset analysis using single-cell RNA sequencing. *Nanotheranostics* 2021; 5: 36–56
- Backer O de, Elinck E, Blanckaert B, Leybaert L, Motterlini R, Lefebvre RA. Water-soluble CO-releasing molecules reduce the development of postoperative ileus via modulation of MAPK/HO-1 signalling and reduction of oxidative stress. *Gut* 2009; 58: 347–356
- Bain CC, Bravo-Blas A, Scott CL, Perdiguero EG, Geissmann F, Henri S, Malissen B, Osborne LC, Artis D, Mowat AM. Constant replenishment from circulating monocytes maintains the macrophage pool in the intestine of adult mice. *Nat Immunol* 2014; 15: 929–937

- Bain CC, Mowat AM. Macrophages in intestinal homeostasis and inflammation. *Immunological Reviews* 2014; 260: 102–117
- Bain CC, Schridde A. Origin, Differentiation, and Function of Intestinal Macrophages. *Front. Immunol.* 2018; 9: 2733
- Barquist E, Bonaz B, Martinez V, Rivier J, Zinner MJ, Taché Y. Neuronal pathways involved in abdominal surgery-induced gastric ileus in rats. *The American journal of physiology* 1996; 270: R888-94
- Berthoud H-R, Powley TL. Characterization of vagal innervation to the rat celiac, suprarenal and mesenteric ganglia. *Journal of the Autonomic Nervous System* 1993; 42: 153–169
- Berthoud H-R, Powley TL. Interaction between parasympathetic and sympathetic nerves in prevertebral ganglia: Morphological evidence for vagal efferent innervation of ganglion cells in the rat. *Microsc. Res. Tech.* 1996; 35: 80–86
- Bevins CL, Salzman NH. Paneth cells, antimicrobial peptides and maintenance of intestinal homeostasis. *Nat Rev Microbiol* 2011; 9: 356–368
- Birch D, Knight GE, Boulos PB, Burnstock G. Analysis of innervation of human mesenteric vessels in non-inflamed and inflamed bowel--a confocal and functional study. *Neurogastroenterology & Motility* 2008; 20: 660–670
- Boeckxstaens GE, Hirsch DP, Kodde A, Moojen TM, Blackshaw A, Tytgat GN, Blommaert PJ. Activation of an adrenergic and vagally-mediated NANC pathway in surgery-induced fundic relaxation in the rat. *Neurogastroenterology and motility : the official journal of the European Gastrointestinal Motility Society* 1999; 11: 467–474
- Boeckxstaens GE, Jonge WJ de. Neuroimmune mechanisms in postoperative ileus. *Gut* 2009; 58: 1300–1311
- Bonaz B, Sinniger V, Pellissier S. The Vagus Nerve in the Neuro-Immune Axis: Implications in the Pathology of the Gastrointestinal Tract. *Front. Immunol.* 2017; 8: 1452
- Borden P, Houtz J, Leach SD, Kuruvilla R. Sympathetic innervation during development is necessary for pancreatic islet architecture and functional maturation. *Cell reports* 2013; 4: 287–301

Borovikova LV, Ivanova S, Zhang M, Yang H, Botchkina GI, Watkins LR, Wang H, Abumrad N, Eaton JW, Tracey KJ. Vagus nerve stimulation attenuates the systemic inflammatory response to endotoxin. *Nature* 2000; 405: 458–462

Bowcutt R, Forman R, Glymenaki M, Carding SR, Else KJ, Cruickshank SM. Heterogeneity across the murine small and large intestine. *World Journal of Gastroenterology : WJG* 2014; 20: 15216–15232

Brinkman DJ, Hove AS ten, Vervoordeldonk MJ, Luyer MD, Jonge WJ de. Neuroimmune Interactions in the Gut and Their Significance for Intestinal Immunity. *Cells* 2019a; 8

Brinkman DJ, Hove AS ten, Vervoordeldonk MJ, Luyer MD, Jonge WJ de. Neuroimmune Interactions in the Gut and Their Significance for Intestinal Immunity. *Cells* 2019b; 8

Browning KN, Travagli RA. Central nervous system control of gastrointestinal motility and secretion and modulation of gastrointestinal functions. *Comprehensive Physiology* 2014; 4: 1339–1368

Bucinskaite V, Kurosawa M, Lundeberg T. Exogenous cholecystokinin-8 reduces vagal efferent nerve activity in rats through CCK(A) receptors. *British Journal of Pharmacology* 2000; 129: 1649–1654

Bueno L, Fioramonti J, Delvaux M, Frexinos J. Mediators and pharmacology of visceral sensitivity: From basic to clinical investigations. *Gastroenterology* 1997; 112: 1714–1743

Bueno L, Fioramonti J, Ruckebusch Y. Postoperative intestinal motility in dogs and sheep. *The American journal of digestive diseases* 1978; 23: 682–689

Burgueño JF, Barba A, Eyre E, Romero C, Neunlist M, Fernández E. TLR2 and TLR9 modulate enteric nervous system inflammatory responses to lipopolysaccharide. *Journal of Neuroinflammation* 2016; 13: 187

Cailotto C, Gomez-Pinilla PJ, Costes LM, van der Vliet J, Di Giovangiulio M, Némethova A, Matteoli G, Boeckxstaens GE. Neuro-anatomical evidence indicating indirect modulation of macrophages by vagal efferents in the intestine but not in the spleen. *PLoS ONE* 2014; 9: e87785

Calvani M, Dabraio A, Bruno G, Gregorio V de, Coronello M, Bogani C, Ciullini S, La Marca G, Vignoli M, Chiarugi P, Nardi M, Vannucchi AM, Filippi L, Favre C.  $\beta$ 3-

Adrenoreceptor Blockade Reduces Hypoxic Myeloid Leukemic Cells Survival and Chemoresistance. *International Journal of Molecular Sciences* 2020; 21

Campos-Acuña J, Elgueta D, Pacheco R. T-Cell-Driven Inflammation as a Mediator of the Gut-Brain Axis Involved in Parkinson's Disease. *Front. Immunol.* 2019; 10: 239

Catala M, Kubis N. Chapter 3 - Gross anatomy and development of the peripheral nervous system. In: Said G, Krarup C, Hrsg. *Handbook of Clinical Neurology : Peripheral Nerve Disorders*: Elsevier, 2013: 29–41

Cheng H, Leblond CP. Origin, differentiation and renewal of the four main epithelial cell types in the mouse small intestine. V. Unitarian Theory of the origin of the four epithelial cell types. *The American journal of anatomy* 1974; 141: 537–561

Choi KM, Kashyap PC, Dutta N, Stoltz GJ, Ordog T, Shea Donohue T, Bauer AJ, Linden DR, Szurszewski JH, Gibbons SJ, Farrugia G. CD206-positive M2 macrophages that express heme oxygenase-1 protect against diabetic gastroparesis in mice. *Gastroenterology* 2010; 138: 2399-409, 2409.e1

Clevers H. The intestinal crypt, a prototype stem cell compartment. *Cell* 2013; 154: 274–284

Cohen G, Heikkila RE, Allis B, Cabbat F, Dembiec D, MacNamee D, Mytilineou C, Winston B. Destruction of sympathetic nerve terminals by 6-hydroxydopamine: protection by 1-phenyl-3-(2-thiazolyl)-2-thiourea, diethyldithiocarbamate, methimazole, cysteamine, ethanol and n-butanol. *The Journal of pharmacology and experimental therapeutics* 1976; 199: 336–352

Coldwell JR, Phillis BD, Sutherland K, Howarth GS, Blackshaw LA. Increased responsiveness of rat colonic splanchnic afferents to 5-HT after inflammation and recovery. *The Journal of Physiology* 2007; 579: 203–213

Collins JT, Nguyen A, Badireddy M. *StatPearls* 2021

Cummings DE, Overduin J. Gastrointestinal regulation of food intake. *Journal of Clinical Investigation* 2007; 117: 13–23

Cummings RJ, Barbet G, Bongers G, Hartmann BM, Gettler K, Muniz L, Furtado GC, Cho J, Lira SA, Blander JM. Different tissue phagocytes sample apoptotic cells to direct distinct

homeostasis programs. *Nature* 2016; 539: 565–569

Desalegn G, Pabst O. Inflammation triggers immediate rather than progressive changes in monocyte differentiation in the small intestine. *Nat Commun* 2019; 10: 3229

Di Y-Z, Han B-S, Di J-M, Liu W-Y, Tang Q. Role of the brain-gut axis in gastrointestinal cancer. *World Journal of Clinical Cases* 2019; 7: 1554–1570

Di Giovangiulio M, Verheijden S, Bosmans G, Stakenborg N, Boeckxstaens GE, Matteoli G. The Neuromodulation of the Intestinal Immune System and Its Relevance in Inflammatory Bowel Disease. *Front. Immunol.* 2015; 6: 590

Eaker EY, Bixler GB, Dunn AJ, Moreshead WV, Mathias JR. Dopamine and norepinephrine in the gastrointestinal tract of mice and the effects of neurotoxins. *The Journal of pharmacology and experimental therapeutics* 1988; 244: 438–442

Engel DR, Koscielny A, Wehner S, Maurer J, Schiwon M, Franken L, Schumak B, Limmer A, Sparwasser T, Hirner A, Knolle PA, Kalff JC, Kurts C. T helper type 1 memory cells disseminate postoperative ileus over the entire intestinal tract. *Nature medicine* 2010; 16: 1407–1413

Farro G, Stakenborg M, Gomez-Pinilla PJ, Labeeuw E, Goverse G, Di Giovangiulio M, Stakenborg N, Meroni E, D'Errico F, Elkrim Y, Laoui D, Lisowski ZM, Sauter KA, Hume DA, van Ginderachter JA, Boeckxstaens GE, Matteoli G. CCR2-dependent monocyte-derived macrophages resolve inflammation and restore gut motility in postoperative ileus. *Gut* 2017; 66: 2098–2109

Furness JB. The enteric nervous system and neurogastroenterology. *Nat Rev Gastroenterol Hepatol* 2012; 9: 286–294

Furness JB, Callaghan BP, Rivera LR, Cho H-J. The Enteric Nervous System and Gastrointestinal Innervation: Integrated Local and Central Control. In: Lyte M, Cryan JF, Hrsg. *Microbial Endocrinology: The Microbiota-Gut-Brain Axis in Health and Disease*. Boston, MA: Springer US, 2014: 39–71

Gabanyi I, Muller PA, Feighery L, Oliveira TY, Costa-Pinto FA, Mucida D. Neuro-immune Interactions Drive Tissue Programming in Intestinal Macrophages. *Cell* 2016; 164: 378–391

- Gallo RL, Hooper LV. Epithelial antimicrobial defence of the skin and intestine. *Nat Rev Immunol* 2012; 12: 503–516
- Ghia J-E, Blennerhassett P, El-Sharkawy RT, Collins SM. The protective effect of the vagus nerve in a murine model of chronic relapsing colitis. *American journal of physiology. Gastrointestinal and liver physiology* 2007; 293: G711-8
- Glebova NO, Ginty DD. Heterogeneous requirement of NGF for sympathetic target innervation in vivo. *The Journal of Neuroscience* 2004; 24: 743–751
- Glinka Y, Gassen M, Youdim MB. Mechanism of 6-hydroxydopamine neurotoxicity. *Journal of neural transmission. Supplementum* 1997; 50: 55–66
- González-Ariki S, Husband AJ. The role of sympathetic innervation of the gut in regulating mucosal immune responses. *Brain, behavior, and immunity* 1998; 12: 53–63
- Grubišić V, Gulbransen BD. Enteric glia: the most alimentary of all glia. *The Journal of Physiology* 2017; 595: 557–570
- Haber AL, Biton M, Rogel N, Herbst RH, Shekhar K, Smillie C, Burgin G, Delorey TM, Howitt MR, Katz Y, Tirosh I, Beyaz S, Dionne D, Zhang M, Raychowdhury R, Garrett WS, Rozenblatt-Rosen O, Shi HN, Yilmaz O, Xavier RJ, Regev A. A single-cell survey of the small intestinal epithelium. *Nature* 2017; 551: 333–339
- Halbgebauer R, Kellermann S, Schäfer F, Weckbach S, Weiss M, Barth E, Bracht H, Kalbitz M, Gebhard F, Huber-Lang MS, Perl M. Functional immune monitoring in severely injured patients-A pilot study. *Scandinavian journal of immunology* 2020; 91: e12837
- Hamilton TA, Zhao C, Pavicic PG, Datta S. Myeloid colony-stimulating factors as regulators of macrophage polarization. *Front. Immunol.* 2014; 5: 554
- Han S, Chen Z, Han P, Hu Q, Xiao Y. Activation of Macrophages by Lipopolysaccharide for Assessing the Immunomodulatory Property of Biomaterials<sup>Tissue engineering. Part A 2017; 23: 1100–1109
- Han W, Tellez LA, Perkins MH, Perez IO, Qu T, Ferreira J, Ferreira TL, Quinn D, Liu Z-W, Gao X-B, Kaelberer MM, Bohórquez DV, Shammah-Lagnado SJ, Lartigue G de, Araujo IE de. A Neural Circuit for Gut-Induced Reward. *Cell* 2018; 175: 665-678.e23
- Hernandez-Baltazar D, Zavala-Flores LM, Villanueva-Olivo A. The 6-hydroxydopamine

model and parkinsonian pathophysiology: Novel findings in an older model. *Neurología (English Edition)* 2017; 32: 533–539

Heuckeroth RO. Hirschsprung disease - integrating basic science and clinical medicine to improve outcomes. *Nat Rev Gastroenterol Hepatol* 2018; 15: 152–167

Holte K, Kehlet H. Postoperative ileus: progress towards effective management. *Drugs* 2002; 62: 2603–2615

Honda T, Wada E, Battey JF, Wank SA. Differential Gene Expression of CCKA and CCKB Receptors in the Rat Brain. *Molecular and Cellular Neuroscience* 1993; 4: 143–154

Hori M, Kita M, Torihashi S, Miyamoto S, Won KJ, Sato K, Ozaki H, Karaki H. Upregulation of iNOS by COX-2 in muscularis resident macrophage of rat intestine stimulated with LPS. *American journal of physiology. Gastrointestinal and liver physiology* 2001; 280: G930-8

Hu D, Al-Shalan HAM, Shi Z, Wang P, Wu Y, Nicholls PK, Greene WK, Ma B. Distribution of nerve fibers and nerve-immune cell association in mouse spleen revealed by immunofluorescent staining. *Sci Rep* 2020; 10: 9850

Huang Y-y, Li X, Li X, Sheng Y-Y, Zhuang P-W, Zhang Y-J. Neuroimmune crosstalk in central nervous system injury-induced infection and pharmacological intervention. *Brain Research Bulletin* 2019; 153: 232–238

Hupa KJ, Stein K, Schneider R, Lysson M, Schneiker B, Hornung V, Latz E, Iwakura Y, Kalff JC, Wehner S. AIM2 inflammasome-derived IL-1 $\beta$  induces postoperative ileus in mice. *Sci Rep* 2019; 9: 10602

Jacobson A, Yang D, Vella M, Chiu IM. The intestinal neuro-immune axis: crosstalk between neurons, immune cells, and microbes. *Mucosal Immunol* 2021; 14: 555–565

Jaensson E, Uronen-Hansson H, Pabst O, Eksteen B, Tian J, Coombes JL, Berg P-L, Davidsson T, Powrie F, Johansson-Lindbom B, Agace WW. Small intestinal CD103+ dendritic cells display unique functional properties that are conserved between mice and humans. *The Journal of Experimental Medicine* 2008; 205: 2139–2149

Jakob MO, Murugan S, Klose CSN. Neuro-Immune Circuits Regulate Immune Responses in Tissues and Organ Homeostasis. *Front. Immunol.* 2020; 11: 308

Jänig W. Autonomic Nervous System. In: Schmidt RF, Thews G, Hrsg. *Human*

Physiology. Berlin, Heidelberg: Springer Berlin Heidelberg, 1989: 333–370

Johnson CD, Barlow-Anacker AJ, Pierre JF, Touw K, Erickson CS, Furness JB, Epstein ML, Gosain A. Deletion of choline acetyltransferase in enteric neurons results in postnatal intestinal dysmotility and dysbiosis. *The FASEB Journal* 2018; 32: 4744–4752

Jonge WJ de, van den Wijngaard RM, The FO, Beek M-L ter, Bennink RJ, Tytgat GNJ, Buijs RM, Reitsma PH, van Deventer SJ, Boeckxstaens GE. Postoperative ileus is maintained by intestinal immune infiltrates that activate inhibitory neural pathways in mice<sup>1</sup> The authors thank Prof. Yvette van Kooyk, Department of Molecular Cell Biology, Free University, Amsterdam, for her gift of blocking antibodies; Drs. Formijn van Hemert and Cynara Veeris, Department of Nuclear Medicine, Academic Medical Center, Amsterdam, for their assistance in the gastric emptying studies; and Dr. Jan M. Ruijter, Department of Anatomy and Embryology, Academic Medical Center, Amsterdam, for statistical assistance. *Gastroenterology* 2003; 125: 1137–1147

Jung S, Aliberti J, Graemmel P, Sunshine MJ, Kreutzberg GW, Sher A, Littman DR. Analysis of fractalkine receptor CX(3)CR1 function by targeted deletion and green fluorescent protein reporter gene insertion. *Molecular and cellular biology* 2000; 20: 4106–4114

Kalff JC, Buchholz BM, Eskandari MK, Hierholzer C, Schraut WH, Simmons RL, Bauer AJ. Biphasic response to gut manipulation and temporal correlation of cellular infiltrates and muscle dysfunction in rat. *Surgery* 1999a; 126: 498–509

Kalff JC, Carlos TM, Schraut WH, Billiar TR, Simmons RL, Bauer AJ. Surgically induced leukocytic infiltrates within the rat intestinal muscularis mediate postoperative ileus. *Gastroenterology* 1999b; 117: 378–387

Kalff JC, Schraut WH, Simmons RL, Bauer AJ. Surgical manipulation of the gut elicits an intestinal muscularis inflammatory response resulting in postsurgical ileus. *Annals of Surgery* 1998; 228: 652–663

Kenney MJ, Ganta CK. Autonomic nervous system and immune system interactions. *Comprehensive Physiology* 2014; 4: 1177–1200

Kim SY, Nair MG. Macrophages in wound healing: activation and plasticity. *Immunology and cell biology* 2019; 97: 258–267

- Knoop KA, Newberry RD. Goblet cells: multifaceted players in immunity at mucosal surfaces. *Mucosal Immunol* 2018; 11: 1551–1557
- Kolter J, Kierdorf K, Henneke P. Origin and Differentiation of Nerve-Associated Macrophages. *Journal of immunology (Baltimore, Md. : 1950)* 2020; 204: 271–279
- Kreis ME, Kasperek MS, Becker HD, Jehle EC, Zittel TT. Postoperativer Ileus: Teil II (Klinische Therapie). *Zentralbl Chir* 2003; 128: 320–328
- Kreiss C, Birder LA, Kiss S, VanBibber MM, Bauer AJ. COX-2 dependent inflammation increases spinal Fos expression during rodent postoperative ileus. *Gut* 2003; 52: 527–534
- Kyösola K, Penttilä O, Salaspuro M. Rectal mucosal adrenergic innervation and enterochromaffin cells in ulcerative colitis and irritable colon. *Scandinavian journal of gastroenterology* 1977; 12: 363–367
- Lee B, Moon KM, Kim CY. Tight Junction in the Intestinal Epithelium: Its Association with Diseases and Regulation by Phytochemicals. *Journal of Immunology Research* 2018; 2018: 2645465
- Leopold Wager CM, Wormley FL. Classical versus alternative macrophage activation: the Ying and the Yang in host defense against pulmonary fungal infections. *Mucosal Immunol* 2014; 7: 1023–1035
- Liu W-F, Wen S-H, Zhan J-H, Li Y-S, Shen J-T, Yang W-J, Zhou X-W, Liu K-X. Treatment with Recombinant *Trichinella spiralis* Cathepsin B-like Protein Ameliorates Intestinal Ischemia/Reperfusion Injury in Mice by Promoting a Switch from M1 to M2 Macrophages. *Journal of immunology (Baltimore, Md. : 1950)* 2015; 195: 317–328
- Lomax AE, Sharkey KA, Furness JB. The participation of the sympathetic innervation of the gastrointestinal tract in disease states. *Neurogastroenterology and motility : the official journal of the European Gastrointestinal Motility Society* 2010; 22: 7–18
- Lueschow SR, McElroy SJ. The Paneth Cell: The Curator and Defender of the Immature Small Intestine. *Front. Immunol.* 2020; 11: 587
- Lundgren O, Jodal M, Jansson M, Ryberg AT, Svensson L. Intestinal epithelial stem/progenitor cells are controlled by mucosal afferent nerves. *PLoS ONE* 2011; 6:

e16295

Manara L, Croci T, Aureggi G, Guagnini F, Maffrand JP, Le Fur G, Mukenge S, Ferla G. Functional assessment of beta adrenoceptor subtypes in human colonic circular and longitudinal (taenia coli) smooth muscle. *Gut* 2000; 47: 337–342

Marino F, Cosentino M. Adrenergic modulation of immune cells: an update. *Amino Acids* 2013; 45: 55–71

Matheis F, Muller PA, Graves CL, Gabanyi I, Kerner ZJ, Costa-Borges D, Ahrends T, Rosenstiel P, Mucida D. Adrenergic Signaling in Muscularis Macrophages Limits Infection-Induced Neuronal Loss. *Cell* 2020; 180: 64-78.e16

McCafferty DM, Wallace JL, Sharkey KA. Effects of chemical sympathectomy and sensory nerve ablation on experimental colitis in the rat. *The American journal of physiology* 1997; 272: G272-80

Mikkelsen HB. Interstitial cells of Cajal, macrophages and mast cells in the gut musculature: morphology, distribution, spatial and possible functional interactions. *Journal of Cellular and Molecular Medicine* 2010; 14: 818–832

Mikkelsen HB, Thuneberg L. Op/op mice defective in production of functional colony-stimulating factor-1 lack macrophages in muscularis externa of the small intestine. *Cell and tissue research* 1999; 295: 485–493

Mikkelsen HB, Thuneberg L, Rumessen JJ, Thorball N. Macrophage-like cells in the muscularis externa of mouse small intestine. *The Anatomical record* 1985; 213: 77–86

Mittal R, Coopersmith CM. Redefining the gut as the motor of critical illness. *Trends in molecular medicine* 2014; 20: 214–223

Moran TH. Gut peptides in the control of food intake. *Int J Obes* 2009; 33 Suppl 1: S7-10

Mueller MH, Glatzle J, Kampiloglou D, Kasperek MS, Grundy D, Kreis ME. Differential sensitization of afferent neuronal pathways during postoperative ileus in the mouse jejunum. *Annals of Surgery* 2008; 247: 791–802

Mueller MH, Karpitschka M, Gao Z, Mittler S, Kasperek MS, Renz B, Sibaevev A, Glatzle J, Li Y, Kreis ME. Vagal innervation and early postoperative ileus in mice. *J Gastrointest Surg* 2011; 15: 891-900; discussion 900-1

Muller PA, Koscsó B, Rajani GM, Stevanovic K, Berres M-L, Hashimoto D, Mortha A, Leboeuf M, Li X-M, Mucida D, Stanley ER, Dahan S, Margolis KG, Gershon MD, Merad M, Bogunovic M. Crosstalk between muscularis macrophages and enteric neurons regulates gastrointestinal motility. *Cell* 2014; 158: 300–313

Nasser H, Adhikary P, Abdel-Daim A, Noyori O, Panaampon J, Kariya R, Okada S, Ma W, Baba M, Takizawa H, Yamane M, Niwa H, Suzu S. Establishment of bone marrow-derived M-CSF receptor-dependent self-renewing macrophages. *Cell Death Discov.* 2020; 6: 63

Nasser Y, Ho W, Sharkey KA. Distribution of adrenergic receptors in the enteric nervous system of the guinea pig, mouse, and rat. *The Journal of comparative neurology* 2006; 495: 529–553

Nijhuis LE, Olivier BJ, Dhawan S, Hilbers FW, Boon L, Wolkers MC, Samsom JN, Jonge WJ de. Adrenergic  $\beta$ 2 receptor activation stimulates anti-inflammatory properties of dendritic cells in vitro. *PLoS ONE* 2014; 9: e85086

Niu X, Liu L, Wang T, Chuan X, Yu Q, Du M, Gu Y, Wang L. Mapping of Extrinsic Innervation of the Gastrointestinal Tract in the Mouse Embryo. *The Journal of neuroscience : the official journal of the Society for Neuroscience* 2020; 40: 6691–6708

O'Carroll C, Fagan A, Shanahan F, Carmody RJ. Identification of a unique hybrid macrophage-polarization state following recovery from lipopolysaccharide tolerance. *Journal of immunology (Baltimore, Md. : 1950)* 2014; 192: 427–436

Olivier BJ, Cailotto C, van der Vliet J, Knippenberg M, Greuter MJ, Hilbers FW, Konijn T, te Velde AA, Nolte MA, Boeckxstaens GE, Jonge WJ de, Mebius RE. Vagal innervation is required for the formation of tertiary lymphoid tissue in colitis. *European Journal of Immunology* 2016; 46: 2467–2480

Orecchioni M, Ghosheh Y, Pramod AB, Ley K. Macrophage Polarization: Different Gene Signatures in M1(LPS+) vs. Classically and M2(LPS-) vs. Alternatively Activated Macrophages. *Front. Immunol.* 2019; 10: 1084

Ozaki H, Kawai T, Shuttleworth CW, Won K-J, Suzuki T, Sato K, Horiguchi H, Hori M, Karaki H, Torihashi S, Ward SM, Sanders KM. Isolation and characterization of resident macrophages from the smooth muscle layers of murine small intestine.

Neurogastroenterology and motility : the official journal of the European Gastrointestinal Motility Society 2004; 16: 39–51

Pellegrini C, Ippolito C, Segnani C, Dolfi A, Errede M, Virgintino D, Fornai M, Antonioli L, Garelli F, Nericcio A, Colucci R, Cerri S, Blandini F, Blandizzi C, Bernardini N. Pathological remodelling of colonic wall following dopaminergic nigrostriatal neurodegeneration. *Neurobiology of Disease* 2020; 139: 104821

Peterson LW, Artis D. Intestinal epithelial cells: regulators of barrier function and immune homeostasis. *Nat Rev Immunol* 2014; 14: 141–153

Plourde V, Wong HC, Walsh JH, Raybould HE, Taché Y. CGRP antagonists and capsaicin on celiac ganglia partly prevent postoperative gastric ileus. *Peptides* 1993; 14: 1225–1229

Randall KJ, Turton J, Foster JR. Explant culture of gastrointestinal tissue: a review of methods and applications. *Cell Biol Toxicol* 2011; 27: 267–284

Rao M, Gershon MD. The bowel and beyond: the enteric nervous system in neurological disorders. *Nat Rev Gastroenterol Hepatol* 2016; 13: 517–528

Raybould HE. Mechanisms of CCK signaling from gut to brain. *Current opinion in pharmacology* 2007; 7: 570–574

Rehfeld JF. Cholecystokinin—From Local Gut Hormone to Ubiquitous Messenger. *Front. Endocrinol.* 2017; 8: 47

Rosas-Ballina M, Olofsson PS, Ochani M, Valdés-Ferrer SI, Levine YA, Reardon C, Tusche MW, Pavlov VA, Andersson U, Chavan S, Mak TW, Tracey KJ. Acetylcholine-synthesizing T cells relay neural signals in a vagus nerve circuit. *Science (New York, N.Y.)* 2011; 334: 98–101

Sanders VM. The beta2-adrenergic receptor on T and B lymphocytes: do we understand it yet? *Brain, behavior, and immunity* 2012; 26: 195–200

Sanidad KZ, Yang H, Wang W, Ozay EI, Yang J, Gu M, Karner E, Zhang J, Kim D, Minter LM, Xiao H, Zhang G. Effects of Consumer Antimicrobials Benzalkonium Chloride, Benzethonium Chloride, and Chloroxylenol on Colonic Inflammation and Colitis-Associated Colon Tumorigenesis in Mice. *Toxicol Sci* 2018; 163: 490–499

Sass V, Schneider T, Wilmes M, Körner C, Tossi A, Novikova N, Shamova O, Sahl H-G.

Human beta-defensin 3 inhibits cell wall biosynthesis in Staphylococci. *Infection and immunity* 2010; 78: 2793–2800

Savitt JM, Jang SS, Mu W, Dawson VL, Dawson TM. Bcl-x is required for proper development of the mouse substantia nigra. *The Journal of Neuroscience* 2005; 25: 6721–6728

Schaefer N, Tahara K, Websky M von, Wehner S, Pech T, Tolba R, Abu-Elmagd K, Kalff JC, Hirner A, Türler A. Role of resident macrophages in the immunologic response and smooth muscle dysfunction during acute allograft rejection after intestinal transplantation. *Transplant international : official journal of the European Society for Organ Transplantation* 2008; 21: 778–791

Schank JR, Ventura R, Puglisi-Allegra S, Alcaro A, Cole CD, Liles LC, Seeman P, Weinschenker D. Dopamine beta-hydroxylase knockout mice have alterations in dopamine signaling and are hypersensitive to cocaine. *Neuropsychopharmacol* 2006; 31: 2221–2230

Scheibner J, Trendelenburg A-U, Hein L, Starke K, Blandizzi C. Alpha 2-adrenoceptors in the enteric nervous system: a study in alpha 2A-adrenoceptor-deficient mice. *British Journal of Pharmacology* 2002; 135: 697–704

Schepper S de, Stakenborg N, Matteoli G, Verheijden S, Boeckxstaens GE. Muscularis macrophages: Key players in intestinal homeostasis and disease. *Cellular Immunology* 2018a; 330: 142–150

Schepper S de, Stakenborg N, Matteoli G, Verheijden S, Boeckxstaens GE. Muscularis macrophages: Key players in intestinal homeostasis and disease. *Cellular Immunology* 2018b; 330: 142–150

Schepper S de, Verheijden S, Aguilera-Lizarraga J, Viola MF, Boesmans W, Stakenborg N, Voytyuk I, Schmidt I, Boeckx B, Dierckx de Casterlé I, Baekelandt V, Gonzalez Dominguez E, Mack M, Depoortere I, Strooper B de, Sprangers B, Himmelreich U, Soenen S, Guilliams M, Vanden Berghe P, Jones E, Lambrechts D, Boeckxstaens G. Self-Maintaining Gut Macrophages Are Essential for Intestinal Homeostasis. *Cell* 2018c; 175: 400-415.e13

Schneider R, Leven P, Glowka T, Kuzmanov I, Lysson M, Schneiker B, Miesen A, Baqi Y,

Spanier C, Grants I, Mazzotta E, Villalobos-Hernandez E, Kalff JC, Müller CE, Christofi FL, Wehner S. A novel P2X2-dependent purinergic mechanism of enteric gliosis in intestinal inflammation. *EMBO Molecular Medicine* 2020; e12724

Schneider T, Kruse T, Wimmer R, Wiedemann I, Sass V, Pag U, Jansen A, Nielsen AK, Mygind PH, Raventós DS, Neve S, Ravn B, Bonvin AMJJ, Maria L de, Andersen AS, Gammelgaard LK, Sahl H-G, Kristensen H-H. Plectasin, a fungal defensin, targets the bacterial cell wall precursor Lipid II. *Science (New York, N.Y.)* 2010; 328: 1168–1172

Seeley JJ, Ghosh S. Molecular mechanisms of innate memory and tolerance to LPS. *Journal of Leukocyte Biology* 2017; 101: 107–119

Seiler R, Rickenbacher A, Shaw S, Haefliger S, Balsiger BM. Role of selective alpha and beta adrenergic receptor mechanisms in rat jejunal longitudinal muscle contractility. *Journal of gastrointestinal surgery : official journal of the Society for Surgery of the Alimentary Tract* 2008; 12: 1087–1093

Sharkey KA, Beck PL, McKay DM. Neuroimmunophysiology of the gut: advances and emerging concepts focusing on the epithelium. *Nat Rev Gastroenterol Hepatol* 2018; 15: 765–784

Shingleton WW, Anlyan W. G., Hart D. Effects of vagotomy, splanchnicectomy and celiac ganglionectomy on experimentally produced spasm of sphincter of Oddi in animals. *Annals of Surgery* 1952; 135: 721–729

Simmons MA. The complexity and diversity of synaptic transmission in the prevertebral sympathetic ganglia. *Progress in Neurobiology* 1985; 24: 43–93

Stakenborg N, Gomez-Pinilla PJ, Boeckxstaens GE. Postoperative Ileus: Pathophysiology, Current Therapeutic Approaches. In: Greenwood-Van Meerveld B, Hrsg. *Gastrointestinal Pharmacology*. Cham: Springer International Publishing, 2017: 39–57

Stein K, Lysson M, Schumak B, Vilz T, Specht S, Heesemann J, Roers A, Kalff JC, Wehner S. Leukocyte-Derived Interleukin-10 Aggravates Postoperative Ileus. *Front. Immunol.* 2018; 9: 2599

Stengel A, Taché Y. Neuroendocrine control of the gut during stress: corticotropin-

releasing factor signaling pathways in the spotlight. *Annual review of physiology* 2009; 71: 219–239

Stoffels B, Hupa KJ, Snoek SA, van Bree S, Stein K, Schwandt T, Vilz TO, Lysson M, Veer CV't, Kummer MP, Hornung V, Kalff JC, Jonge WJ de, Wehner S. Postoperative ileus involves interleukin-1 receptor signaling in enteric glia. *Gastroenterology* 2014; 146: 176-87.e1

Strader AD, Woods SC. Gastrointestinal hormones and food intake. *Gastroenterology* 2005; 128: 175–191

Straub RH, Wiest R, Strauch UG, Härle P, Schölmerich J. The role of the sympathetic nervous system in intestinal inflammation. *Gut* 2006; 55: 1640–1649

Tack JF, Wood JD. Actions of noradrenaline on myenteric neurons in the guinea pig gastric antrum. *Journal of the Autonomic Nervous System* 1992; 41: 67–77

Tamada H, Kiyama H. Suppression of c-Kit signaling induces adult neurogenesis in the mouse intestine after myenteric plexus ablation with benzalkonium chloride. *Sci Rep* 2016; 6: 32100

Tan CMJ, Green P, Tapoulal N, Lewandowski AJ, Leeson P, Herring N. The Role of Neuropeptide Y in Cardiovascular Health and Disease. *Front. Physiol.* 2018; 9: 1281

The FO, Jonge WJ de, Bennink RJ, van den Wijngaard RM, Boeckxstaens GE. The ICAM-1 antisense oligonucleotide ISIS-3082 prevents the development of postoperative ileus in mice. *British Journal of Pharmacology* 2005; 146: 252–258

Tieu K. A guide to neurotoxic animal models of Parkinson's disease. *Cold Spring Harbor Perspectives in Medicine* 2011; 1: a009316

Torihashi S, Ozaki H, Hori M, Kita M, Ohta S, Karaki H. Resident macrophages activated by lipopolysaccharide suppress muscle tension and initiate inflammatory response in the gastrointestinal muscle layer. *Histochemistry and cell biology* 2000; 113: 73–80

Tracey KJ. The inflammatory reflex. *Nature* 2002; 420: 853–859

Tracey KJ. Reflex control of immunity. *Nat Rev Immunol* 2009; 9: 418–428

Türler A, Schnurr C, Nakao A, Tögel S, Moore BA, Murase N, Kalff JC, Bauer AJ. Endogenous endotoxin participates in causing a panenteric inflammatory ileus after

colonic surgery. *Annals of Surgery* 2007; 245: 734–744

Uesaka T, Young HM, Pachnis V, Enomoto H. Development of the intrinsic and extrinsic innervation of the gut. *Developmental Biology* 2016; 417: 158–167

van Itallie CM, Holmes J, Bridges A, Gookin JL, Coccaro MR, Proctor W, Colegio OR, Anderson JM. The density of small tight junction pores varies among cell types and is increased by expression of claudin-2. *Journal of cell science* 2008; 121: 298–305

Vanuytsel T, Vanormelingen C, Vanheel H, Masaoka T, Salim Rasoel S, Tóth J, Houben E, Verbeke K, Hertogh G de, Vanden Berghe P, Tack J, Farré R. From intestinal permeability to dysmotility: the biobreeding rat as a model for functional gastrointestinal disorders. *PLoS ONE* 2014; 9: e111132

Varol C, Vallon-Eberhard A, Elinav E, Aychek T, Shapira Y, Luche H, Fehling HJ, Hardt W-D, Shakhar G, Jung S. Intestinal lamina propria dendritic cell subsets have different origin and functions. *Immunity* 2009; 31: 502–512

Vasina V, Abu-Gharbieh E, Barbara G, Giorgio R de, Colucci R, Blandizzi C, Bernardini N, Croci T, Del Tacca M, Ponti F de. The beta3-adrenoceptor agonist SR58611A ameliorates experimental colitis in rats. *Neurogastroenterology & Motility* 2008; 20: 1030–1041

Vather R, O'Grady G, Bissett IP, Dinning PG. Postoperative ileus: mechanisms and future directions for research. *Clinical and Experimental Pharmacology and Physiology* 2014; 41: 358–370

Vaughan-Shaw PG, Fecher IC, Harris S, Knight JS. A meta-analysis of the effectiveness of the opioid receptor antagonist alvimopan in reducing hospital length of stay and time to GI recovery in patients enrolled in a standardized accelerated recovery program after abdominal surgery. *Diseases of the colon and rectum* 2012; 55: 611–620

Veiga-Fernandes H, Pachnis V. Neuroimmune regulation during intestinal development and homeostasis. *Nat Immunol* 2017; 18: 116–122

Verheijden S, Boeckxstaens GE. Neuroimmune interaction and the regulation of intestinal immune homeostasis. *American journal of physiology. Gastrointestinal and liver physiology* 2018; 314: G75-G80

- Vilz TO, Overhaus M, Stoffels B, Websky M von, Kalff JC, Wehner S. Functional assessment of intestinal motility and gut wall inflammation in rodents: analyses in a standardized model of intestinal manipulation. *JoVE (Journal of Visualized Experiments)* 2012: e4086
- Wang F-B, Powley TL. Vagal innervation of intestines: afferent pathways mapped with new en bloc horseradish peroxidase adaptation. *Cell and tissue research* 2007; 329: 221–230
- Wang X, Chan AKK, Sham MH, Burns AJ, Chan WY. Analysis of the sacral neural crest cell contribution to the hindgut enteric nervous system in the mouse embryo. *Gastroenterology* 2011; 141: 992-1002.e1-6
- Watson CJ, Hoare CJ, Garrod DR, Carlson GL, Warhurst G. Interferon-gamma selectively increases epithelial permeability to large molecules by activating different populations of paracellular pores. *Journal of cell science* 2005; 118: 5221–5230
- Weber B, Saurer L, Schenk M, Dickgreber N, Mueller C. CX3CR1 defines functionally distinct intestinal mononuclear phagocyte subsets which maintain their respective functions during homeostatic and inflammatory conditions. *European Journal of Immunology* 2011; 41: 773–779
- Wehkamp J, Salzman NH, Porter E, Nuding S, Weichenthal M, Petras RE, Shen B, Schaeffeler E, Schwab M, Linzmeier R, Feathers RW, Chu H, Lima H, Fellermann K, Ganz T, Stange EF, Bevins CL. Reduced Paneth cell alpha-defensins in ileal Crohn's disease. *Proceedings of the National Academy of Sciences of the United States of America* 2005; 102: 18129–18134
- Wehner S, Behrendt FF, Lyutenski BN, Lysson M, Bauer AJ, Hirner A, Kalff JC. Inhibition of macrophage function prevents intestinal inflammation and postoperative ileus in rodents. *Gut* 2007; 56: 176–185
- Wehner S, Buchholz BM, Schuchtrup S, Rocke A, Schaefer N, Lysson M, Hirner A, Kalff JC. Mechanical strain and TLR4 synergistically induce cell-specific inflammatory gene expression in intestinal smooth muscle cells and peritoneal macrophages. *American journal of physiology. Gastrointestinal and liver physiology* 2010; 299: G1187-97
- Wehner S, Engel DR. Resident macrophages in the healthy and inflamed intestinal

muscularis externa. *Pflugers Arch - Eur J Physiol* 2017; 469: 541–552

Wehner S, Schwarz NT, Hundsdorfer R, Hierholzer C, Tweardy DJ, Billiar TR, Bauer AJ, Kalff JC. Induction of IL-6 within the rodent intestinal muscularis after intestinal surgical stress. *Surgery* 2005; 137: 436–446

Wehner S, Straesser S, Vilz TO, Pantelis D, Sielecki T, La Cruz VF de, Hirner A, Kalff JC. Inhibition of p38 mitogen-activated protein kinase pathway as prophylaxis of postoperative ileus in mice. *Gastroenterology* 2009; 136: 619–629

Wen L, Tang F. Boosting the power of single-cell analysis. *Nat Biotechnol* 2018; 36: 408–409

Willemze RA, Welting O, van Hamersveld HP, Meijer SL, Folgering JHA, Darwinkel H, Witherington J, Sridhar A, Vervoordeldonk MJ, Seppen J, Jonge WJ de. Neuronal control of experimental colitis occurs via sympathetic intestinal innervation. *Neurogastroenterology & Motility* 2018; 30: e13163

Willemze RA, Welting O, van Hamersveld P, Verseijden C, Nijhuis LE, Hilbers FW, Meijer SL, Heesters BA, Folgering JHA, Darwinkel H, Blancou P, Vervoordeldonk MJ, Seppen J, Heinsbroek SEM, Jonge WJ de. Loss of intestinal sympathetic innervation elicits an innate immune driven colitis. *Molecular medicine (Cambridge, Mass.)* 2019; 25: 1

Worthington JJ, Reimann F, Gribble FM. Enteroendocrine cells-sensory sentinels of the intestinal environment and orchestrators of mucosal immunity. *Mucosal Immunol* 2018; 11: 3–20

Wynn TA, Chawla A, Pollard JW. Macrophage biology in development, homeostasis and disease. *Nature* 2013; 496: 445–455

Yan Y, Ramanan D, Rozenberg M, McGovern K, Rastelli D, Vijaykumar B, Yaghi O, Voisin T, Mosaheb M, Chiu I, Itzkovitz S, Rao M, Mathis D, Benoist C. Interleukin-6 produced by enteric neurons regulates the number and phenotype of microbe-responsive regulatory T cells in the gut. *Immunity* 2021; 54: 499-513.e5

Yang H, Sanidad KZ, Wang W, Xie M, Gu M, Cao X, Xiao H, Zhang G. Triclocarban exposure exaggerates colitis and colon tumorigenesis: roles of gut microbiota involved. *Gut Microbes* 2020; 12: 1690364

Yoo BB, Griffiths JA, Thuy-Boun P, Cantu V, Weldon K, Challis C, Sweredoski MJ, Chan KY, Thron TM, Sharon G, Moradian A, Humphrey G, Zhu Q, Shaffer J, Wolan DW, Dorrestein PC, Knight R, Gradinaru V, Mazmanian SK. Targeted Neuronal Activation of the Gastrointestinal Tract Shapes the Environment of the Gut in Mice 2021

Yoo BB, Mazmanian SK. The Enteric Network: Interactions between the Immune and Nervous Systems of the Gut. *Immunity* 2017; 46: 910–926

You X-Y, Zhang H-y, Han X, Wang F, Zhuang P-W, Zhang Y-J. Intestinal Mucosal Barrier Is Regulated by Intestinal Tract Neuro-Immune Interplay. *Front. Pharmacol.* 2021; 12: 1197

Zasloff M. Antimicrobial peptides of multicellular organisms. *Nature* 2002; 415: 389–395

Zeng Z, Mukherjee A, Varghese AP, Yang X-L, Chen S, Zhang H. Roles of G protein-coupled receptors in inflammatory bowel disease. *World Journal of Gastroenterology : WJG* 2020; 26: 1242–1261

Zhang H, Miao J, Li F, Xue W, Tang K, Zhao X, Jing X, Zhang J, Huang C, Hou N, Han J. Norepinephrine transporter promotes the invasion of human colon cancer cells. *Oncology Letters* 2020; 19: 824–832

Zhang J, Fan W, Wang H, Bao L, Li G, Li T, Song S, Li H, Hao J, Sun J. Resveratrol Protects PC12 Cell against 6-OHDA Damage via CXCR4 Signaling Pathway. *Evidence-Based Complementary and Alternative Medicine* 2015; 2015: 1–12

Zheng D, Liwinski T, Elinav E. Interaction between microbiota and immunity in health and disease. *Cell Res* 2020; 30: 492–506

Zheng Z, Wan Y, Liu Y, Yang Y, Tang J, Huang W, Cheng B. Sympathetic Denervation Accelerates Wound Contraction but Inhibits Reepithelialization and Pericyte Proliferation in Diabetic Mice. *Journal of Diabetes Research* 2017; 2017: 7614685

Zigmond E, Jung S. Intestinal macrophages: well educated exceptions from the rule. *Trends in immunology* 2013; 34: 162–168

Zigmond E, Varol C, Farache J, Elmaliah E, Satpathy AT, Friedlander G, Mack M, Shpigel N, Boneca IG, Murphy KM, Shakhar G, Halpern Z, Jung S. Ly6C hi monocytes in the inflamed colon give rise to proinflammatory effector cells and migratory antigen-presenting

cells. *Immunity* 2012; 37: 1076–1090

Zihni C, Mills C, Matter K, Balda MS. Tight junctions: from simple barriers to multifunctional molecular gates. *Nat Rev Mol Cell Biol* 2016; 17: 564–580

Zittel TT, Rothenhöfer I, Meyer JH, Raybould HE. Small intestinal capsaicin-sensitive afferents mediate feedback inhibition of gastric emptying in rats. *The American journal of physiology* 1994; 267: G1142-5

## 9. Acknowledgments

First and most importantly, I wish to sincerely thank Prof. Dr. Sven Wehner for providing me with an opportunity to pursue my Ph.D. career in his group. Thank you for being strict whenever necessary and providing me excellent guidance throughout these years. Your mentoring and immense support motivated and helped me to develop independently as a better scientist. You gave me freedom and let me face professional challenges that boosted my confidence. You encouraged me constantly and I cannot thank you enough for assisting me throughout my research.

I would like to thank the whole Ph.D. committee. Thank you for all the work you have put into this process. I especially would like to thank Prof. Dr. Daniel Robert Engel for being part of the committee. I would like to express my deepest gratitude for the effort you put into reviewing my thesis. I thank Prof. Dr. Jörg C. Kalff for providing me an opportunity to start this research work in your institute and also for being part of my thesis committee. I would also like to thank Prof. Dr. Wolfgang Kastenmüller for joining the dissertation committee. I would like to thank Ms. Sarah Funk, for answering my hundreds of questions regarding the thesis submission, the documents required as well as all the effort you put into processing this thesis. I would like to thank Prof. Wouter J. de Jonge who is a great collaborator. I appreciate your liveliness in all our wonderful discussions. Thank you for your great contributions in suggesting experiments and editing my paper.

I would like to thank Dr. Reiner Schneider for his experimental support and editing of my paper as well as this thesis. You never missed a single chance to complain, but I learned a lot from you. Thank you for being supportive and listening to my problems in the lab. Talking to you gave me strength and support. I thank Dr. Balbina Garcia-Reyes for correcting this work and lending me moral support. Thank you for always trying to solve my problems and providing me with fresh energy so I could push the thesis forward.

I like to thank Dr. Kathy Stein who greatly contributed to my peaceful stay in Bonn. You were always kind and helpful. Thank you for teaching me flow cytometry and other necessary techniques needed for my Ph.D. I thank Dr. Jana Enderes for making use of my technical skills and finally publishing a paper together. Thank you for also providing me advice on medical care whenever needed.

Special thanks to our technical assistant staff Mariola Lysson, Patrik Efferz, Bianca Schneiker, Jana Müller and Sabine Schmitt. I thank Mariola Lysson, an expert in several techniques for providing experimental support. Your way of working in the lab is very precise and I got to learn a lot from you. Thank you for helping me find a nice place to stay in Bonn for the past 4 and a half years.

I thank Patrik Efferz for being kind and creating a fun environment in the lab. Talking to you always cheered my mood. We had great discussions throughout my time in this lab. Thank you for listening to my stories and providing me moral support. Your warm words kept motivating me to work harder. A big thank you for doing a great job in the background by taking care of animals. Because of you, I could plan my experiments smoothly. I thank Bianca Schneiker for helping me with most of my experiments. You are always calm and happy that cheers everybody in the lab. You never said no to me whenever I asked for your help. I knew I could always depend on you with the experimental help. Thank you for baking yummy cookies and sharing them with us.

I thank Jana Müller for always agreeing to help me in my experiments. You are very sweet and a quick learner. Thank you for always being in a good mood and creating a warm environment in the lab. I thank Sabine Schmitt for helping me in some of my experiments. Although it was a very short period, I still got to learn some things from you. I thank Dr. Alexandra Seinsche for helping me with the animal proposal and shipping of packages. You were kind enough to help me even on quick notice.

I thank Patrick Leven, my fellow doctoral researcher, for providing me experimental advice and motivating me to work harder. We not only discussed science but topics ranging from escape room games and spicy food. Thanks for being a good friend and sharing all the fun moments. I thank Linda Schneider for all the talks especially, on fitness topics. Thank you to always listen to my stories no matter how boring they were. I thank Hilal Sengül for being honest and providing me research advice. I am happy to have worked with you.

I thank Vasiliki Bantavi for remaining good friends for all these times. We had a great time together and shared each other's problems. I will surely miss all our lab talks and fun moments we had. Thank you for always encouraging me and making me feel strong. I thank Mona Bresser for her trust in my skills and for learning the techniques from me. You

are very hardworking, enthusiastic and had lots of questions. Therefore, I learned a lot by trying to find answers for you. I would like to thank Svenja Gysser and Xenia Zoller, our past and present secretaries for being professional and making our work easier. Thank you for working hard and keeping us up to date on laboratory and administration work.

I thank Dr. Klaas Yperman for teaching me how to use Illustrator and ImageJ. You were always there no matter what. Thank you for helping me, providing unlimited support, and for being the person to know me the best. Finally, I would like to thank my family for being my biggest support and motivating me unconditionally to reach my goals. Thank you for always having trust in my decisions and giving me complete freedom.

You all immensely contributed to this work and I am proud of what we achieved together. I had a great experience being a part of this team. It was my first job and I moved to a foreign country 7500 kilometers away from my family. I met wonderful people and had fantastic discussions. I faced many ups and downs but I surely learned something from each one of you. It was a deep journey with thousands of experiences that turned me into a better person than I was. I will carry all the best and fun moments I had here for the rest of my life. It surely is and will be one of the best experiences of my life. I will miss you all and hope you remember me now and then.